Earthquake-Induced Ground Fissuring in Foot-Slope Positions of the Port Hills, Christchurch

---

A thesis

submitted in partial fulfilment of

Master of Science in Engineering Geology

in the

University of Canterbury

by

C J Stephen-Brownie

University of Canterbury

2012

Acknowledgements

Over the time spent working on this thesis, I have been incredibly fortunate to receive the kind support of many people.

I would like to express my sincere gratitude to my supervisors David Bell and Dr Marlène Villeneuve for their time, expertise and constructive suggestions relating to this research work.

I would also like to extend my thanks to the University of Canterbury Geology Department technicians: Matt Cockcroft, Chris Grimshaw, Cathy Higgins, and Vanessa Tappenden, for their assistance with laboratory analysis and the resistivity survey. Also from the University of Canterbury, Dr Cédric Lambert who offered valuable advice on the use of *FLAC*, and Janet Warburton, whose administrative assistance was greatly appreciated.

Many Christchurch residents allowed me to access to their properties, in particular, Alan Hawkins from number 3 Glenview Terrace, and Dr Kari Basset, of the University of Canterbury Geology Department, from number 40 Rapaki Road. Thank-you for your support, and for allowing me to dig holes in your back yards.

I am particularly grateful for the insights into the behaviour of springs and groundwater in the Hillsborough area offered by Helen Rutter from Aqualinc Research Ltd., Christchurch.

Thank-you to Tobi, my field assistant and champion.

Finally, thank-you to my parents, whose support and encouragement has been tremendous throughout all my years of university study. I could not have done it without you.

Abstract

Following the 22 February 2011, M_W 6.2 earthquake located on a fault beneath the Port Hills of Christchurch, fissuring of up to several hundred metres in length was observed in the loess and loess-colluvium of foot-slope positions in north-facing valleys of the Port Hills. The fissuring was observed in all major valleys, occurred at similar low altitudes, showing a contour-parallel orientation and often accompanied by both lateral compression/extension features and spring formation in the valley floor below. Fissuring locations studied in depth included Bowenvale Valley, Hillsborough Valley, Huntlywood Terrace–Lucas Lane, Bridle Path Road, and Maffeys Road–La Costa Lane.

Investigations into loess soil, its properties and mannerisms, as well as international examples of its failure were undertaken, including study of the Loess Plateau of China, the Teton Dam, and palaeo-fissuring on Banks Peninsula. These investigations lead to the conclusion that loess has the propensity to fail, often due to the infiltration of water, the presence of which can lead to its instantaneous disaggregation. Literature study and laboratory analysis of Port Hills loess concluded that is has the ability to be stable in steep, sub-vertical escarpments, and often has a sub-vertically jointed internal structure and has a peak shear strength when dry.

Values for cohesion, c (kPa) and the internal friction angle, ϕ (degrees) of Port Hills loess were established. The c values for the 40 Rapaki Road, 3 Glenview Terrace loess samples were 13.4 kPa and 19.7 kPa, respectively. The corresponding ϕ values were thought unusually high, at 42.0° and 43.4°.The analysed loess behaved very plastically, with little or no peak strength visible in the plots as the test went almost directly to residual strength.

A geophysics resistivity survey showed an area of low resistivity which likely corresponds to a zone of saturated clayey loess/loess colluvium, indicating a high water table in the area. This is consistent with the appearances of local springs which are located towards the northern end of each distinct section of fissure trace and chemical analysis shows that they are sourced from the Port Hills volcanics.

Port Hills fissuring may be sub-divided into three categories, Category A, Category B, and Category C, each characterised by distinctive features of the fissures. Category A includes fissures which display evidence of, spring formation, tunnel-gullying, and lateral spreading-like behaviour or quasi-toppling. These fissures are several metres down-slope of the loess-bedrock interface, and are in valleys containing a loess-colluvium fill. Category B fissures are in wider valleys than those in Category A, and the valleys contain estuarine silty sediments which

liquefied during the earthquake. Category C fissures occurred at higher elevations than the fissures in the preceding categories, being almost coincident with bedrock outcropping.

It is believed that the mechanism responsible for causing the fissuring is a complex combination of three mechanisms: the trampoline effect, bedrock fracturing, and lateral spreading. These three mechanisms can be applied in varying degrees to each of the fissuring sites in categories A, B, and C, in order to provide explanation for the observations made at each. Toppling failure can describe the soil movement as a consequence of the a three causative mechanisms, and provides insight into the movement of the loess. Intra-loess water coursing and tunnel gullying is thought to have encouraged and exacerbated the fissuring, while not being the driving force *per se*. Incipient landsliding is considered to be the least likely of the possible fissuring interpretations.

Table of Contents

List of Tables

List of Figures

1. Introduction

1.1 Project background

Christchurch is located on the east coast of the South Island of New Zealand, adjacent to the ancient volcanic calderas of Banks Peninsula (Figure 1.1). On Saturday September 4th 2010, at 4.35 am Christchurch was shaken by a M_W 7.1 earthquake, sourced on an hitherto unknown fault located west of the city, near the small town of Darfield (Figure 1.1). This earthquake, referred to henceforth as the Darfield Earthquake, signalled the beginning of a series of major earthquakes and aftershocks in the region over the following weeks and months. This thesis provides a detailed documentation and attempted explanation of one geotechnical aspect of the earthquakes, specifically the appearance of extended (up to 500 m) fissuring in the loess foot-slope positions of north-facing valleys of the Port Hills near the location of the sub-surface fault rupture of the M_W 6.2 earthquake of 22 February 2011.

Figure 1.1 Christchurch, Darfield and the Port Hills. Inset: New Zealand. Base map source: Google Maps.

The February 2011 earthquake, henceforth known as the Christchurch Earthquake, while lower in magnitude than the Darfield Earthquake, caused the most damage to the region, both geotechnically and socially. The earthquake was caused by the movement of an oblique thrust fault located beneath the Port Hills of Christchurch, dipping to the South, with an epicentre beneath the Heathcote Valley (Kaiser et al. 2012). The fault trace did not reach the surface

however when projected it is thought to trend 058°, along the base of the hills to where the Heathcote river enters the estuary, and then out to sea at the northern end of the New Brighton spit (Smyrou et al. 2011; Kaiser et al. 2012).

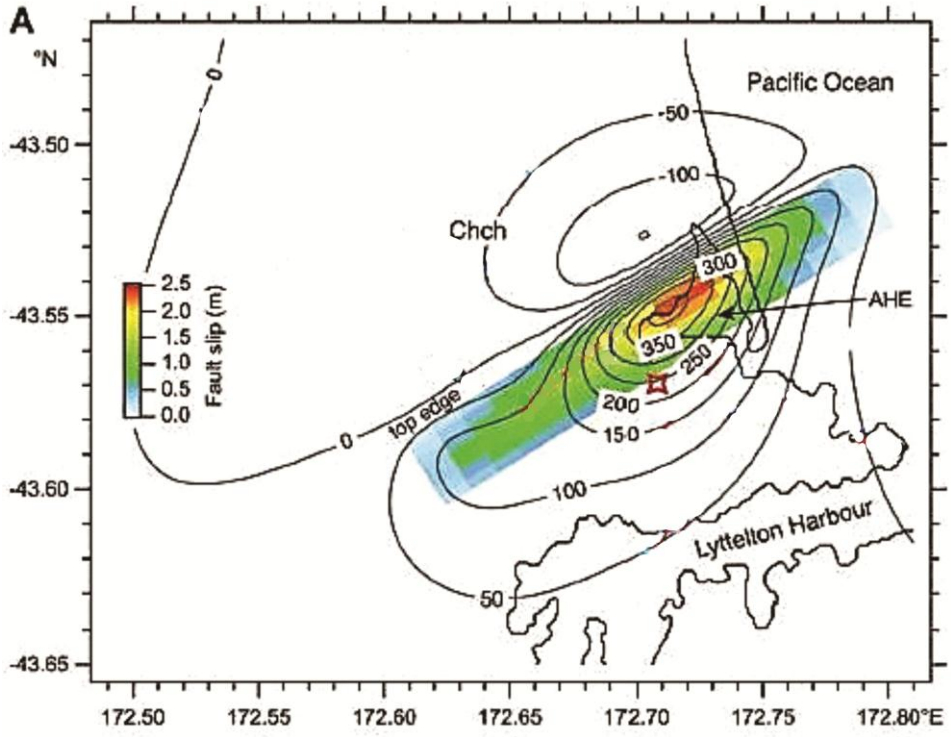

Figure 1.2 Geodetic source model of the Christchurch Earthquake, after Kaiser et al. 2012.Black contours indicate relative vertical ground displacement in millimetres, as shown by Kaiser et al.'s model. Coloured rectangle shows the modelled fault plane, trending northeast, and dipping to the southwest, with its top edge at a depth of one kilometre.

Movement on the fault of the Christchurch Earthquake was an oblique-thrust motion, ultimately causing sites on the Port Hills to increase in elevation relative to the Avon-Heathcote Estuary. Arguably, the most striking geotechnical feature of the 22 February 2011 earthquake was the extreme ground acceleration recorded in the Port Hills area. In the Heathcote Valley, readings of 2.2lg peak vertical ground acceleration were recorded (Bradley & Cubrinovski 2011), far surpassing the peak ground acceleration (PGA) values of most earthquakes of a similar magnitude world-wide, for example Anderson (2010) labels PGA values greater than 1.0 g as 'extraordinary'.

These intense vertical and horizontal forces caused boulders, some up to 5 t, to be lifted and dropped in place. Many houses built in areas which suffered such forces were irreparably damaged, as were many historic buildings in Lyttelton, a small town on the south side of the Port Hills.

Following the Christchurch Earthquake much geotechnical damage was reported over the Port Hills as well as in the City itself. In Christchurch City the main problems were due to liquefaction of the Springston Formation silts and sands, while on the hills the main issues were from rockfall and movement of the loess soil on the foothills.

Fissuring in the Port Hills caused severe damage to many hill-side properties, with fissures mostly less than 0.2 m in width extending segmentally for several hundred metres. These fissures are present in nearly all major valleys, occur at similar low altitudes, show a contour-parallel orientation and are often accompanied by both lateral compression/extension features and spring formation in the valley floor below.

1.2 Thesis objectives

This project was undertaken to provide explanations for the fissuring behaviour observed in the Port Hills of Christchurch following the series of significant earthquakes which occurred near the city in 2010 and 2011, in particular the Christchurch Earthquake of 22 February 2011. Such explanations would be useful for planners and developers, as well as residents currently adversely affected by the fissuring. As such, the principal objectives of this project are:

a) To research literature on loess soils and failures which take place in them, and to confirm whether there are any links between the fissuring behaviour seen in Christchurch and that observed in previously documented locations world-wide.
b) To establish and document the extent of the of the fissure traces on the Port Hills through extensive field investigation and collation of post-earthquake data.
c) To conduct in-depth study at specific locations, including laboratory analysis of loess taken from fissuring sites to ascertain its geotechnical properties and propensity to form fissures.
d) To establish working hypotheses on the geotechnical mechanisms responsible for the formation of the fissures, as well as exploring their geotechnical implications and possible remediation measures. A preferred mechanism for loess fissuring is presented, along with recommendations for further research.

1.3 Geological setting

1.3.1 Geological evolution of Canterbury

New Zealand is situated on an oblique continental convergence zone along the south-western edge of the Pacific Plate. Convergence rates of approsimately 38 mm per year are accommodated between the Pacific and Australian plates (DeMets et al. 2010) along the South Island's Alpine Fault (Figure 1.3). This motion has resulted in the formation of the Southern Alps, in an event beginning about 25 million years ago and , and continuing today, known as the Kaikoura Orogeny. The mountains are currently being uplifted at rates of 10-20 mm per year (Coates 2002). In the northern South Island a series of strike-slip faults comprise the Marlborough Fault System, and active faults have been mapped in the foothills of the Southern Alps west of the Canterbury Plains (Kaiser et al. 2012).

The Kaikoura Orogeny has resulted in a total of about 20 kilometres of uplift taking place along the Alpine Fault. Weathering and erosion have been in opposition to the orogenic processes, constantly removing rock through actions such as glaciation, rock avalanches, and

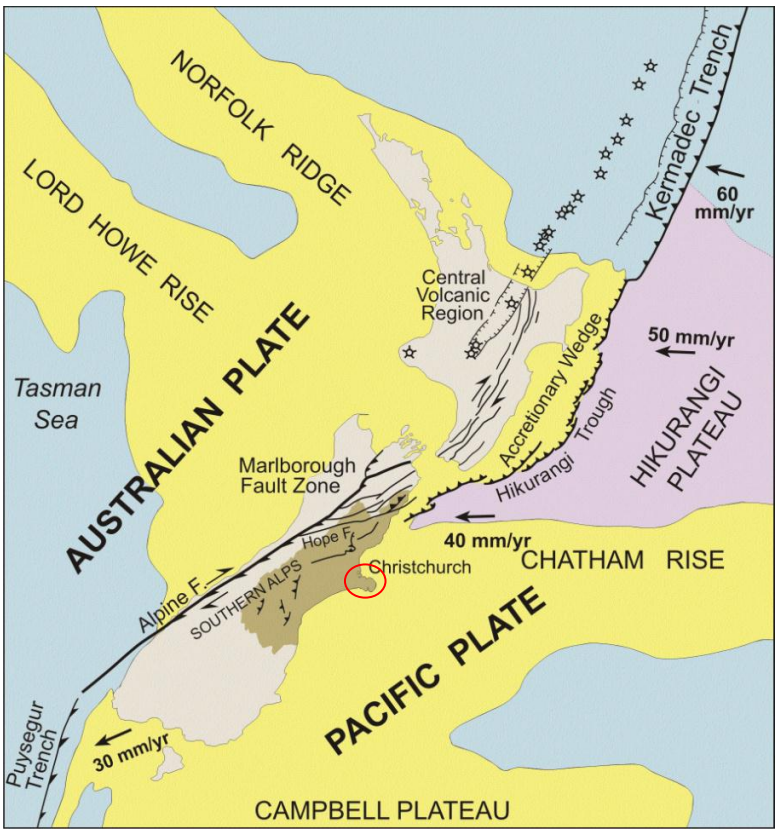

Figure 1.3 Australian-Pacific plate boundary through New Zealand and convergence rates of Pacific relative to Australian Plate. Christchurch and Banks Peninsula (circled red) on the east coast of the South Island. (Image courtesy of J. Pettinga, University of Canterbury Geology Department, 2012).

river and debris flow transportation. The Canterbury Plains were largely constructed by the sediment deposition from the Waimakariri and Rakaia Rivers, in particular during the glaciations of the Quaternary period, when thick layers of gravel and sand accumulated on the rivers' flood plains, and extended several kilometres beyond the present-day coastline (Figure 1.4).

Banks Peninsula (Figure 1.3) commenced volcanic activity in the mid- to late-Miocene, between 12-10 million years ago, and was predominantly of the "Hawaiian" style of eruption. The peninsula was originally an island, separate from the larger landmass of the Southern Alps forming in the west. The eruptions resulted in the formation of roughly symmetrical, cone-shaped, basaltic lava flow deposits (Brown & Weeber 1992) which radiate outwards from three principal eruptive centres. Volcanic activity on Banks Peninsula ceased around the mid-Pliocene, and the area remained relatively tectonically stable during the Pleistocene when widespread aeolian deposits of loess accumulated (Griffiths 1973). Aggradation of outwash from glaciations of the Southern Alps progressively infilled the seaway between the Southern Alps and Banks

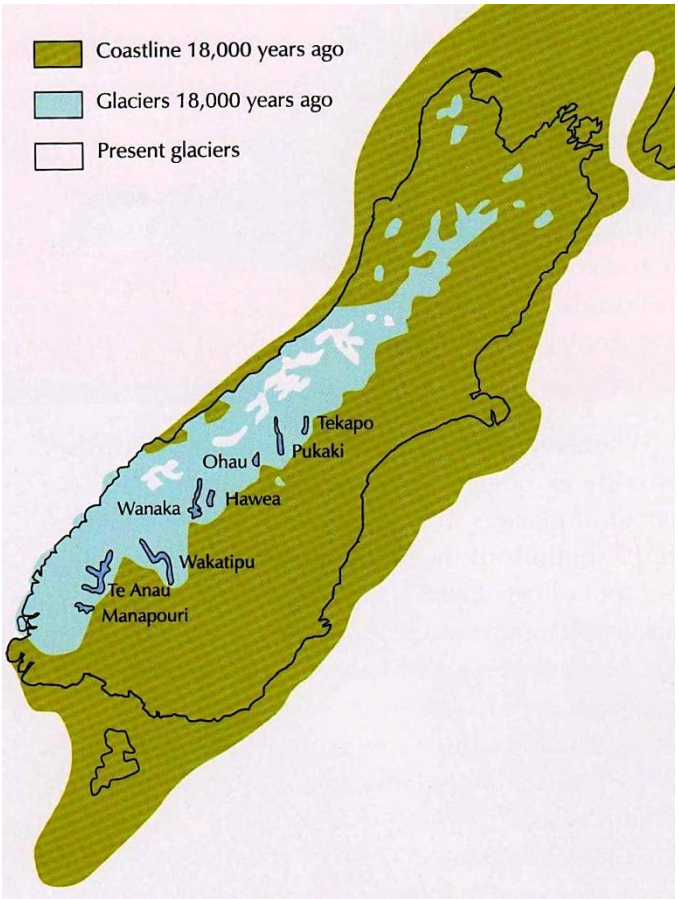

Figure 1.4 The coastline of New Zealand and glacial coverage during the Late Otiran Glaciation of 18000 B.P. After Coates (2002).

Peninsula until the current day, where some 300 m of fluvioglacial gravels underlie the Canterbury Plains (Figure 1.7) (Bell et al. 1986; Coates 2002).

The Port Hills of Christchurch form the south-eastern boundary of the city. They are part of the eroded caldera surrounding the volcanic crater lake, occupied by Lyttelton Harbour. Andesitic and basaltic lava flows radiate from the caldera northwards towards Christchurch City, forming a series of valleys, the flanks of which are mantled by a thick loess layer, and the floors filled with alluvial silts and sands, peat, and loess colluvium. The north-facing slopes contain the thickest loess deposits, up to 40 m thick in some valleys. Volcanic bedrock extends tens of metres below the ground surface at the base of the hills; along Centaurus Road the bedrock depth is variable, but predominantly between 50 m and 100 m deep, with one Environment Canterbury well (No.M35/w4135), which is located near the junction of Centaurus Road and Rapaki Road, reaching bedrock at c. 55.5 m (Brown & Weeber 1994).

1.3.2 Seismicity of the Christchurch and Port Hills area

Being located near the centre of the East Coast of the South Island, Christchurch has the potential to be impacted by seismic activity occurring not only in Canterbury, but also in adjacent regions, and even offshore (Pettinga et al. 2001). The Darfield and Christchurch Earthquakes were both relatively shallow (<15 km) crustal earthquakes, with their hypocentres in the basement Torlesse Composite Terrane of sandstone (greywacke) and mudstone (argillite) (Browne et al. 2012). It is believed that these faults, which originally formed due to either Mesozoic to Cenozoic extension or the emplacement of the nearby volcanics, were reactivated during the Darfield and Christchurch Earthquakes (Browne et al. 2012).

Drilling at Charteris Bay on Banks Peninsula in the late 1980s revealed highly sheared Torlesse and volcanic rocks, which were interpreted to be the indicative of a northeast-striking fault (Field et al. 1989; Browne et al. 2012), which , while separate from the location of the Christchurch fault, has a similar strike and shows that the area has a history of rupture from such features.

The general trend of fault traces in the Canterbury region is in a northeast-southwest orientation, with movement in a right-lateral sense, which has come about most recently due to the plate movement related to the Kaikoura Orogeny. Figure 1.6 shows the mapped faults of the northern Canterbury Plains, and their various type groups, many being oblique thrust faults. The varying sets of fault orientations in the area have originated in different time periods, in response to the stress fields of the time.

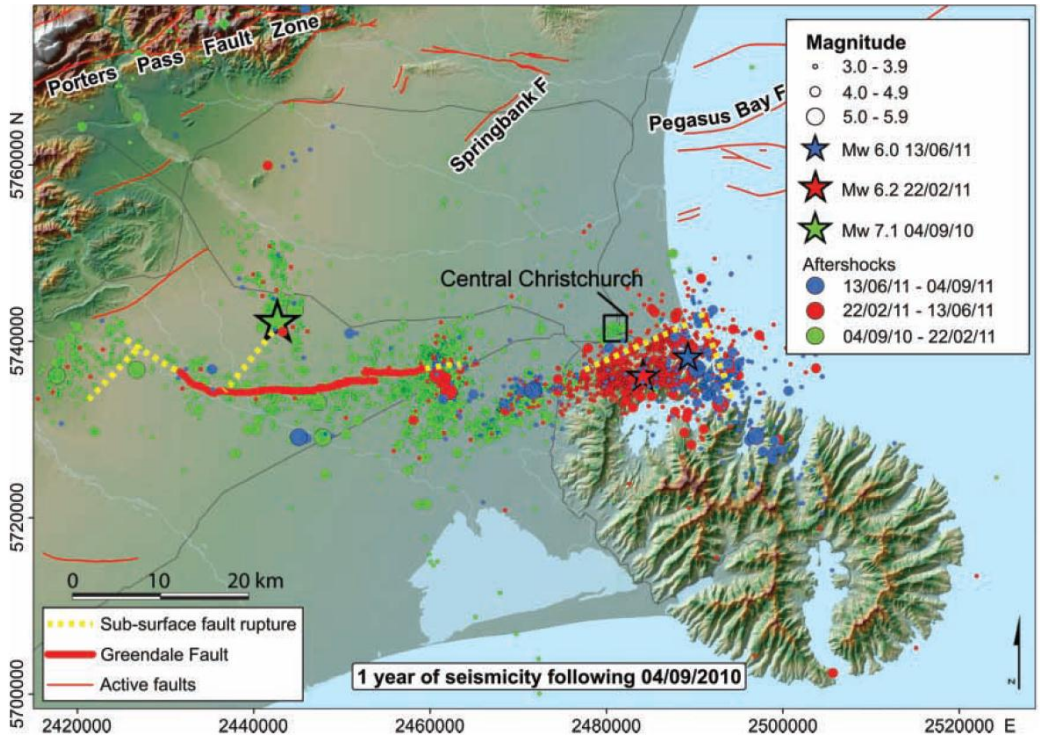

Figure 1.5 The MW 6.2 Christchurch earthquake (red star) in the context of the Darfield main shock (green star) and aftershock sequence up until 04 September 2011. After Kaiser et al. (2012).

The Darfield Earthquake fault trace is shown at the bottom of the image and it trends nearly east-west. Figure 1.5 provides an overview of the Christchurch and Darfield Earthquake sequences, and the location of the faults responsible for these earthquakes. Other east-striking faults, such as the Ashley and Loburn Faults, in the region were Late Cretaceous faults which were reactivated in the Neogene to Quaternary (Campbell et al. 2012), and it is likely that the Darfield Earthquake, and potentially the Christchurch Earthquake, occurred on such reactivated structures.

The proximity of both of these fault traces to the city of Christchurch and to the Port Hills has meant that there has been widespread damage to the city during the earthquake and subsequent aftershocks. This thesis deals predominantly with the effects appearing from movement on the fault beneath the Port Hills that was responsible for the Christchurch Earthquake, on 22 February 2011. During this earthquake, the fault trace did not break the ground surface, however the oblique thrust movement along the southeast-dipping fault plane induced a broad warping of the surrounding ground (Browne et al. 2012), resulting sections of the Port Hills having been uplifted by nearly 1.0 m relative to down-thrown regions within Christchurch City. The fissuring which appeared in the lower flanks of the north-facing valleys of the Port Hills can be directly attributed to the intensity and shallowness of the Christchurch earthquake.

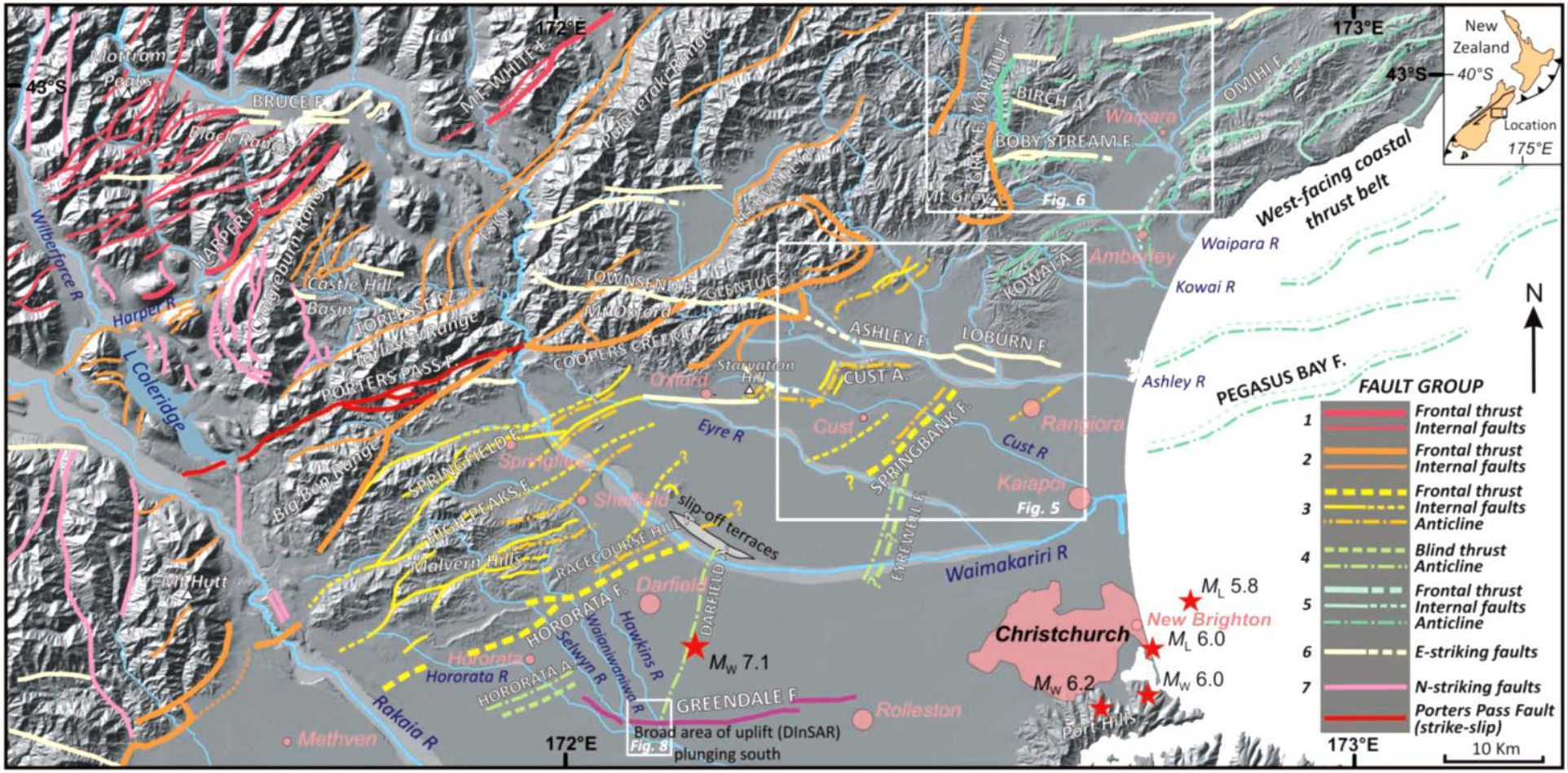

Figure 1.6 Map of the north Canterbury region showing main fault groups (colour coded).Dashed lines represent faults concealed underneath Quaternary gravels or offshore. Geographic localities referred to in text are also shown. The location of the epicentres triggering cycles of seismicity are shown by red stars. F, Fault; FZ, Fault zone; A, Anticline; R, River. Insets show location of other figures from Campbell et al.'s publication. From Campbell et al 2012.

1.4 Hydrogeology of the Christchurch Area

The city of Christchurch is underlain to a depth of up to approximately 300 m by complex layering of glacial outwash gravels and interglacial estuarine muddy sediments (Figure 1.7) These alternating deposits resulted from sea level fluctuations of up to 150 m between the glacial periods of the Quaternary, and continuing until about 14 000 B.P. (Coates 2002). The fluvial gravel outwash beds form a large aquifer system which abuts the coast of the Canterbury Plains adjacent to Banks Peninsula. These are confined, upper Quaternary, alluvial aquifers, with recharge derived from influent seepage from the bed of the Waimakariri River to the northwest of Christchurch (Brown & Weeber 1994).

The Banks Peninsula bedrock aquifers form a second aquifer system in the Christchurch area. These carry groundwater in inter-connected joints, cracks, and fissures of the volcanic rock, with recharge sourced predominantly from the slow circulation of local Banks Peninsula rainfall, which has been ascertained through chemical and isotope analysis of the water (Brown & Weeber 1994).

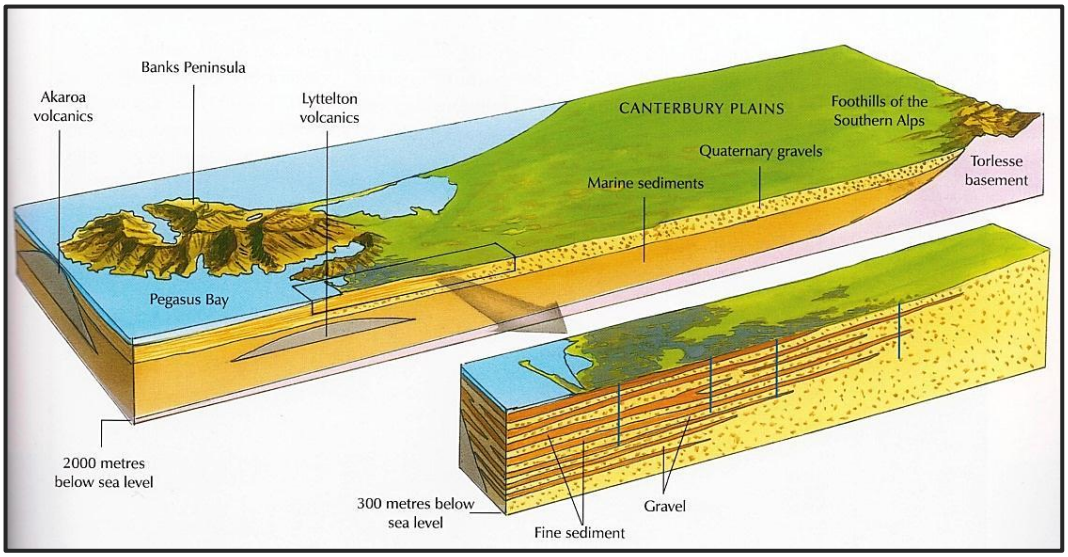

Figure 1.7 Simplified cross-section (vertical exaggeration x 5) of the sedimentary layers underlying the Canterbury Plains. Zoomed section highlighting Canterbury alluvial aquifer system to depth of 300 metres below sea level. After Coates (2002).

1.5 Geographical setting

The local climate is subhumid on the Canterbury Plains and in the lower slopes of the hills, becoming humid higher up the hills (Griffiths 1974). Freeze-and-thaw conditions in winter can have a significant influence on erosion of Port Hills soils at higher elevations on the south-facing slopes (Griffiths 1974).

Prior to European colonisation of the Christchurch area, vegetation on the Port Hills was comprised of a variety of native fauna. Valley floors were mostly raupo (*Typha orientalis*) swamp, with flax (*Phorium tenax*), toetoe (*Cortaderia richardii*), and bracken (*Pteridium aquilinum* var. *esculentum*) in the upper, narrower parts of the valleys (Griffiths 1974). Patches of mixed podocarp forest occurred on the summits and some distance down south-facing shady faces of the hills, but the remainder were predominantly covered with tussock grassland, predominantly hard tussock (*Festuca novae-zelandiae*) (Griffiths 1974). European colonisation of the area meant that the Port Hills began to be used for farming, and as such the valley floors have been drained, cultivated with pasture crops, and subdivided for housing. With the advent of farming, much remnant native forest cover was destroyed through burning to create land for grazing, although this practice is now prohibited.

1.6 Methodology and format

Research methods include mapping of the occurrence of foot-slope damage from the Christchurch earthquakes of 2010 and 2011, a detailed engineering geological study of two sites where fissuring has occurred, and soil testing of the loess from these sites including shear box soil strength analysis.

Also conducted was a geophysical resistivity survey through one of the fissure locations in Hillsborough, a study of groundwater and spring behaviour in the case-study area, and research into the suitability of the computer programme FLAC to model the behaviour of the hillslope.

The outline of this thesis is as follows:

Chapter Two covers the formation and geotechnical properties of loess, and provides a review of slope failure in loess soils from around the world both in natural slopes and in loess-filled embankment dams. The chapter concludes with a review of loess stabilisation methods. Background on the Christchurch Earthquakes and the impacts that were observed in the Port Hills in particular are described in Chapter Three, as well as an overview of the fissuring problem. Chapter Four provides detailed analysis of the fissuring as it occurred in one valley in Huntsbury. The chapter includes engineering geological maps of the fissuring, laboratory testing analysis, geophysical resistivity survey results, and groundwater data analysis. Documentation of remedial work undertaken at several sites is also included. The information provided in Chapter Four is analysed in Chapter Five, where possible interpretations of the mechanism of formation of the fissures are discussed. Chapter Six is a summary of the findings of the previous chapters, with specific conclusions and recommendations.

2 Loess Soils: Review

2.1 Loess

Pale yellow-brown, silt-sized blanket deposits of *loess* are widespread throughout the world, and it is generally considered that they were formed from aeolian deposition at the time of the Pleistocene glaciations (Claridge & Campbell 1987). Glaciers produce large quantities of *rock flour* (silt-sized particles, whose mineral content is directly attributable to the rock type of the source area) as a result of the grinding action of ice against the surrounding bedrock. These clayey silt deposits are removed by fluvial action, and collect along the margins of glacial outwash plains. The fine material is then picked up and carried as suspended load by strong catabatic winds which form at the margin of glaciers. Airfall loess deposits consist of accumulated layers of this fine-grained clayey or sandy silt which has been entrained and subsequently deposited, often far away from the source area (Claridge & Campbell 1987; Marshak 2001).

Loess bodies consist of multiple layers, usually each topped with a fragipan layer, which is often visible 0.7 – 1.0 m below the surface, and there is a sharp boundary between this fossil soil and the next layer of loess above (Raeside 1964). When weathering takes place, the loess bodies tend to form distinct layers, coincident with chemical weathering stages within the loess, which are indicated by differences in the nature and relative proportions of micas and chlorite minerals. This was observed in Churchman and Bruce's (1987) study on loess in Southland, New Zealand. Loess in the Port Hills also displays such layering within the soil profile, which, together with soil properties such as clay mineral dispersion and moisture-dependent strength changes, can control the occurrence and severity of mass movement and tunnel-gully erosion (Bell et al. 1986).

Loess may be grouped into two main categories; primary loess of aeolian origin, and secondary loess, also known as *loess colluvium* which includes primary loess that has been altered or degraded *in situ* or deposited by water(Ives 1973).

Loess colluvium is comprised of a mixture of loessial materials which have been transported down slope by erosional processes sometime after their initial deposition on the hill side. Approximately 10 % of the loess colluvium is made up of volcanic rock fragments, the proportion of which increases with proximity to bedrock (Bell & Trangmar 1987). The loess deposits themselves are usually divided into pedogenic layers. Uppermost is the topsoil and

lower surface layer, a firm, plastic sandy silt from 0.25 m to 0.70 m deep. Then the fragipan, which is a clayey silt from 0.40 m to 1.20 m deep, and finally the parent layer, which is up to 6.00 m deep and may be in situ or redeposited stiff, non-plastic sandy silt. These layers are depicted in Figure 2.1.

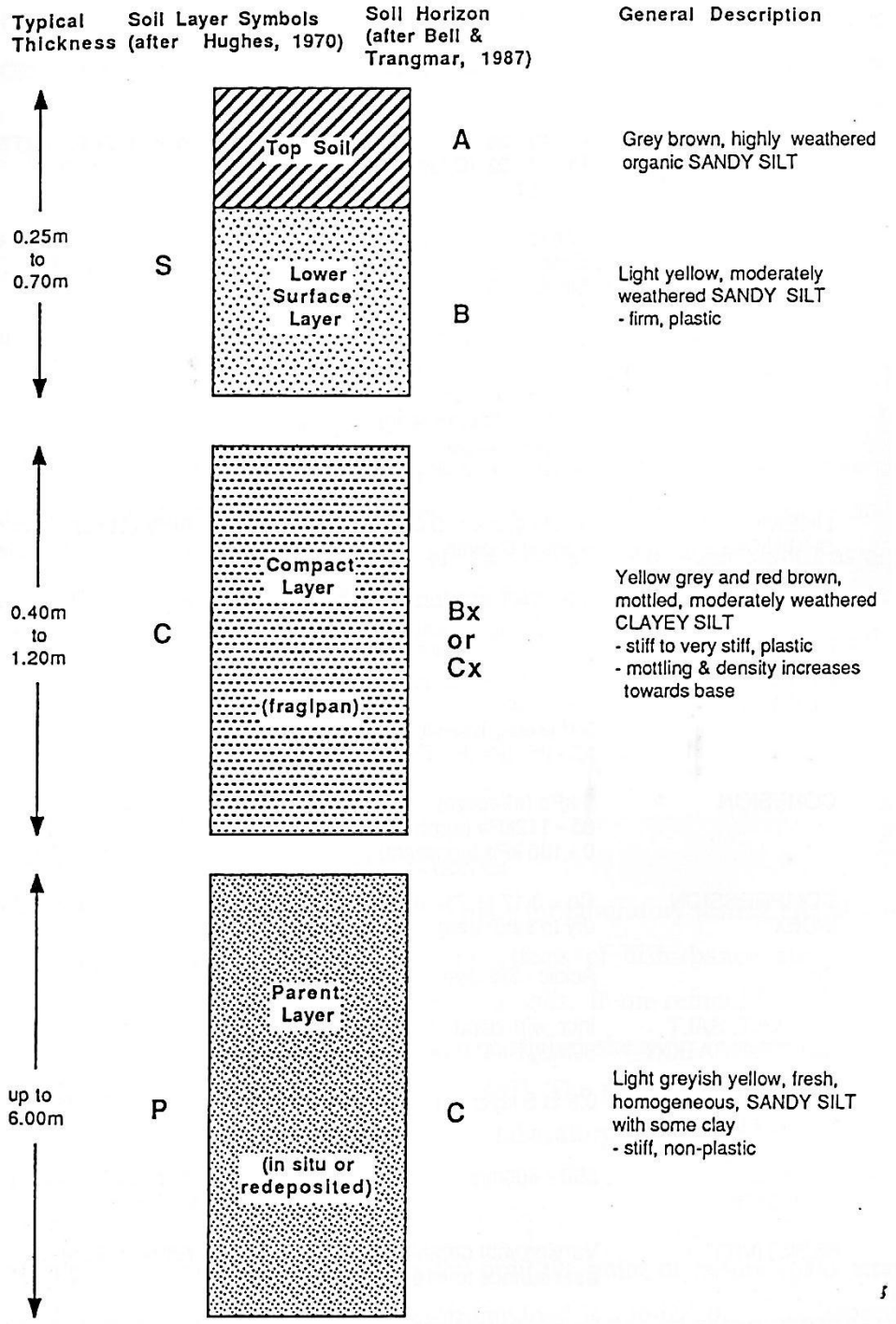

Figure 2.1 Pedogenc layering that develops in Banks Peninsula loess. After Goldwater (1990)

Loess and other windblown deposits have the unusual characteristic of being stable in steep, sub-vertical escarpments (Figure 2.2), and may exhibit sub-vertical columnar jointing (Bell 2007; Ishihara 2009). Vertical exposures of loess are relatively resistant to weathering, and can form several metre high, stream-gouged cliff formations (Raeside 1964; Blyth 1969; Ives 1973). When loess is excavated, these sub-vertical fractures mean that the soil may fall off in blocks. There are several reasons for this structure in the loess soils, including the presence of electrical charges on the clay particles which bind the sediment together (Marshak 2001), and the fact that by nature the slopes are often be under-saturated (Derbyshire 2001). Bell (2007) indicates that in loess the silt-sized particles are held together by bonds of clay-sized particles (which may be clay minerals, or fine quartz, feldspar or calcite), and it is the strength of these bonds that governs the mechanical behaviour of the loess.

Loess has a peak shear strength when dry, but when water seeps into the characteristic vertical joints of loess, they can become enlarged conduits and eventually may develop into underground piping systems and tunnel-gullies (Bell & Trangmar 1987). During high discharge events, water flows through these gully systems and erosion occurs through particle entrainment along the base of the tunnel (Derbyshire 2001).

Figure 2.2 Example of near-vertical loess cutting at Stonehaven Terrace, Christchurch.

2.2 Occurrence, origin and geological history of Banks Peninsula loess

Loess deposits of variable thickness are found over 26% of the land surface of Canterbury (Ives 1973). Around Christchurch, dispersive loess of late Pleistocene age (Figure 2.3) has been wind-deposited on the slopes of the Port Hills (Raeside 1964; Brown & Weeber 1992). It is largely sourced from the braided river beds of the Canterbury Plains which are comprised of greywacke from the Southern Alps. Over time the loess has accumulated mostly in the valleys, as well as mantling the topography, with thicknesses ranging from 1 m – 20+ m (Griffiths 1973; Brown & Weeber 1992). A secondary, minor, source area for loess of the more seaward slopes of Banks Peninsula could be from continental shelf (Figure 2.4), which was exposed during sea-level recessions of the Pleistocene (Raeside 1964). The primary minerals found in the Canterbury loess are quartz and plagioclase feldspar, which together, in equal proportion, make up nearly 90% of the loess (Raeside 1964).

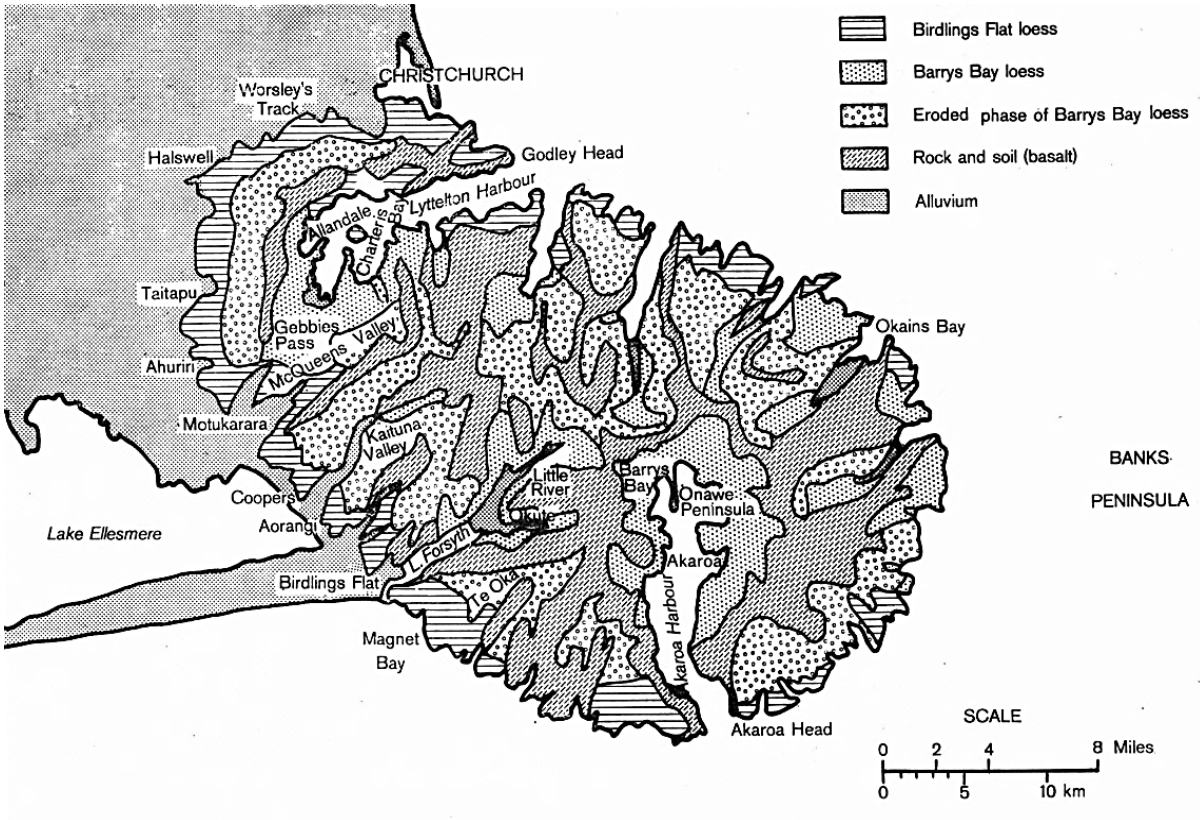

Figure 2.3 Loess deposits on Banks Peninsula (Griffiths 1973, p.659).

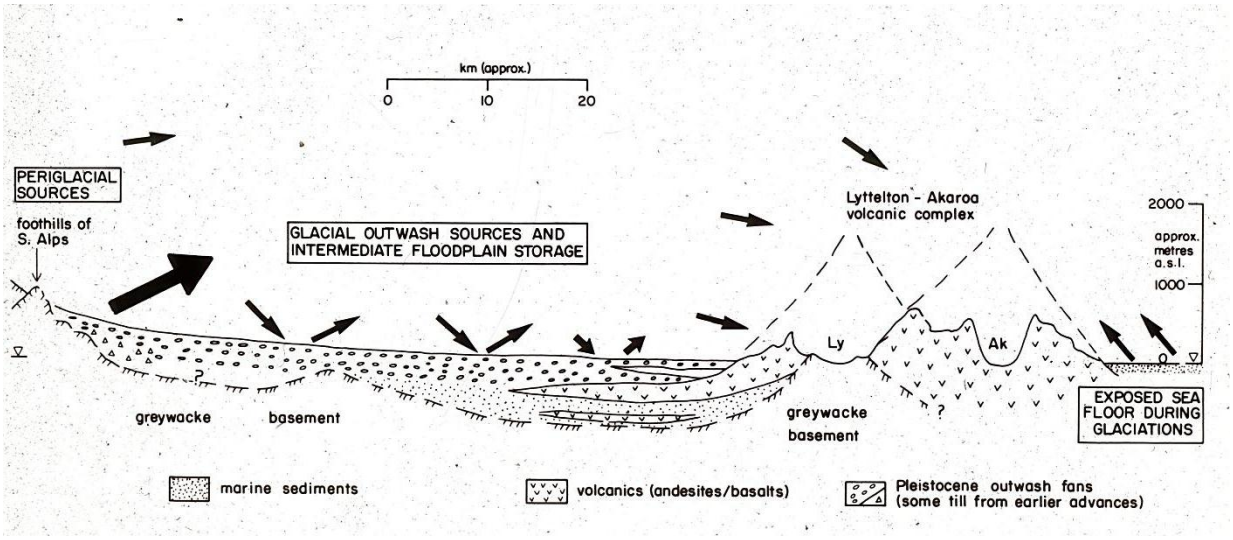

Figure 2.4 Suggested origin for Banks Peninsula Loess Deposits. After Bell and Trangmar (1987)

As seen in Figure 2.3, the Banks Peninsula loess deposits can be divided into two distinct facies; the Birdlings Flat loess, and the Barrys Bay loess. The loess of Christchurch's Port Hills is the Birdlings Flat variety, which is coarser than the Barrys Bay loess, is locally calcareous and is comprised of silt, fine sand and clay particles (Griffiths 1973). The Birdlings Flat loess is at its thickest at lower elevations on the north-facing slopes of the Port Hills, and loess-colluvium is found in valley floors (Griffiths 1973).

Hillslopes on the Port Hills can be divided into subsections based on elevation, whereby each subsection contains a different soil type (Figure 2.5) which form as a result of sediment deposition, and secondary transportation. The steep and hilly terrain of Banks Peninsula has meant that much of the *in situ* (primary airfall) loess mantle has been eroded and redeposited downslope in valley-floor locations as colluvium. Loess depths tend to be no greater than 15 m (Bell et al. 1986), however post-earthquake drilling has recorded depths of valley floor loess to 40 m. It is likely that freeze-and-thaw processes during the glacial environments of the Pleistocene induced much of this down-slope sediment transfer, although the exact volumes of loess redeposited through these processes can only be conjectured (Griffiths 1973). It is also thought that the north and west sides of the Port Hills may have been drier and subject to more rapid fluctuations in temperature, resulting in relatively reduced vegetation cover, and thus more of the loess would have been stripped away, exposing the volcanic rock underneath (Griffiths 1973). In general, the presence of loess-colluvium and the varying proportions of weathered volcanic fragments within the reworked loess reflects proximity to bedrock outcrops and slope morphology (Bell et al. 1986).

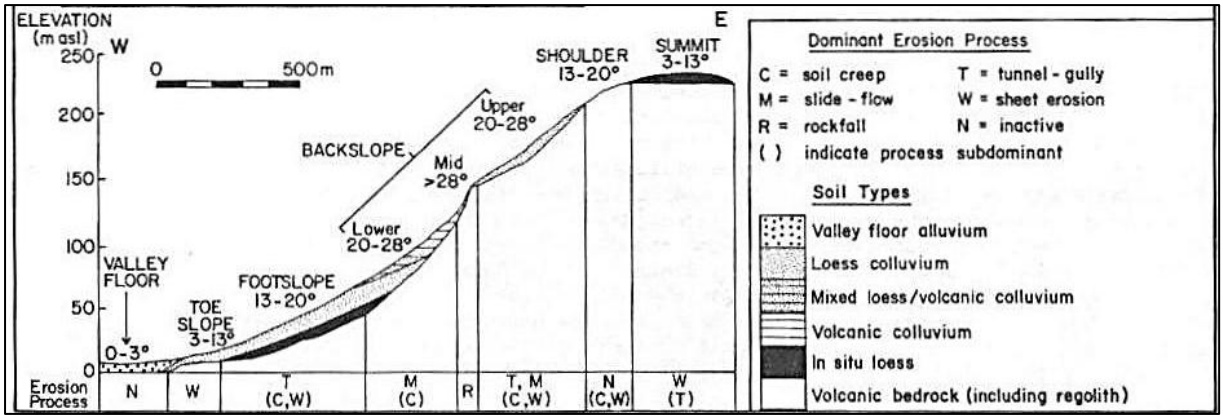

Figure 2.5 Schematic profile for Port Hills loess showing soil types against elevation. After Bell et al. 1986.

The expansion of the city of Chistchurch over the last century has led to large numbers of subdivisions being built on the Port Hills. Excavation for subdivision has often led to the development of many steep, erosion-prone sites (Bell 1981), as well as substantial erosion by tunnel-gully and overland processes.

2.3 General properties of Loess

Bell (2007) explains that loess' ability to retain its structure is dependent upon the clay-sized particles which form bonds between the larger silt-sized particles, which generally make up 50-90% of a loess deposit. This formation occurs as a result of the aeolian deposition of the loess, which gives it an initially loose structure. Bell further explains how, when loess comes in contact with water, it is these bonds which become soft, ultimately leading the structure of the soil to collapse under its own weight.

Because it can be difficult to obtain undisturbed samples of loess, Lutenegger (1987) investigated the shear strength of loess using the Borehole Shear Test (BST) to directly obtain the soil friction angle and cohesion. He found that the BST was a very efficient method to determine the Mohr-Coulomb failure envelope of friable loess. When dry, loess is both strong and incompressible and able to withstand a fairly large overburden pressure. However upon wetting, the highly porous nature of loess means that water will be drawn into the pores, and is able to break down the strong matrix structure (Ishihara 2009). In this way, the addition of water can lead to a reduction in bulk volume, and a loss of shear strength in a loess body, this is referred to as hydraulic collapsibility (Ishihara 2009). It is interesting to note also, that the permeability of loess tends to be significantly higher in the vertical direction than the horizontal, as a result of the vertically stable structure, whereby water will more easily flow along the sub-vertical fracture sets (Bell 2007).

The plasticity of loess tends to be low, with the plasticity index being generally between 5 and 10 (Goldwater 1990; Ishihara 2009), and it is well known that soils of low-plasticity are known to be more prone to liquefaction and flow-type failure (Ishihara & Koseki 1989), although only when saturated.

When considering the geotechnical properties of loess, it is important to consider the Mohr-Coulomb failure criterion and the effective stress theory for saturated soils. The Mohr-Coulomb equation (Equation 1) shows that the shear strength (τ) on any plane in a soil is related to the effective normal stress (σ'_n) and the soil parameters, effective cohesion (C') and effective angle of internal friction (ϕ').

$$\tau \leq C' + \sigma'_n \tan\phi' \qquad \mathbf{1}$$

The Mohr-Coulomb failure criterion is used to represent soils and rock subject to a shear stress, and is suitable to be applied to landslide situations with both shallow (10 – 13 m) and intermediate sliding planes of up to 30 m deep (Sciarra et al. 2011). The Mohr-Coulomb failure criterion may have limited applicability in loess soils due to their idiosyncratic nature, but for straight-forward analysis, the Mohr-Coulomb failure criterion may be used to modelling the shear strength of a loess body. In this way, it is possible to predict the likelihood of its sliding along a basal plane, or in the case of toppling failures, the likelihood of movement occurring between the multiple sub-vertical joint sets. Such analysis is of use in the realm of computerised modelling of a hillside, such as that conducted on the stability of rock masses by Sciarra et al. (2011) , whereby the use of input parameters of cohesion and internal friction, combined with information on the physical shape of the landscape, can help to predict the failure mechanism of an area under load.

2.4 Properties of Port Hills loess

On the Port Hills of Christchurch and other parts of Banks Peninsula there have been significant concerns surrounding stability issues within the loess mantle, particularly as Christchurch has grown and the demand for subdivision space on the Port Hills has increased. Throughout the latter half of the 20th century many authors have studied the geotechnical properties of Port Hills loess, including several students at the University of Canterbury who completed their MSc Engineering Geology theses on the Port Hills Loess. Table 2.1 provides a summary of their findings.

The properties of loess are inherently dependent upon local conditions, in particular the source rock material, the local climate at the time of deposition, and the manner in which

deposition occurs. This means that geotechnical properties of a loess sample from one area may be markedly different to those of another, for example within the Port Hills alone there are two distinct loess facies (Figure 2.3), each with individual properties (Griffiths 1973).

The loess facies of the Port Hills contain predominantly clayey silts, and vary from those of other regions of New Zealand, such as those in Blenheim as discussed by Laffan and Southerland (1987), as well as around the world, such as the landslide-prone loess of the China Plateau, discussed by Derbyshire (2001). As an example, loess from Hungary typically has higher Atterberg Limits than the Port Hills loess, in particular the liquid limit, which may be as much as 42 (Fodor & Kleb 1994); 11 % higher than the highest Port Hills loess reading. In general, however, loess deposits tend to be relatively similar, in that they have similar grain size distributions, mineral composition, and all display the granular skeleton bound by micro-aggregates (Bell 2007).

Table 2.1 Geotechnical properties of Banks Peninsula Loess. The pedogenic layering references are as follows: A: topsoil; B: lower surface layer; Bx/Cx/C: compact layer; C/P: parent layer. After Yetton (1986), Goldwater (1990) and Jowett(1995).

Parameter	Typical Range of Values	Reference
Porosity	30 – 40 %	Birrel and Packard (1953)
Void Ratio	0.4 – 0.7	Birrel and Packard (1953), Miller (1971)
Atterberg Limits	LL: 18 – 33 PL: 17 – 22 PI < 12	Crampton (1985), Yetton (1986), Alley (1966), Trangmar (1991)
Grain Size	Sand: ~10 % Silt: 65 – 80 % Clay: 11 – 25 %	Alley (1966), Crampton (1985), Yetton (1986)
Dry Density	B horizon average = 1.54 $t.m^{-3}$ Cx horizon average = 1.64 $t.m^{-3}$ (1.51 – 1.88 $t.m^{-3}$ range) C horizon average = 1.55 $t.m^{-3}$ (1.32 – 1.70 $t.m^{-3}$ range)	Evans (1977), Crampton (1985), Yetton (1986)
Linear Shrinkage	0 – 1 %	Alley (1966)
Permeability	1.5 x 10^{-7} $m.s^{-1}$ (undisturbed) ~1 x 10^{-7} $m.s^{-1}$ (in situ test) 2 x 10^{-8} $m.s^{-1}$ (remoulded)	Birrel and Packard (1953), Sanders (1986), Tehrani (1988)
Internal Angle of Friction	28° (peak, direct shear: drained)	Goldwater (1990)
Cohesion	0 – 20 kPa (peak, direct shear: drained)	Goldwater (1990)
Dispersion (Crumb class)	B horizon: 2 - 4 Cx horizon: 2 - 3 C horizon: 2 – 4	Yetton (1986)
Resistivity	Varying with depth from around 90 ohm-metres at depth in P layer.	Yetton (1986)
Conductivity	From 1.0 $mho.cm^{-1}x10^{-4}$ to 14 $mho.cm^{-1}x10^{-4}$ with depth.	Birrell and Packard (1953), Yetton (1986)

2.5 Slope failures in Loess

Worldwide, loess landscapes are subject to a variety of slope processes. On the Port Hills of Christchurch, loess failures include mass movement and tunnel-gully erosion, which are controlled by a combination of manifest soil layering and the properties of the loess soil itself such as clay mineral dispersion and changes in strength as a result of moisture content (Bell et al. 1986). The following section discusses failure mechanisms observed world-wide in loess terrains, detailing case studies in natural slopes as well as failures of a similar style which have taken place in earth dam structures.

2.5.1 Failure mechanisms observed in loess terrains

In their 1986 paper, Bell et al. recognised distinct forms of erosion on Banks Peninsula which are a direct result of the presence of the loess mantle. These mechanisms of erosion have the potential to lead to slope failure, the processes being: tunnel-gullying, slope movement, soil creep, sheet and rill erosion, and wind erosion.

When loess banks are in under-saturated, nearly-vertical orientations they are relatively stable, however instantaneous disaggregation and hydrocompaction can occur if they are locally saturated (Derbyshire 2001). Sub-vertical jointing can form loess bodies, an idiosyncrasy of this soil which is not observed in other gravels or sands. These are thought to form as a result of the presence of electrical charges on the clay particles which bind the sediment together (Marshak 2001).

Lutenager and Hallberg (1988) discuss the relationship of the stability of loess with the soil's Attaberg Limits, water content and void ratio, based on studies of loess from the upper midwest, U.S.A. They cite experience in the U.S.A. as showing that when the liquidity index (a value derived from the field moisture content, and the liquid and plastic limits of the loess) of loess approaches or exceeds a value of 1 then collapse or subsidence of the loess may be imminent, particularly if the soil undergoes an increase in load. The loess property of *collapsibility* is related to bulk density, pore size and particle size distribution (Dijkstra et al. 1994). Sometimes areas of collapsible, nearly liquid, loess may occur as isolated zones within the main body, and other times the entire loess column may be collapsible. Lutenager and Hallberg explain that these collapsible loess soils tend to be confined to low-density, low-clay-content loess, which has a readily-available source of groundwater and thus a higher water content.

Water will infiltrate the sub-vertical joints throughout the loess body, and can ultimately create complex drainage systems which run roughly parallel to the ground surface (Figure 2.6),

and result in values of hydraulic conductivity which are much higher than those of undisturbed loess. These processes can result in slope failure depending on the shear strength of the properties of the soil(Bell et al. 1986; Derbyshire 2001). The strength of a loess body is dependent to a great extent on its density, which then directly influences the shear strength properties of the soil. When the loess has a density below 1300 kg.m^{-3} large settlements occur in the loess which has a low shearing resistance. However, if the density is higher than 1450 kg.m^{-3} then settlements are small and the shearing resistance is higher(Bell 2007). The latter applies to Port Hills loess, which has a density of ~1650-1700 kg.m^{-3} (Goldwater 1990).

The types of landslides which may occur in loess vary depending on the conditions of the loess mass, for example it may fail as a single mass of material that displaces along interconnected joint systems. Failures may also occur as extensional or translational slides, or as lateral spreads (Derbyshire 2001). Moisture content of the loess plays a major role in determining how, and by what mechanism, a soil body will fail. On Banks Peninsula, rapid slope movements can occur following prolonged wetting of slope, while gradual infiltration of groundwater through subsurface erosion can cause failure after a much longer time frame (Bell et al. 1986).

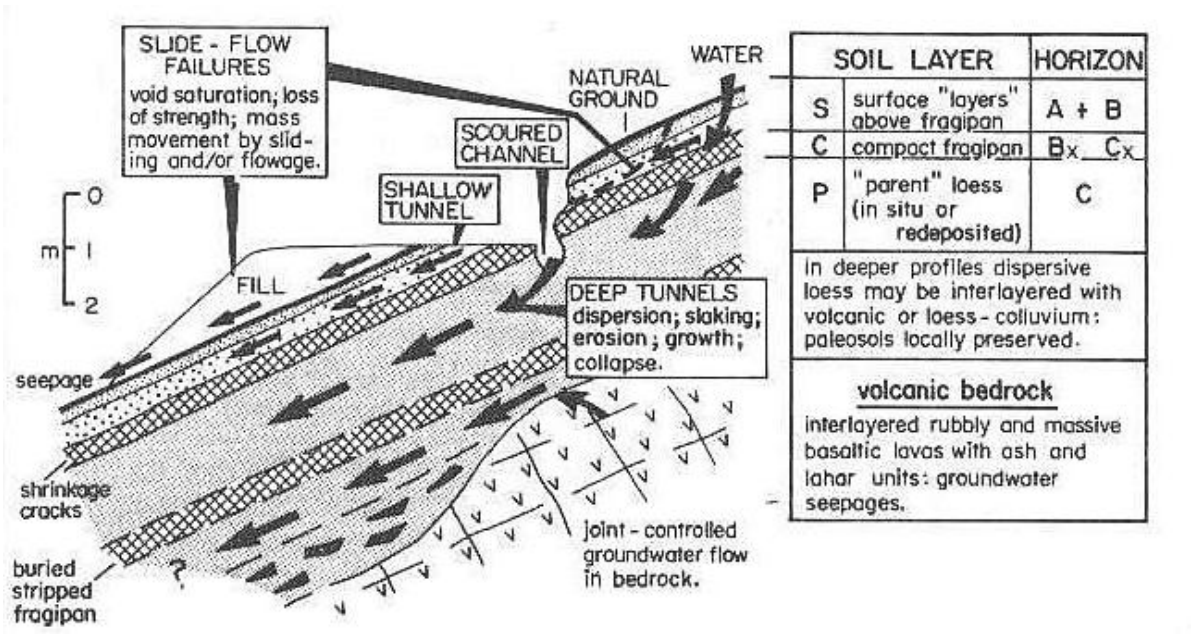

Figure 2.6 Schematic model of water routing in loess leading to slope instability. After Bell et al. 1986.

Tunnel-gully erosion in loess occurs in many locations in New Zealand, and was dramatically accelerated by burning and over-grazing of native grassland by early European settlers in the

middle of the 19th century. The appearance of tunnel gullying on Banks Peninsula was first described by Cumberland (1944), who defined it as:

> *"the culturally induced removal by running water of parts of the soil or subsoil at varying depths beneath the surface without, at first, disturbing the surface sod or soil."*

Tunnel-gullying begins with the formation of subsurface water "pipe-like" tunnels above or below the fragipan, whose subsequent enlargement often leads to surface collapse, which is then followed by open gullying, as shown in Figure 2.7 (Bell et al. 1986; Laffan & Sutherland 1987).

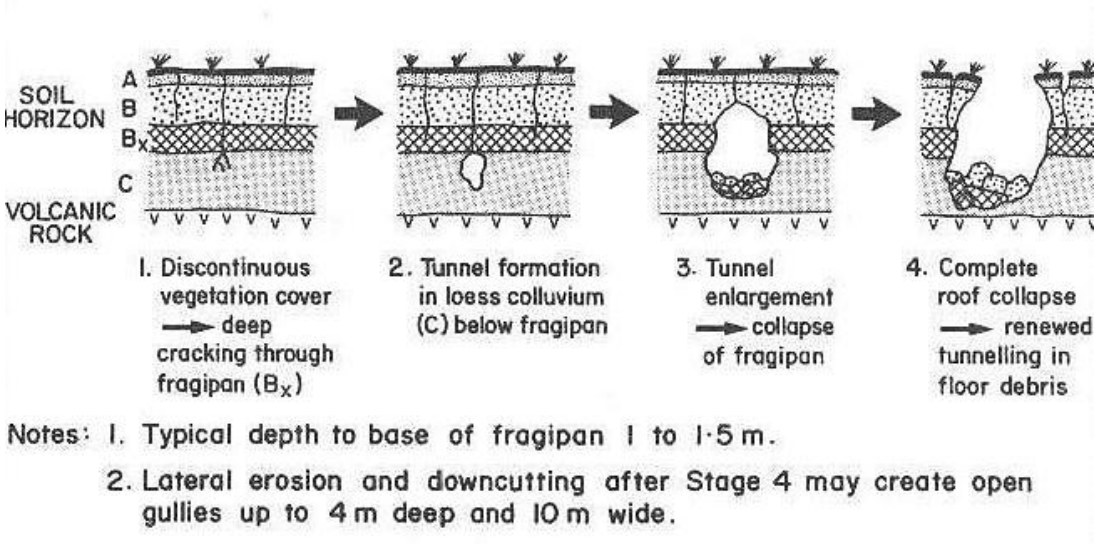

Figure 2.7 Deep tunnel-gully development model. After Bell et al. 1986.

2.5.2 Fissuring behaviour in Loess

Fissuring has been observed to occur in loess soils world-wide, and it can happen for a number of reasons. Most common is incipient landsliding, where fissures form along the head scarp area of a landslide. Also common triggers tare earthquakes, prolonged rainfall or dessication due to drought. Fissures are elongate, up to several hundred metres long in some cases, and of varying widths from a few centimetres to a metre or more.

The physical processes behind the formation of fissures in loess depend on the composition of the loess itself, often most importantly its clay content, as well as local environmental factors. If we consider an inclined mass, and assuming a linear Mohr-Coulomb failure envelope, tension will be at a maximum on the ground surface, and decreases linearly to zero with depth (Lohnes & Handy 1968). This can be illustrated by imagining a vertical cut of height *Hc* in a block of gelatine: the upper gelatine will edge over into the cut, allowing tension cracks to form parallel

to the face of the cut (Lohnes & Handy 1968). These tension cracks essentially leave a parallelogram-shaped slab of soil between them, which may have sufficient weight, *W*, to provide normal, *N*, and shear, *Sa*, forces to exceed the shear strength, *Sr*, of the underlying soil, and induce a slab failure (Figure 2.8).

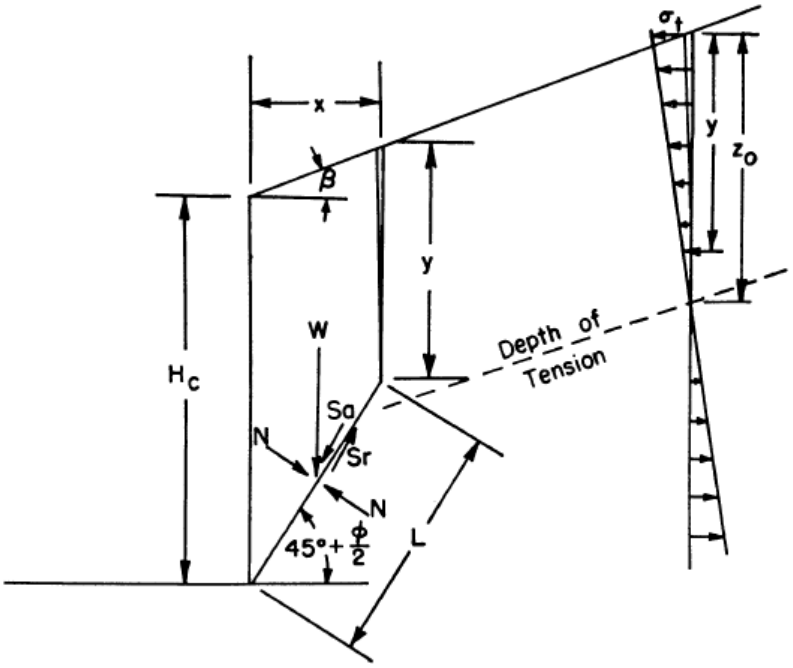

Figure 2.8 Rankine earth pressure theory indicates tension leading to vertical cracking in upper soil adjacent to a cut, and if the cut is high enough, slab failure. After Lohnes (1968).

In his 2009 paper, Ishihara made calculations to estimate the greatest potential depth of fissures in Chinese loess, based on the relationship between the pressure of the overburden of soil acting vertically and the uniaxial compressive strength of the soil. If the vertical stress at depth *Z* given by ρZ exceeds the compressional strength, q_u, then the soil will fail, producing deformation in the lateral direction, and thereby closing the fissure (Figure 2.9).

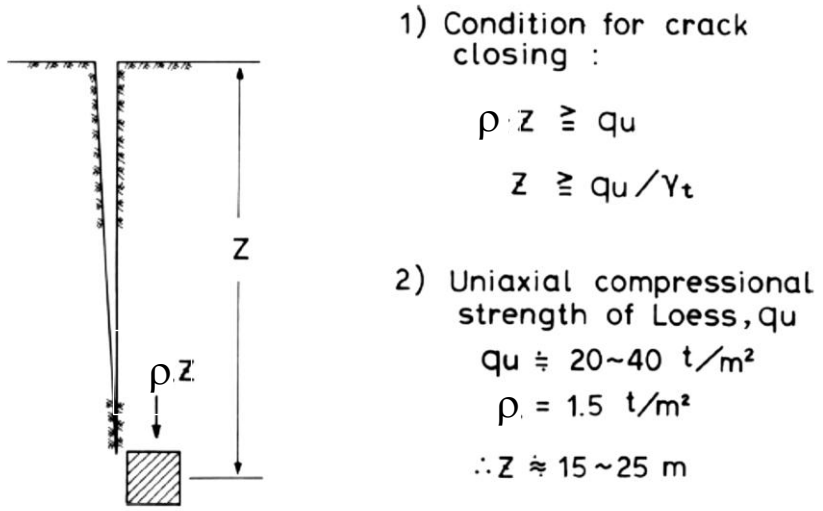

Figure 2.9 Conditions of fissure development after Ishihara 2009. New Zealand loess has density values (ρ) of 1.65 – 1.7 t/m³. Z is depth at which a fissure will be closed.

The depth at which a fissure will be closed is given by Equation 2, where q_u is the uniaxial compressive strength of the soil (t/m²), and γ_t is the unit weight of the soil (t/m³).

$$Z \geq \frac{q_u}{\rho} \qquad 2$$

Sun et al. (2009), whose work showed that an increase in water content reduced the tensile strength of loess, gave an alternative reason for the fissures to be closed at depth. They considered that the lower dry density of the loess towards the surface meant that it had a greater potential to absorb rainfall, thus increasing in water content, and higher likelihood to develop slope fissuring due to loss of tensile strength.

2.6 Loess failure case studies in natural slopes

2.6.1 The Loess Plateau of China

Loess accumulations in China mantle about 613 000 km² and can be up to 500 m thick in the area known as the Loess Plateau of China (Figure 2.10), located in the middle reaches of the Hwang He (Yellow River). Large zones of ground fissuring are apparent in regions of the Loess Plateau, and landslides have been recorded throughout the 2000-year Chinese written history, including a large earthquake-triggered landlside in the Kansu Province, in the 1920 Haiyuan

Earthquake which was combined with techtonically-triggered fissuring in the up to 200 m-deep loess plateau (Zhang & Lanmin 1995). The two triggering mechanisms for fissuring and land failure on the Loess Plateau of China are over-saturation of the soil by monsoonal summer rains (with a minimal rainfall intensity required to be about 1.6-2.4 mm h^{-1}), as well as ground acceleration due to earthquakes (Derbyshire 2001).

Loess from the Loess Plateau of China has particle sizes which lie mainly in the coarse to medium silt grades (0.01-0.06 mm), with up to 65% consisting of quartz particles, and a clay percentage of up to 30% (Derbyshire 2001). Being relatively unconsolidated aeolian deposits, the Chinese loess has a very high porosity and a low bulk density, which, when combined with the low average moisture contents, leads to high pore water tension within the loess. This encourages clay particles to cluster between the coarser grains and ultimately strengthens the undisturbed dry loess. Some secondary calcium carbonate between the quartz grains also adds local strength through cementation (Derbyshire 2001).

Fissure zones in the Loess Plateau of China have been traced for distances up to 8 km, with individual fissures reaching 1 km in length. The reason for the formation of these fissures is debated, with Sun et al. (2009) indicating that the fissures may result from tensile stress generated by deep deformations in the earth's crust, however Xu (2010) disagrees, believing rather that the fissures form as a result of the loess' sensitivity to water and that when rainfall coincides with fault activities providing shear or tensile stress, the loess fails in collapse, forming fissures. The area is extremely prone to subsidence, which has been noted to closely follow a pattern of local depression of the water table (Sun et al. 2009).

Derbyshire (2001) recognised six types of loess landslides in China, based on composition of the slide mass and on the location of the failure plane. Earthquakes historically trigger large rotational mass movements, with large semi-circular failure planes. Fissuring is produced along with landsliding in the Loess Plateau of China, both as a precursor to sliding, and in the nearby land. The six landslide types recognised by Derbyshire are:

- *Bedrock contact landslides* - the sliding of a mass of loess along an impermeable bedrock surface which forces groundwater to accumulate and form a zone of saturation in the loess. This landslide type is very common throughout the Chinese Loess Plateau, and is often exacerbated by the presence of smectitic clay in the weathered bedrock.
- *Palaeosol contact landslides* - the sliding of a mass of loess along a palaeosol surface within the loess. The palaeosols are clay-enriched and thus less permeable, creating a saturated layer in the loess.

- *Mixed landslides* - these are slow-moving slides comprised of a combination of both loess and bedrock, which slides along planes or joints in the bedrock. In the Chinese Loess Plateau, the slip surface is within a mudstone, and dips at 10°-25° in the same direction as the slope.
- *Slides within loess* - large landslides composed entirely of loess which fail only where earthquake shock or undercutting occurs. These are relatively uncommon on the Chinese Loess Plateau due to the low moisture content of the area, which gives the loess higher shear strength.
- *Terrace landslide* - where fluvial or colluvial gravels in terraces act as an aquifer between bedrock and loess. Failure occurs when cracks develop throughout the loess after the strength of the bedrock is lowered.
- *Tan-ta* - small-scale planar slip displacements, up to 10 m in diameter and at a depth of one to several metres, which occur as a result of snowmelt, rainwater, slope undercutting or earthquakes.

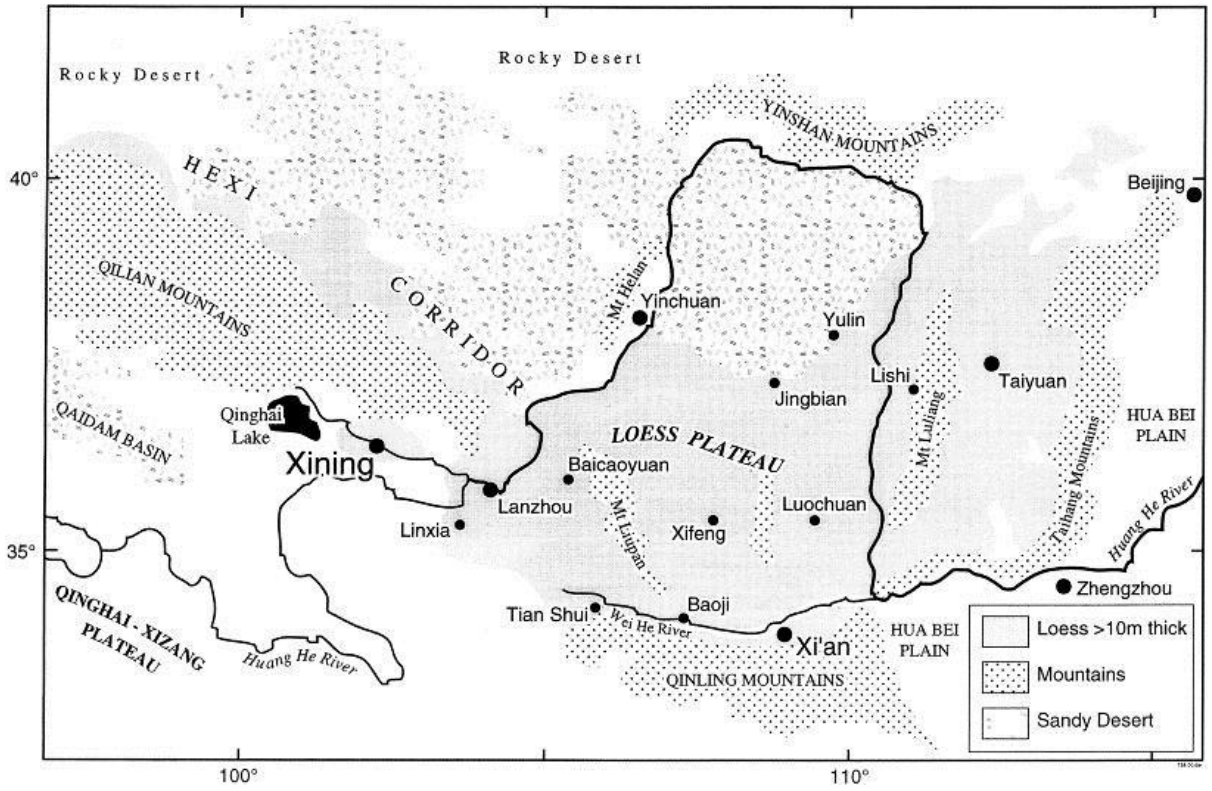

Figure 2.10 The Loess Plateau of north China and adjacent regions. After Derbyshire 2001

Based on Derbyshire's (2001) descriptions, the landslides known as *tan-ta* appear to be most similar to the movement observed in the Port Hills of Christchurch, however it is important to

remember that Chinese loess has distinctly different properties to Port Hills loess, for example the Chinese loess is in a more loose state structurally, as it has not undergone the same pedogenic processes which have resulted in the high dry strength of the Christchurch loess. The Chinese loess is superficially similar to that of the Port Hills, in that it indicates that loess has the propensity to split in sub-vertical fissures.

In their 2009 paper, Sun et al. attempted to establish the relationship between the tensile characteristics of loess and the developmental mechanism of ground fissures in north-western China through the use of a uniaxial soil tensile apparatus. The fissures studied (Figure 2.11) were larger than those which formed in Christchurch, mapping of the fissures showed they run sub-parallel to ground contours, in a similar way to those seen in Christchurch. Sun et al. used a uniaxial soil tensile apparatus to study the influence of water on the tensile characteristics of undisturbed loess, and found the material in which the failures formed showed an exponential reduction in tensile strength (σ_t) with an increase of water content (w), as shown by the relationship in Equation 3.

$$\sigma_t = 144.937e^{-0.1252w} \quad \textbf{3}$$

Sun et al.'s experiments showed that the tensile strength of the loess was generally very low, generally less than 25 kPa. They concluded that when the water content is high, and the dry density is low, the loess will be prone to fissuring under the action of tensile stress.

In his paper commenting on the work by Sun et al., Xu (2010) questioned their results by noting that the natural water content of loess in the Chinese Loess Plateau is 10.7-23.4%, with an average of 18.0%, which is lower than the range of water content used in the study by Sun et al.. Xu notes that tension cracks in loess may form due to either shear or tensile stresses resulting from deep deformations in the earth's crust, when the strength of the loess can no longer resist load applied by fault activities and/or rainfall conditions.

Figure 2.11 Ground fissure development in farmland in north-western China. After Sun et al. 2009

2.6.2 Infilled Fissures in Banks Peninsula Loess

In 1983 a small study was undertaken by S.A. Harris into the occurrence of infilled fissures at the interface of two loess deposits on Banks Peninsula, New Zealand. The fissures he observed were narrow, and up to 165 cm deep, and were infilled with loess from the overlying layer (Figure 2.12). The fissures are polygonal in plan view (implying a desiccation-induced origin), and occur predominantly in the surface on the Stony Bay loess deposits, being infilled by Te Oka loess, with occasional vertically-oriented elongate stones in the infilling material. The fissures are most commonly between 5 and 15 cm in width, although may be up to 60 cm.

Based on Harris' study, and the author's own observations of Port Hills fissures, three causes for the formation of these palaeo-fissures are thought possible: frost wedging of the loess during periglacial climates, shrink-swell due to wetting and drying cycles, and, finally that these palaeo-fissures were earthquake-derived in a similar manner to those formed in the Christchurch Earthquake.

Harris concluded that the most likely cause for their formation was seasonal frost fissuring or ice wedges, however Bell (2007) states that loess does not appear to be frost susceptible. For the formation of such features an almost continuous permafrost would have been required, with average temperatures at least 16 to 18°C cooler than today, however such a drop is far greater

than any which has been reported from climate reconstructions which have shown a 5 to 8°C drop at most (Dr. S.Winkler, University of Canterbury, pers. comm. 2012).

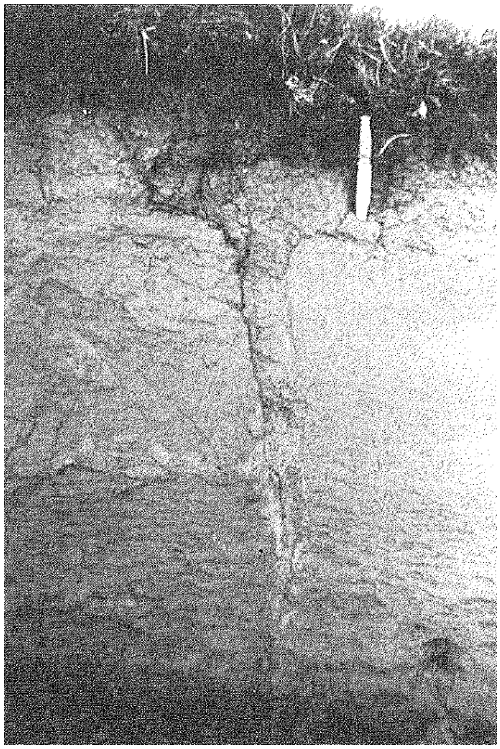

Figure 2.12 A typical fissure developed in Stony Bay loess, Banks Peninsula. After Harris 1983.

Also hypothesised by Harris (1983) was that the fissures were as the result of shrink-swell desiccation of the loess due to seasonal temperature changes. Harris notes that it is strange that the infilling loess does not disturb the host loess, implying that the host soil did not expand to its original volume when temperatures became warmer after each glacial contraction phase.

The fissures which formed during the Christchurch Earthquake have a distinctly similar appearance to the palaeo-fissures observed by Harris, which signifies the potential for ancient earthquakes to have provided the trigger for the formation of these fissures. Further research into these palaeo-fissures, in particular locating and mapping their orientation, could provide further evidence for the hypothesis that they are earthquake-derived.

2.7 Failure case studies in man-made structures

The failure of earth-fill dams is a useful corrolary to the failure of loess in natural landscapes worldwide. Internal erosion or subsurface erosion may take place within an earth-fill dam, and studies have been done on multiple failure sites where such an occurrence has lead to major failure of a dam.

2.7.1 The Teton Dam

The Teton Dam in south-eastern Idaho, USA, failed on June 5, 1976 upon its first filling (Figure 2.13), resulting in serious loss of life and major economic costs (Smalley 1992; Muhunthan & Pillai 2008). It was a 93 m high earth-fill dam. A minor leak, which was evident as a dampness on the downstream slope, developed when the reservoir reached an elevation of 1615 m. This expanded overnight and led to the complete breach about 20 hours later. A combination of failure mechanisms have been suggested, particularly the presence of internal erosion/piping within the loess core, and defects in the abutment rock (Smalley 1992; Muhunthan & Pillai 2008).

Figure 2.13 Looking downstream through the break in the Teton Dam after the crest of the water had passed. After Smalley 1992.

The Teton Dam was an embankment dam with an impermeable core of recompacted, not clayey, loess, built in a steep-walled canyon in the Teton River (Figure 2.14). The canyon walls were of volcanic origin, being primarily intensely layered and jointed rhyolite with minor inclusions of basalt, breccia and welded ash-flow tuff. The joints in the rhyolite are closely spaced and open, with no infilling apparent and some fractures with widths of up to 915 mm were found (Smalley 1992). The impervious core in the centre of the dam was constructed using locally-sourced loess, a uniform clayey silt of aeolian origin that had a low plasticity index (PI) of around 4, a low liquidity index (LI), and unified soil classification system (USCS) of CL-ML (Muhunthan & Pillai 2008). This loess core was carefully placed in 15 cm layers; each compacted by 12 passes with a heavy sheepsfoot roller. Even with this attention to detail, the silt-rich loess was not adequately compacted due to its low clay-mineral content (Smalley 1992), and due to the fact that compaction destroys the natural bonds in loess soils (Bell 2012 pers. comm.). The foundation seepage control was designed to be effected by the construction of

a deep grout curtain as well as narrow, excavated trenches through the rock to depths of 21 m, backfilled with compacted loess (Smalley 1992).

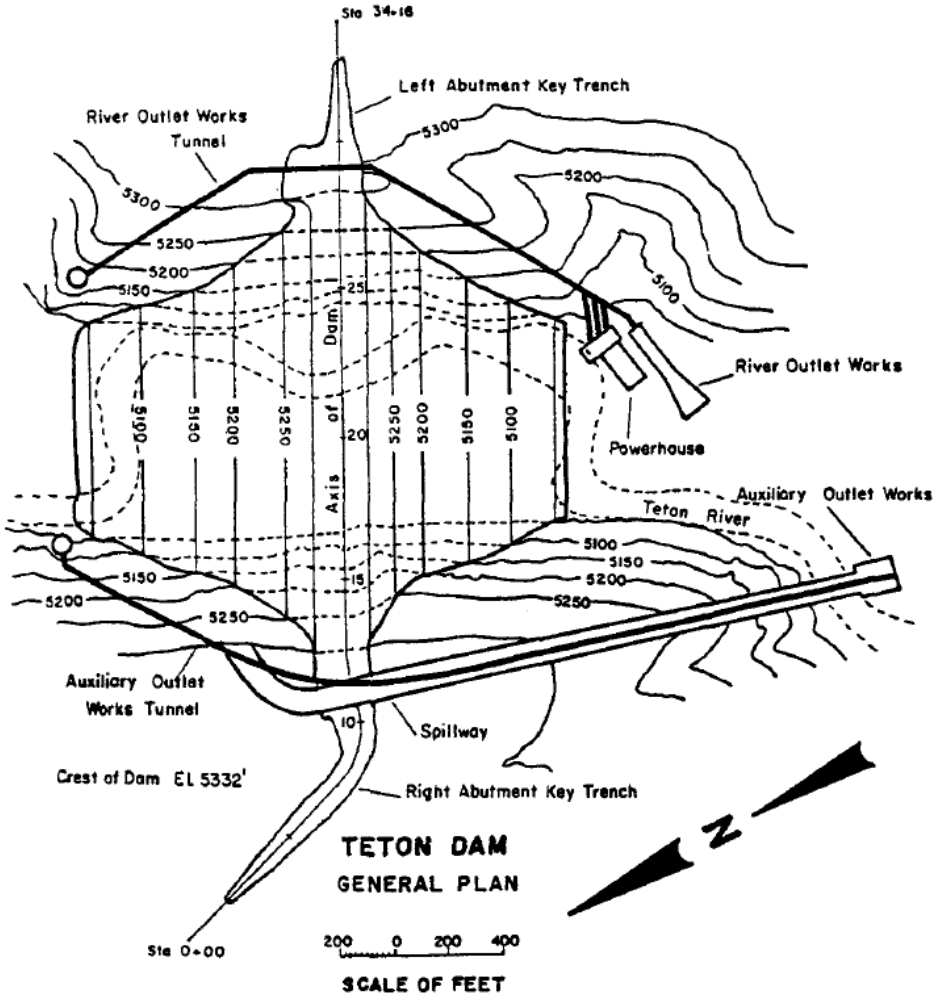

Figure 2.14 General plan of the Teton Dam, based on the original design drawings of the US Bureau of Reclamation, with dimensions in feet (1 ft = 0.305 m). The failure initially occurred in the right abutment, where the dam meets the canyon wall. After Smalley 1992

The core of the dam was filled with approximately 4 million cubic metres of local loess. Unfortunately the loess was unsuitable for use in the dam core , in particular due to its low plasticity index of 4 (Smalley 1992). Under high shear stresses and low confining stresses, highly compacted soils of low plasticity tend to crack in an environment of low liquidity index (Muhunthan & Pillai 2008).Mechanical properties of soils with such a low plasticity value can be affected hugely by even a tiny change in water content, and a compacted loess core, while initially impermeable is brittle and dilatant, thus allowing the passage of water (Smalley 1992).

After two main engineering investigations of the failure, it was concluded that the failure began in the right cut-off trench, and was triggered by water coming through the rhyolite fractures, which eroded the compacted loess. With no seepage-control filter zone between the compacted loess core and its contact with the open joints and fissures in the excavated rhyolite face downstream of the grout curtain, water was free to move into the dam core (Smalley 1992).

2.8 Relevance of case studies to Port Hills fissuring

The case studies discussed in this chapter have varied relevance to the causes of the Port Hills fissuring which occurred during the Christchurch Earthquake. While not all examples provided were earthquake-derived fissuring, and remembering that loess deposits have by nature widely varying characteristics, these examples are still able to provide relevant data on the fissure-forming abilities of loess and what may trigger these fissures, as well as on loess stabilisation methods which have been undertaken worldwide.

Additionally, there has been continued pressure on the leaders of Christchurch to provide solutions to residents of areas of the Port Hills affected by geotechnical hazards following the earthquake. Stabilisation methods which have been utilised successfully elsewhere may be adopted for use in the Port Hills, following site-specific studies of the loess to ensure their suitability.

Lutenager and Hallberg's (1988) explanation that collapsible loess soils tend to be confined to low-density, low-clay-content loess, which has a readily-available source of groundwater has marked similarities to a description of Port Hills loess, thus indicating that their analysis of collapsible loess soils may be relevant to the Christchurch situation, with necessary adaptations due to varying constituents. Mechanical properties of soils with a low plasticity value can be affected hugely by even a tiny change in water content, as shown in the Teton Dam example, where a compacted loess core, while initially impermeable is brittle and dilatant, thus allowing the passage of water (Smalley 1992). These comments are highly important as they show the potential impact that the passage of groundwater could have on Port Hills loess.

The fact that loess has a tendency to form sub-vertical fissures has been observed in locations other than the Port Hills, and this tendency has been attributed by the Chinese studies to be a tensile failure. Lohnes et al. (1968) made the comment that a cut face in loess will topple inwards along the internal sub-vertical fractures within the loess. This is a useful corollary to the Port Hills case, where instead of a cut batter; it is possible that lateral support was removed as a result of the shaking intensity of the earthquake.

2.9 Loess stabilisation methods

Numerous methods of loess stabilisation have been investigated and trialed world-wide. Loess requires individual treatment depending on its constituent particles, and care must be taken when undertaking excavation work. Loess has been shown to be relatively stable when in a sub-vertical orientation, however when angled it will rapidly form rills upon exposure to rain.

In the case of the Port Hills of Christchurch, the loess soils are most stable in their natural state, reliant on strong interstitial bonds (described by many authors, such as Marshak (2001)), and unaltered by anthropogenic changes. With the growth of Christchurch city, however, methods are required to counteract the dispersive nature of the loess as well as the formation of the tunnel-gullies. Apart from vertical orientation of batter slopes, and water infiltration prevention, one particularly successful method utilised on the Port Hills is that of chemical stabilisation whereby the soils are rendered non-dispersive by the addition of certain chemicals (Bell et al. 1986). The chemicals most often added to the soil are hydrated lime ($Ca(OH)_2$), quicklime (CaO), or Portland cement and orthophosphoric acid (H_3PO_4). These are applied to the soil either by a process whereby the soil is excavated and mixed with the stabiliser and then recompacted in layers at optimum moisure content, or by utilising a slurry or grout which is added at depth (Bell et al. 1986). Of the aforementioned chemicals, hydrated lime usually the preferred option as it does not undergo volume expansion on hydration (as quicklime does), and it is the safer of the chemicals to handle and store (Glassey 1986).

In his 1986 thesis, Glassey showed that the addition of lime to a soil in small percentages (1% - 12%) increases the strength of the soil. Glassey found that by adding lime to loess soil the material becomes erosion resistant and non-dispersive. It also displays a reduction in slaking and swelling strain. Optimum moisture content was shown to have increased, with the maximum dry density of the soil decreasing. Glassey also found that the plasticity of the soil was increased due to an increase in overall grain size.

The use of a slurry to fill larger cavities has been shown by Bell et al. (1986) and Yetton (1986) to be efficient in their stabilisation. The slurry is made up of an orthophosphoric acid-loess-fine sand, sand-lime, or sandy gravel-lime-cement mixture, which becomes an erosion-resistant body when cured (Bell et al. 1986). Use of this method can, however, mean that new cavities may form outside the stabilised area if water seepage control is not implemented (Bell et al. 1986).

Surface and subsurface water flows can have a huge impact on loess stability. Water infiltration has been shown by many authors to have the ability to cause quasi-instantaneous

disaggregation of a loess body. It is therefore of great importance that drainage control is implemented when loess stabilisation is required. Methods which may be utilised include the use of lime-stabilised cut-off channels which can intercept active shallow tunnels, or the construction of deeper interception drains which use a gravel filter to drain groundwater flow on a longer-term basis (Bell et al. 1986; Yetton 1986).

Laffan and Sutherland's (1987) methods of treating tunnel-gully erosion are as follows:

- Natural vegetation: removal of grazing stock to allow recovery of remaining vegetation.
- Plantation forestry and closely spaced planting of pine trees.
- Pasture improvement and grazing management.
- Contour works and gully infilling: bulldozers to infill severe tunnel gullies, bench terraces (unsuccessful) to control runoff
- Angle-bulldozing and re-vegetation with permanent pasture: a "high-powered bulldozer is used to excavate the eroded hillside at an angle of 30-45 degrees to the horizontal. The excavations are made to a depth at least equal to the deepest gullies so that all traces of the tunnel-gullies and original drainage pattern are erased."
- Chemical ameliorants: to promote flocculation and aggregate stability in highly dispersible soils, for example, the application of calcium salts like gypsum or hydrated lime which can lower the exchangeable sodium levels or increase the cation concentration of the soil solution.

On the Loess Plateau of China, various remedial methods have been attempted in effort to prevent further failure of loessial soils but with minimal success. Consolidation, tamping, structural reinforcement, and leakage detection are methods which have proved useful for remediation in some areas in China although they are rarely successful in the younger loess of the Loess Plateau which has been found to be prone to collapse upon wetting, even without an applied load. Piling into subjacent non-collapsible layers or bedrock is an effective but rarely used remedial measure due to its expense (Derbyshire 2001).

Loess stabilisation methods are many and varied. World-wide, methods of loess stabilisation have been developed with the specific requirements of the site being taken into account. Stabilisation methods range from engineering solutions such as the construction of complex drainage routes and chemical stabilisation, to preventative measures such as vertical batter angles and the incorporation of stabilising vegetation. Attempts to control the dispersive nature of loess by shear force without taking into account its unique properties have been found to be

unsuccessful, for example bulldozing poorly designed bench terraces into loess without adequate drainage and run-off solutions will lead to water infiltration, and thus has the potential to cause failure.

2.10 Synthesis

- Loess is a pale yellow-brown, silt-sized deposit, blankets of which are widespread throughout the world. It was predominantly formed from aeolean transportation and deposition of glacially formed rock flour during the Pleistocene glaciations. Loess has many idiosyncratic properties such as its ability to be stable in steep, sub-vertical escarpments, as well as having vertical jointing and cleavage, and a peak shear strength when dry.
- The loess of the Port Hills of Christchurch is up to 20 m thick, and mantles many of the mid-slopes of the hills. Loess-colluvium, a re-worked combination of loess and volcanic bedrock is found in the valley floors and has been found to be 40 m thick in places.
- Failure in loess can take several forms, but predominantly originates with the infiltration of water, the presence of which leads to the instantaneous disaggregation and hydrocompaction of the loess structure. Failure such as tunnel-gully erosion, slope movement, soil creep, or rilling can then occur.
- Loess failure case studies include fissuring on the Loess Plateau of China, a flow slide in the Republic of Tajikistan, and infilled, frost-induced cracking in the loess of Banks Peninsula. Earth-fill dams also offer a useful corollary to the natural failure of loess, and the Teton Dam, Idaho, USA is an example where water infiltrated the loess core of the dam and a colossal failure ensued.
- Loess is both strong and incompressible when dry but this structure immediately breaks down upon the infiltration of water as the highly porous nature of loess means that water will easily infiltrate into the pores, and is able to break down the strong matrix structure, resulting in a reduction of bulk volume and a loss of shear strength. Loess tends to have cohesion of ~10 kPa, making it more prone to liquefaction and flow-type failure. The Mohr-Coulomb failure criterion may be used when modelling the shear strength of a loess body, and thus predicting the likelihood of its sliding.
- Many loess stabilisation methods are in use world-wide. The most appropriate method for a particular site depends on the individual characteristics of the site itself. Methods popular on the Port Hills include chemical stabilisation and grout infilling of fissures, as well as suitably designed drainage control, vegetation and sub-vertical batter slopes in excavations.

3 2010 and 2011 Christchurch Earthquakes

3.1 Introduction to the Christchurch Earthquakes

The first of the series of large earthquakes to take place near Christchurch, New Zealand occurred at 4.35 am (NZ Standard Time) on 4 September 2010. This was an M_W 7.1 earthquake, which became known as the Darfield Earthquake. It occurred along a previously unknown fault; the Greendale Fault (Figure 1.5, Figure 3.2), which ruptured in dextral strike-slip fashion, resulting in intense shaking that was felt throughout the Canterbury region. This was followed by a series of aftershocks, including a large M 5.3 earthquake on Boxing Day, 2010, each of which resulted in further cases of liquefaction and lateral spreading along the banks of the Heathcote River, with semi-continual fissuring in the sandy silt deposits alongside the river for most of its length.

The Christchurch Earthquake, the largest of the Darfield Earthquake aftershock sequence to date at M_W 6.2, took place at 12.51 pm (NZ Standard Time) on 22 February 2011 (Figure 3.2) on a previously unknown fault beneath the Port Hills of Christchurch. The fault rupture plane, while it did not reach the ground surface, has been estimated to be 14 kilometres long and seven kilometres wide (down-dip), extending from Cashmere, through the Avon-Heathcote estuary, and offshore a few kilometres. The hypocentral location of the earthquake was shallow, and beneath the Heathcote Valley in the Port Hills (Kaiser et al. 2012). The fault was a reverse-oblique mechanism, which resulted in part of the Port Hills and southern Christchurch being raised by up to half a metre relative to the rest of the city. The ground acceleration recorded during the February earthquake was greater than any experienced in New Zealand, and among the highest recorded worldwide. Ground accelerations were recorded at strong motion recorder sites (Figure 3.1), and in or immediately adjacent to the Port Hills, and they ranged from 0.3g to 1.4g (horizontal) and 0.4g to 2.2g (vertical) (Bradley & Cubrinovski 2011; Kaiser et al. 2012).

The strongest of the several large aftershocks following the February earthquake was a M_W 6.0 event on the 13th June 2011, henseforth referred to as the June Earthquake, which occurred on a strike slip fault with its epicentre near the suburb of Sumner (Kaiser et al. 2012). This earthquake also produced extremely high ground accelerations (c. 2g) at the southeastern edge of the city (Kaiser et al. 2012).

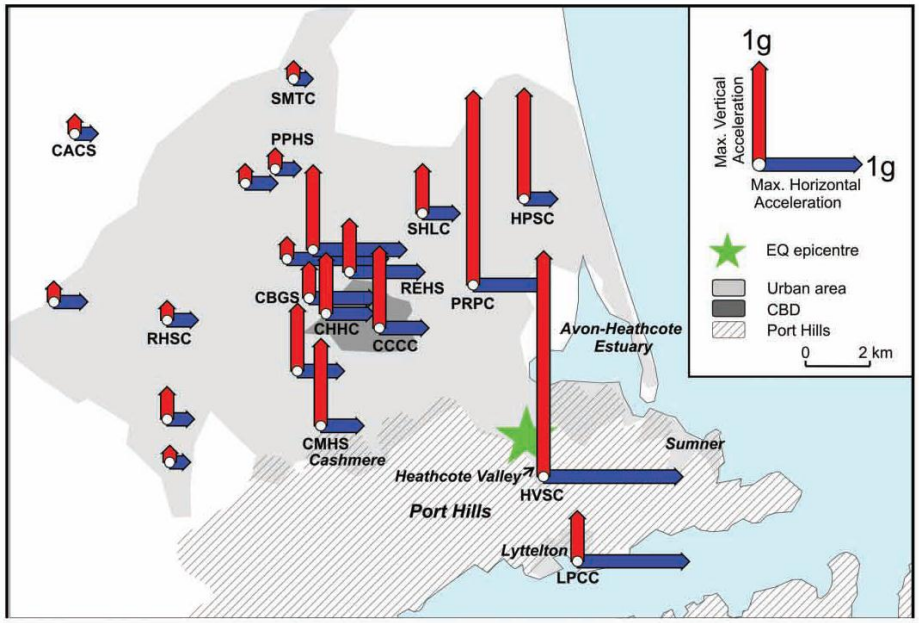

Figure 3.1 Map of the Christchurch urban area showing maximum peak ground accelerations (vertical and horizontal vector components) recorded at GeoNet national and regional network seismic stations (labelled) and temporary low-cost Quake-Catcher Network accelerometers. After Kaiser et al. (2012).

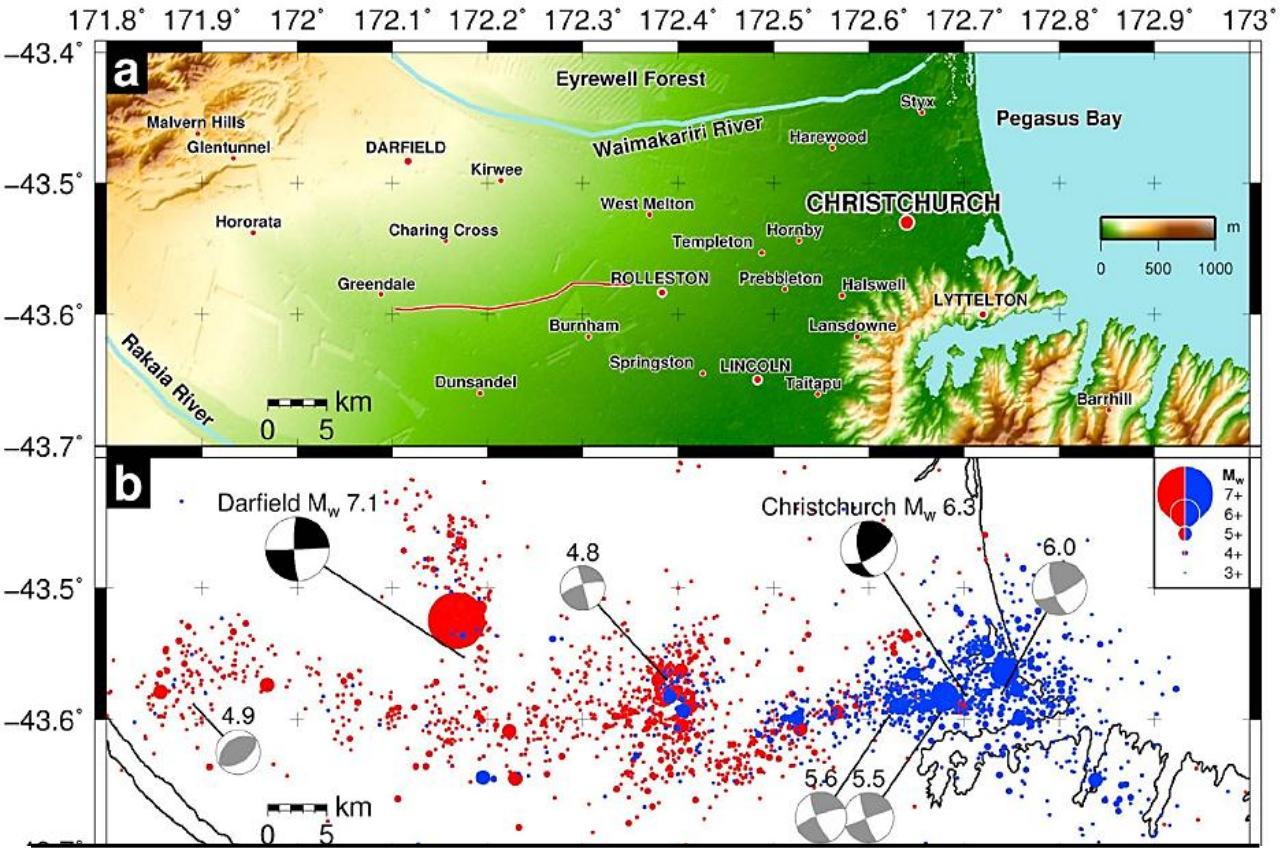

Figure 3.2 (a) The Christchurch region with mapped trace of the Greendale fault. (b) Distribution of aftershocks greater than M3 following the September (red circles) and February (blue circles) earthquakes, together with focal mechanisms for the larger earthquakes. After Elliot et al. (2012).

3.2 Post-earthquake Ground Damage in the Port Hills

3.2.1 Land damage following the Darfield Earthquake

Minor land damage was reported in or near the Port Hills of Christchurch; there were scattered instances of rockfall from unstable outcrops, and some liquefaction of the sandy deposits in the valley beside Bridle Path Road. Residents of 211 Centaurus Road reported the appearance of a flowing spring beneath their house following the this earthquake, and have been pumping water from their property since. Some residents of Vernon Terrace also reported the first appearance of springs on their properties immediately following this earthquake, many of which had flows that were exacerbated by the subsequent earthquakes. The springs in this area are discussed in more detail in Section 4.7.

Some fissuring of the foot-slope loess in the Port Hills was recorded by GNS after this earthquake, with a little damage being reported in the Vernon Terrace (Figure 3.5) area (Dellow et al. 2011a), together with the nearby spring formation. This movement appeared to reactivate during the February and subsequent earthquakes.

3.2.2 Land damage following the Christchurch Earthquake

The Christchurch Earthquake caused severe geotechnical damage to the Port Hills and to the rest of Christchurch City, and was by far the most devastating of the earthquakes. Large scale rockfall and cliff collapse occurred in the hills, as well as extensive fissuring of valley-wall loess deposits. Cliff collapse occurred around Whitewash Head, Peacock's Gallop and Redcliffs with related deep fissuring in the loess cap of the bedrock cliffs behind. In low-lying areas of sand and silt deposits, liquefaction occurred over vast areas, with lateral spreading taking place alongside rivers and streams.

This earthquake caused severe damage to the Huntsbury reservoir, a rectangular reservoir located on the Huntsbury Hill at the intersection of Huntsbury Avenue and Milhill Lane (Figure 3.3). Information on the shearing through the Huntsbury reservoir has been collected by Beca Infrastructure Ltd (2011). The earthquake caused the formation of a series of *en echelon* fractures through the floor of the reservoir in a NW – SE orientation, and the contents (32 000 m^3) of the reservoir drained. It is still uncertain as to where the water flowed, as the water was not observed to be concurrently flowing out at any particular location on the hillside. Fractures continued out either side of the reservoir onto nearby roads, with an average strike of 290 - 315°, a dip of 65 - 85° ± 10° SW. The fractures have been interpreted as an historic feature which propagated to the ground surface as a result of the earthquake shaking. This theory

results from the discovery of several well-formed slickenside surfaces, as well as the soft clay "gouge" in the tunnel containing the inlet/outlet pipe to the reservoir.

The orientation of the fractures through the Huntsbury reservoir is of further interest as they appear to line up approximately with the contour-parallel "dog-leg" observed in the Ramahana Road–Albert Terrace fissure trace (Figure 4.11).

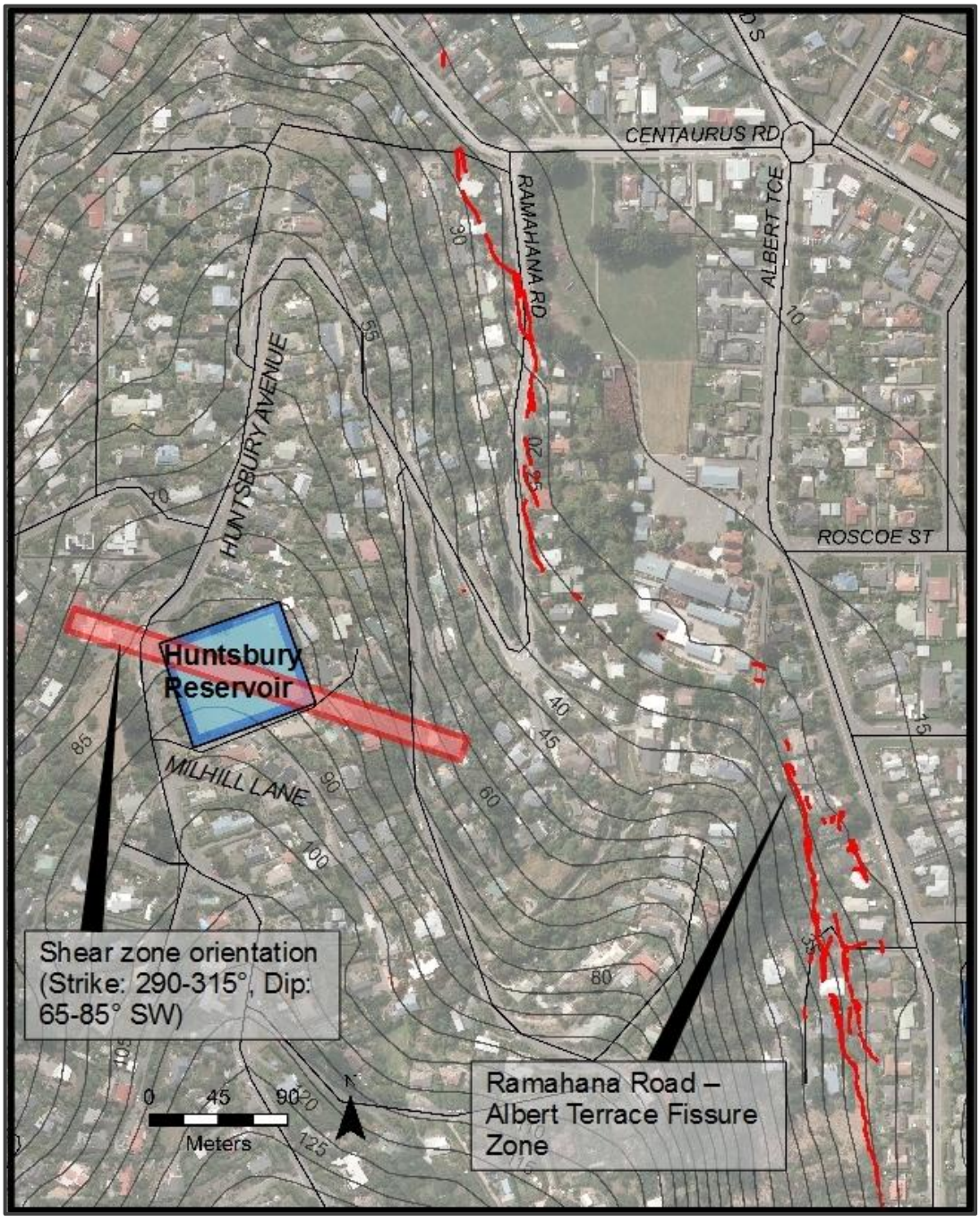

Figure 3.3 Location of Huntsbury Reservoir with orientation of fracture zone shown by red rectangle. Relationship to Ramahana Road-Albert Terrace fissure zone shown, with shear zone appearing to align with the fissure "dog-leg".

3.2.3 Land damage following the June Earthquake

The June 13th aftershock caused further rock fall across much of the Port Hills, and some fissuring in the valley bottoms showed further movement after the June earthquake, producing similar movement patterns to the Christchurch Earthquake (Dellow et al. 2011a).

Cliff collapse at Whitewash Head and Sumner Cliffs was prevalent in the June Earthquake, with cracks that had developed parallel to the cliff faces in February becoming head-scarps of major bedrock landslides.

3.3 Foot-slope Fissuring – overview of the fissures

Several authors, for example, Dellow et al. (2011a) and Kaiser et al. (2012), have described the Port Hills loess fissuring as incipient deep-seated landsliding, characterised by small amounts of vertical displacement in the head-scarp area and compressional features near the toe areas. However none of the fissure sites have yet failed catastrophically, even after Christchurch has experienced two wet winters with snow fall and further aftershocks. Importantly, drilling in the Hillsborough Valley has not located any basal shear surface which would be fundamental to landsliding. This implies that incipient landsliding is not necessarily the cause of the fissuring, and as such this and the following chapter provide results of detailed investigations into the fissuring with the ultimate aim to define their formation mechanism.

There are five main valley sites of post-earthquake fissuring in the north-facing valleys of the Port Hills, as shown in Figure 3.5, page 52. These sites, from west to east, are: Bowenvale Valley, Hillsborough Valley, Huntlywood Terrace–Lucas Lane, Bridle Path Road, and Maffeys Road–La Costa Lane. The following chapter section will examine the five main fissuring sites and provide a brief overview of each.

The fissure traces are predominantly discontinuous segments, which extend in a zone of varying width along the hillside, in an approximately contour-parallel orientation. When overlaid onto a moderate-resolution geologic map of Christchurch (Brown & Weeber 1992), the fissure traces appear to coincide approximately with the boundary between the hill-mantling loess deposits and the colluvial valley fill (a mixture of re-deposited loess and fragments of volcanic bedrock) as shown in Figure 3.4. In the field it was observed that in most locations (Maffeys Road–La Costa Lane being a notable exception) the fissures appear at least 20 m overland distance below the beginning of outcropping bedrock.

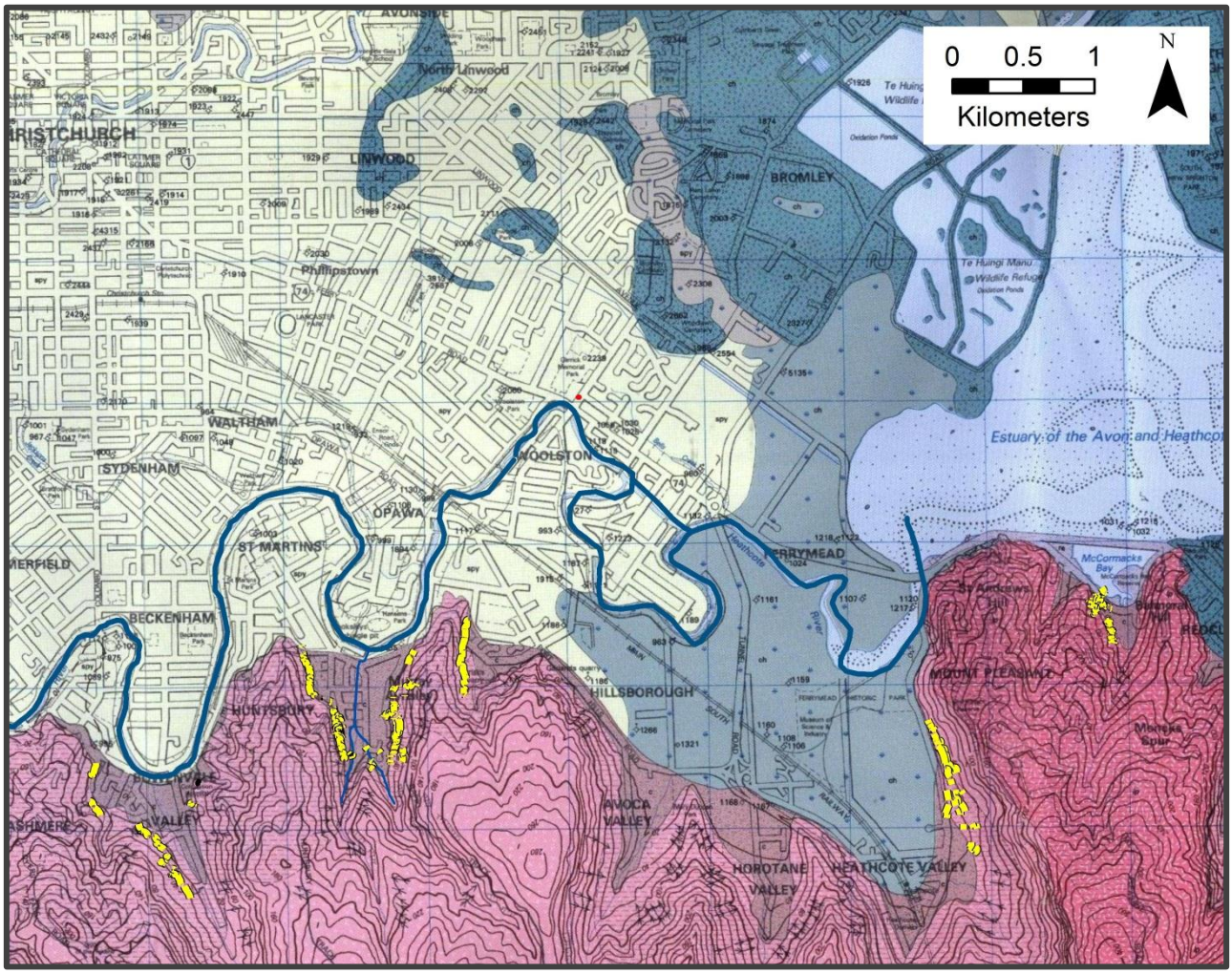

Figure 3.4 Fissure traces overlaid onto geological map of the Christchurch urban area. Fissure traces shown in yellow. Pink rocks are Miocene volcanics, predominantly basalt. Dark pinkish brown shows valley-fill loess colluvium. Pale yellow is alluvial sand and silt overbank deposits. Blue and grey are Christchurch Formation sands, silts and peats. Geologic map is asection from Geology of the Christchurch urban area. Scale 1:25 000. Institute of Geological and Nuclear Sciences geological map by Brown and Weeber (1992).

Nearly every section of fissure trace with measureable extension is accompanied by lateral compression features in the valley floor below. These were commonly observed in sealed roads and kerbing where linear sections have been truncated, "concertina-fashion". The total extent of compression is difficult to measure accurately without the use of precise land survey equipment with measurements having been taken both prior to, and after, the earthquakes. Field observation indicates that the extent of compression is comparable to the extent of lateral extension in the fissures above, and fence offset along driveways on Vernon Terrace indicates

compression in the order of 700-800 mm. The cumulative displacements across the tension cracks rarely exceed one metre (Dellow et al. 2011a).

One feature of the fissuring has been the contemporaneous formation of new springs and seepages in some of the valley floors, information on which has been kindly shared through communication with Helen Rutter of Aqualinc, Christchurch. Springs appeared in many locations over Christchurch following the Darfield Earthquake and subsequent aftershocks, in particular following the Christchurch Earthquake, and in places appear to have some correlation with the locations of the fissuring. The two prevailing locations where springs formed were the western side of the valley opposite Bridle Path Road, alongside Tunnel Road, and around the entrance to the Hillsborough Valley. Individual spring locations were observed elsewhere near the fissuring – two springs have been located below the Huntlywood Terrace–Lucas Lane fissures, and one spring has been located below Rossmore Terrace in the Bowenvale Valley fissure area. Detailed discussion on the Hillsborough Valley springs is provided in Chapter 4.

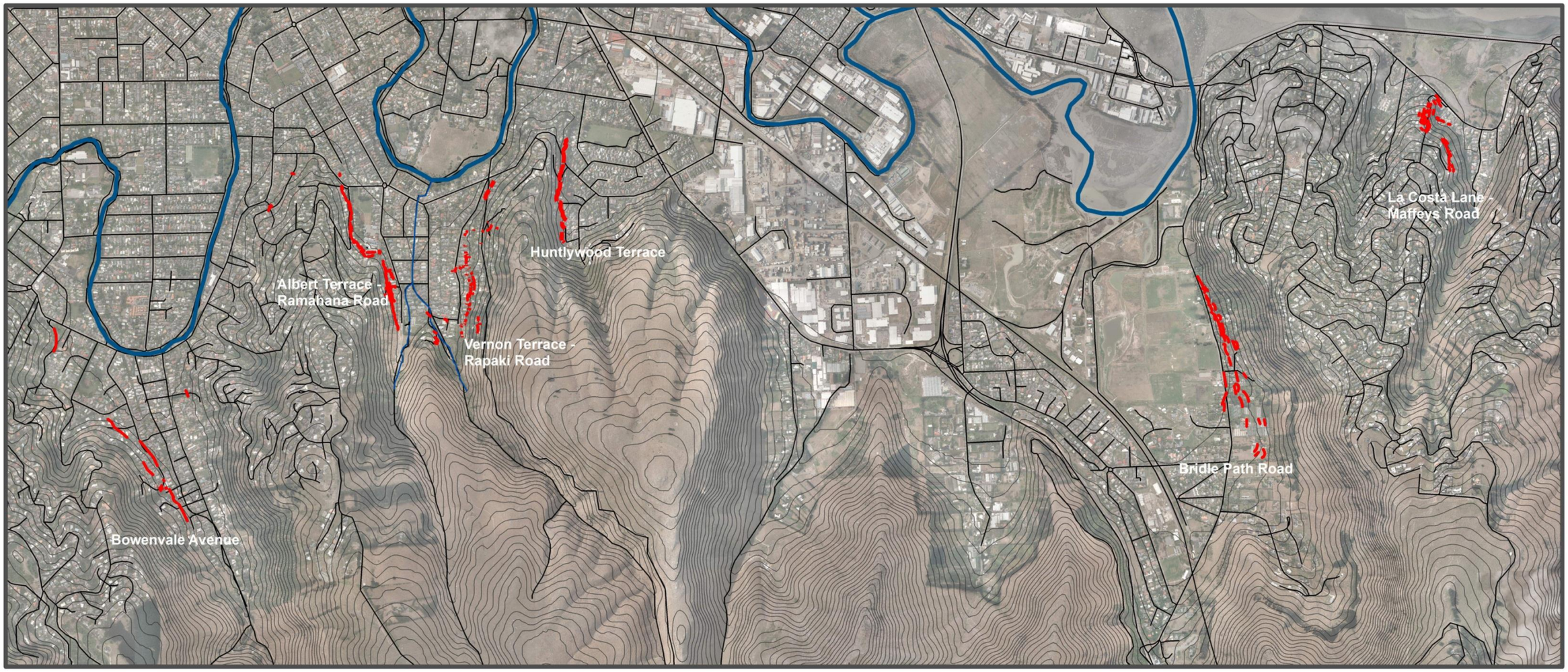

Figure 3.5 Overview map of all fissure traces (red). Mapped by author. Bridle Path Road and Maffeys Road-La Costa Lane traces after maps produced by SKM and URS, Christchurch. Huntlywood Terrace-Lucas Lane trace after pers. comm. R. Hunter.

3.2 Bowenvale Valley Fissuring

Aside from occasional smaller instances of fissuring near Princess Margaret Hospital, Bowenvale Valley is the westernmost site of major fissuring on the Port Hills (Figure 3.6). The fissuring in the Bowenvale Valley area occurs predominantly on the western side of the valley, extending from a vacant section on Maurice Knowles Lane, through properties to Landsdowne Terrace, and ending in Roseneath Place. Two 20-30 m sections of fissuring also occurred in the upper end of Rossmore Terrace, a short distance west of Roseneath Place, as well as a 50-60 m section near the bottom of Rossmore Terrace. A short section of fissuring was noted to cross Sunvale Terrace on the eastern side of Bowenvale Valley, outside 7 Sunvale Terrace; however this did not appear to extend further than roughly 20 m. The trace is discontinuous and roughly contour-parallel, as is typical for the Port Hills fissures, in this case being predominantly between the 25 m and 30 m (above sea level) contours. A detailed cross section of the Bowenvale Valley fissure trace is provided in Figure 3.7.

In the Bowenvale Valley, in particular near Plumwood Lane (Figure 3.6), the fissure trace orientation appears dependent on factors which cause it to follow a path of least resistance, or least tensile strength. The fissure trace divides and re-forms several times in the area. Fissures pass directly through 8 Plumwood Lane. Since the fissure appears to have divided into several smaller traces at this point, most of which circumvent the house, the impact on the house at 8 was lessened, although the lower storey and garage did separate slightly from the upper half. A larger fissure was observed at 5 Plumwood Lane, of approximately 100 mm wide, passing beneath the centre of the house. This was evident as several cracks in the patio area which combined to form a single large split through the house. There is extensive evidence of land and fill movement in this area with the retaining wall to the north of the house having moved eastwards towards the centre of the valley, causing cracking to form in the fill behind. The crack continues into 9 Fineran Lane where it passes beneath the house, effectively splitting the house in two down the peak of the roof.

Figure 3.6 Bowenvale Valley fissure traces.

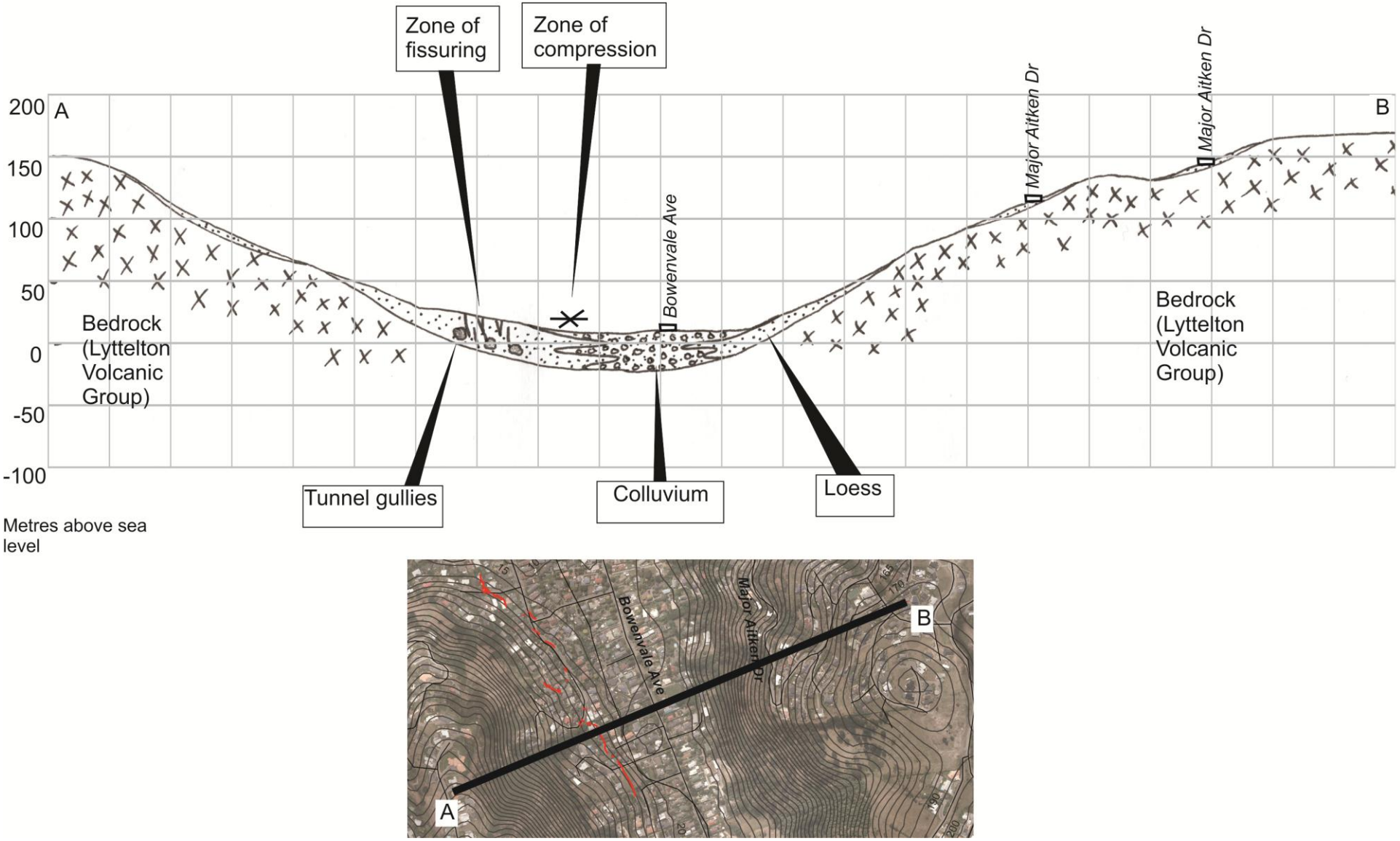

Figure 3.7 Schematic cross-section through Bowenvale Valley, at natural scale however size of fissures exaggerated approximately 10x, in order for clarity of observation. In reality they would extend only slightly into the loess layer. Bedrock and valley fill loess-colluvium mapped based on geological map in Brown and Weeber (1992).

3.3 Hillsborough Valley Fissures

The next major group of fissuring eastward of the Bowenvale fissures are those in the valley around Hillsborough Terrace (Figure 3.7). This valley has extensive fissuring on both sides, extending from the start of Ramahana Road through to the end of Albert Terrace on the west, and following the length of Vernon Terrace and Rapaki Road on the east with the fissure traces following a roughly contour-parallel orientation, each extending for a distance of 500-600m. Shorter, <2 m sections of fissuring were also observed in The Crescent, at the head of the valley.

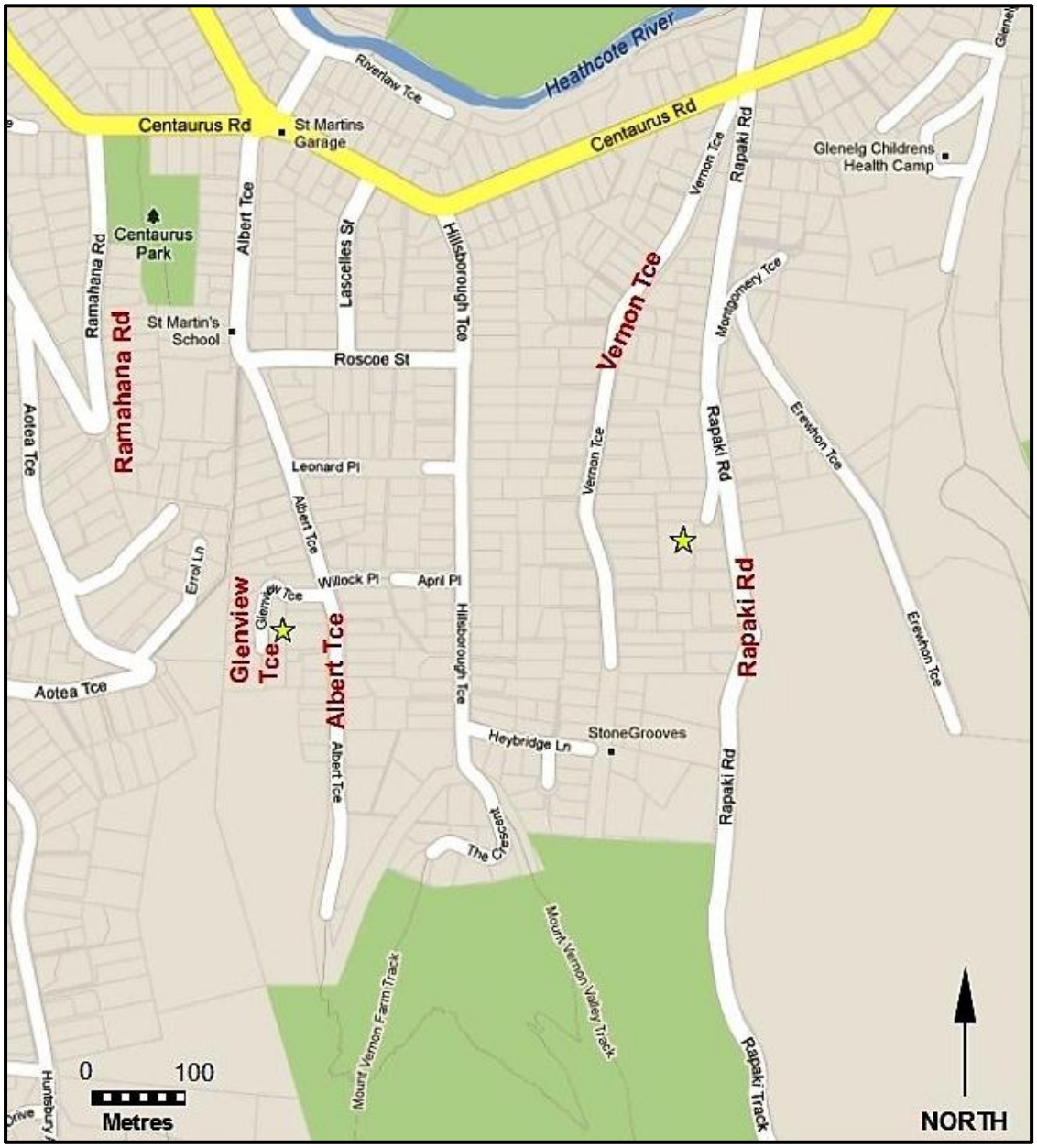

Figure 3.8 Case-study locations, Huntsbury, streets noted in text highlighted. Locations of case study focus locations indicated by yellow stars. Base map source: GoogleMaps.

The Vernon Terrace fissures were observed to continue to creep for some time following the Christchurch Earthquake, and it has been postulated that the fissures formed on a pre-historic landslide head-scarp (Dellow et al. 2011a). A detailed cross section of the Hillsborough Valley fissures is provided in Figure 3.9.

The Hillsborough Valley system was selected as a suitable site for further detailed case study analysis, including laboratory soil testing, a resistivity survey, and analysis of the springs which emerged in this valley is discussed in greater detail in Chapter Four.

Post-earthquake spring formation was unprecedented in the Hillsborough Valley, with the formation of at least two dozen new springs whilst other valleys had only one or two in general.

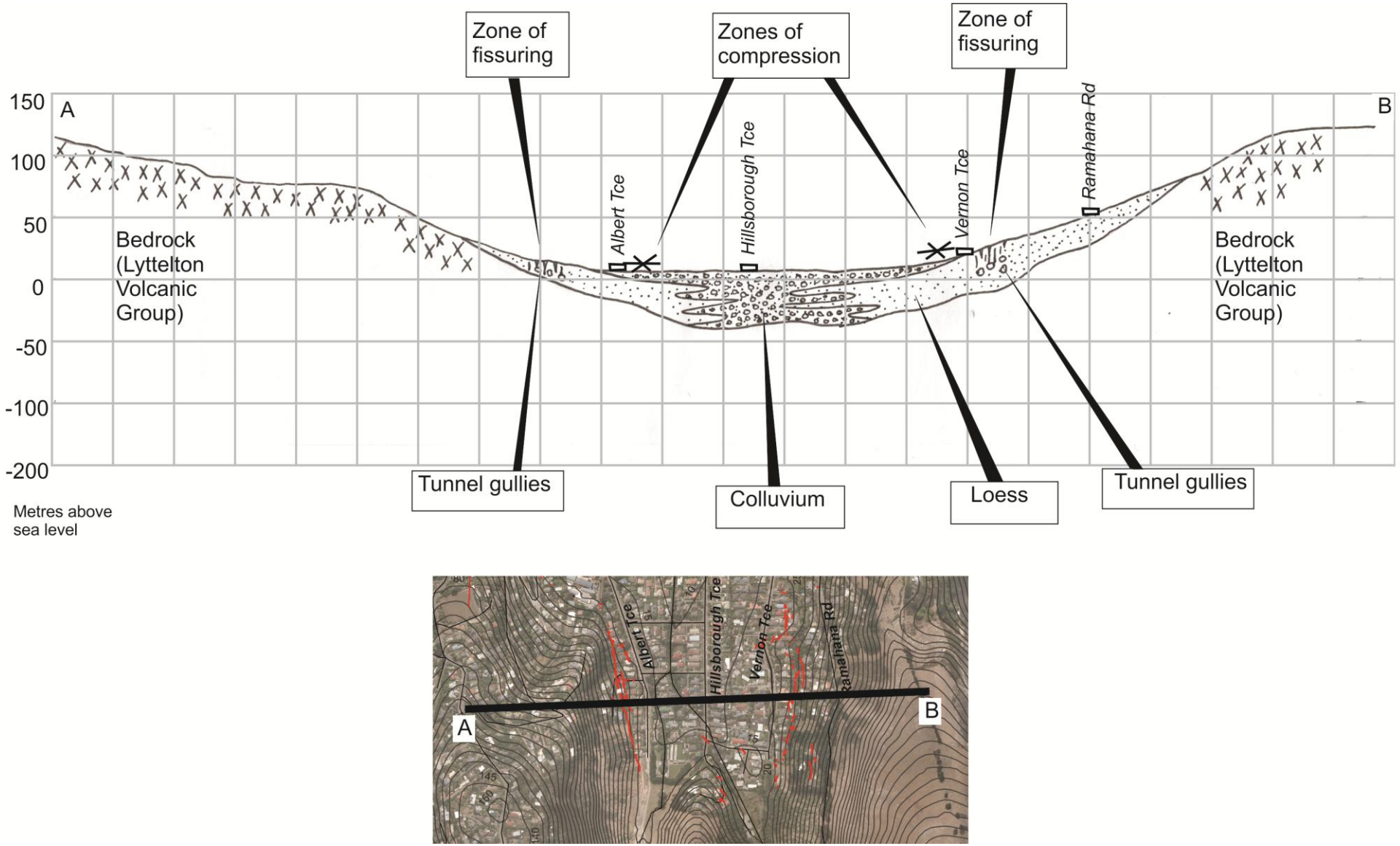

Figure 3.9 Schematic cross-section through Hillsborough Valley. Scale: natural scale, however size of fissures exaggerated approximately 5x, in order for clarity of observation. In reality they would extend only slightly into the loess layer. Bedrock and valley fill loess-colluvium mapped based on geological map in Brown and Weeber, 1992.

3.4 Huntlywood Terrace Fissures

The fissure traces trending from Huntlywood Terrace to Lucas Lane are mapped in Figure 3.10. At the time of writing, a landslide hazard has been declared for Lucas Lane, following heavy rainfall in the winter of 2012. Christchurch newspaper, The Press of 18 August 2012, reported that residents of six houses in Lucas Lane were forced to evacuate on the 14th of August. The paper also reported that review of aerial photographs of the area had indicated the presence of an historic slip on the slope above Lucas Lane. An historic brick quarry was located in the Lucas Lane area, which may have been a contributing factor to the landslide risk in the area.

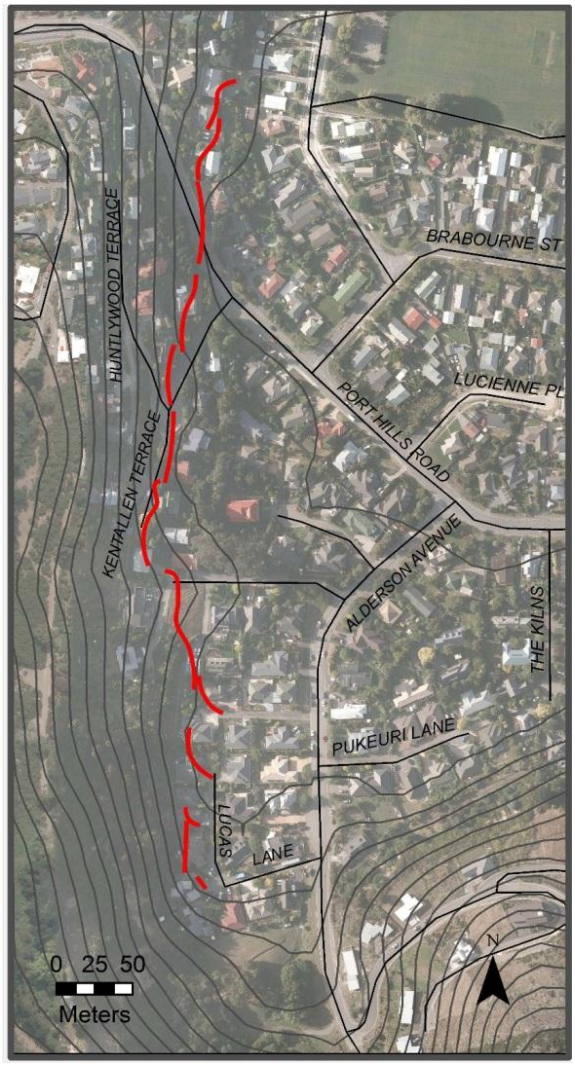

Figure 3.10 Fissure trace from Huntlywood Terrace to Lucas Lane. Mapped following pers. comm. R. Hunter.

3.5 Bridle Path Road Fissures

The Bridle Path Road fissure traces extend for some 400 m, in a semi-continuous manner (Figure 3.11). The Christchurch Earthquake's epicentre was directly below the Heathcote Valley, and the high vertical ground acceleration of 2.2g was recorded nearby. Extensive fissuring formed along driveways leading uphill from Bridle Path Road (Figure 3.12), as well as many failures of areas of fill, and liquefaction occurred in the valley floor. Movement monitoring devices set up following the Christchurch Earthquake indicated that the Bridle Path Road fissures continued to creep for some time afterwards (Dellow et al. 2011a). The fissure traces were discontinuous, with lengths of up to approximately 20 m. These sections of fissures overlapped and extended the 400 m distance of Bridle Path Road in effect forming a linear fissure "zone", passing through the houses and drives to the east of Bridle Path Road. Driveways perpendicular to the fissure zone showed the movement most readily, with paved areas being separated by fissures of up to 200 mm in width, such as those seen in Figure 3.12. In Hammerton Lane, being at a slightly higher elevation to the fissures along Bridle Path Road properties, fissuring was also observed, however it was attributed to being the result of localised fill failure (Figure 3.11).

Bridle Path Road fissures differed from those of, for example, Bowenvale Valley or Hillsborough Valley, in the fact that the valley on Bridle Path Road is at least three times wider than these other valleys, and there were no similar "paired" fissure traces apparent on the western side of the valley. Liquefaction was observed in the farmland in the valley floor below Bridle Path Road, in both the Darfield and Christchurch Earthquakes, and in the Christchurch Earthquake springs developed towards the western side of the valley (H.Rutter, Aqualinc Research Ltd, pers. comm., 2012).

A schematic cross section of the Bridle Path Road fissures is provided in Figure 3.13, showing the relationship of the fissuring to the location of the bedrock outcrops higher up the hillslope, and to the valley floor sediments below. Springs are shown reaching the surface towards the west of the valley, and liquefaction is indicated where it was observed in the central valley sediments.

Figure 3.11 Bridle Path Road fissure traces. Map adapted from Engel and MacFarlane, unpublished memo, 2011.

Figure 3.12 Upper: cracking in the driveway of 158A Bridle Path Road, and lower: tension cracks across Hammerton Lane, looking towards Bridle Path Road. Engel and MacFarlane, unpublished memo, 2011.

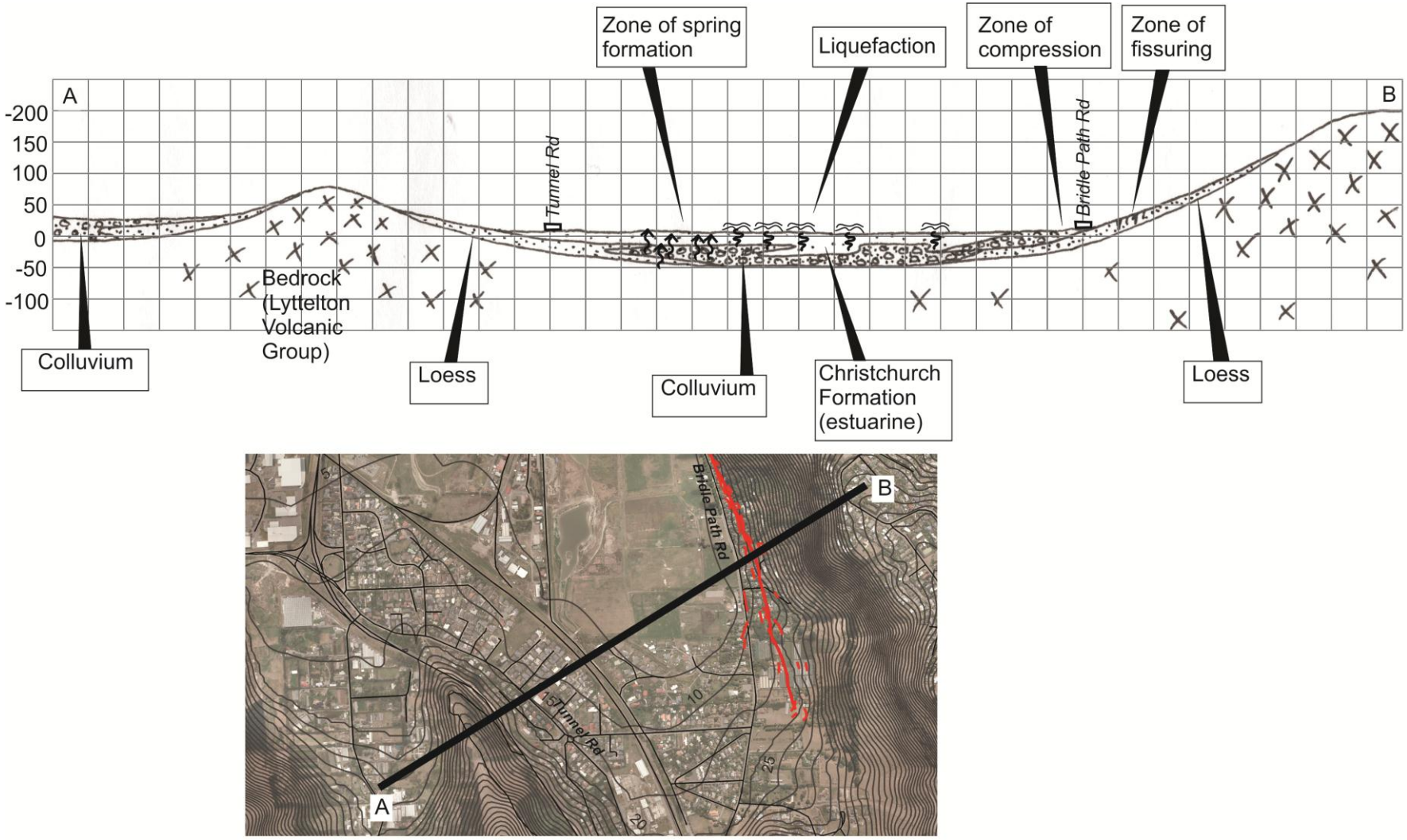

Figure 3.13 Schematic cross section through Bridle Path Road valley, with bedrock and Christchurch Formation mapped based on geological map in Brown and Weeber, 1992. Springs indicated by upwards wavy arrows, and liquefaction by wavy lines on surface. Scale: natural scale, however size of fissures exaggerated in order for clarity of observation. In reality they would extend only slightly into the loess layer.

3.6 Maffeys Road-La Costa Lane and Basil Place Fissures

The fissuring at La Costa Lane (Figure 3.14 and Figure 3.15) was first noted during ground inspections during March 2011. The fissuring had severely damaged the land at 16 La Costa Lane, and the owners indicated that their house had moved east from the road-side by the fissuring. At 14 La Costa Lane, fissuring had similarly caused a wooden car port structure to detach from the road and collapse. The Maffeys Road fissures are aligned with the crest of the hill, thus trending approximately perpendicular to the contours. These may or may not be related to the La Costa Lane fissures, which do follow the more common contour-parallel alignment. The La Costa Lane fissures differ from those further to the west in that they are at a higher elevation, being up to 65 m above sea level, and being almost directly on the loess-bedrock interface. Some minor fissuring was also noted along Basil Place, in the valley below La Costa Lane. Again this is unusual, as in other locations, fissuring has been accompanied by lower level compression, rather than further fissuring. The Basil Place fissuring is on slopes of lower gradient, and only approximately 15 metres above sea level.

Figure 3.14 Cracking outside 22 La Costa Lane. Engel and MacFarlane, unpublished memo, 2011.

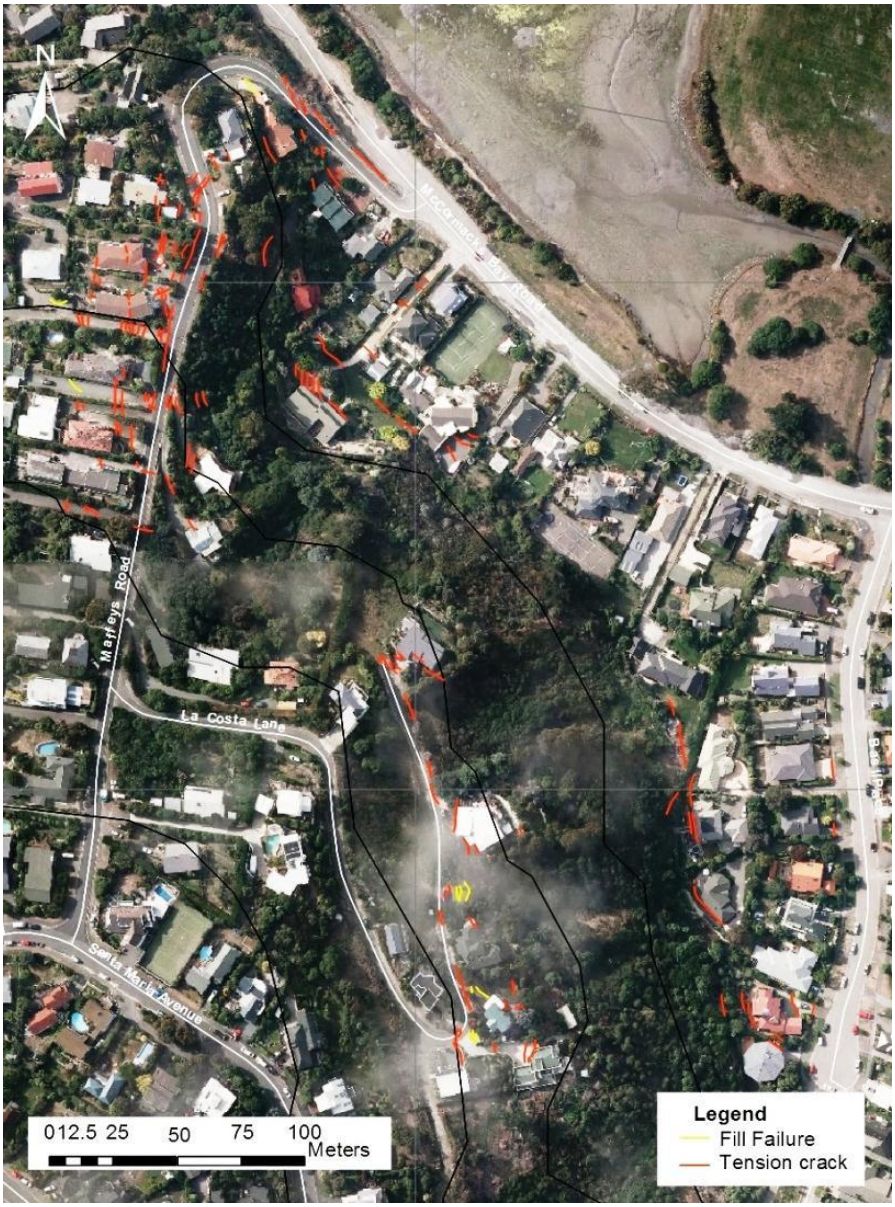

Figure 3.15 Tension cracks at Maffeys Road, La Costa Lane and Basil Place to right. Engel and MacFarlane, unpublished memo, 2011.

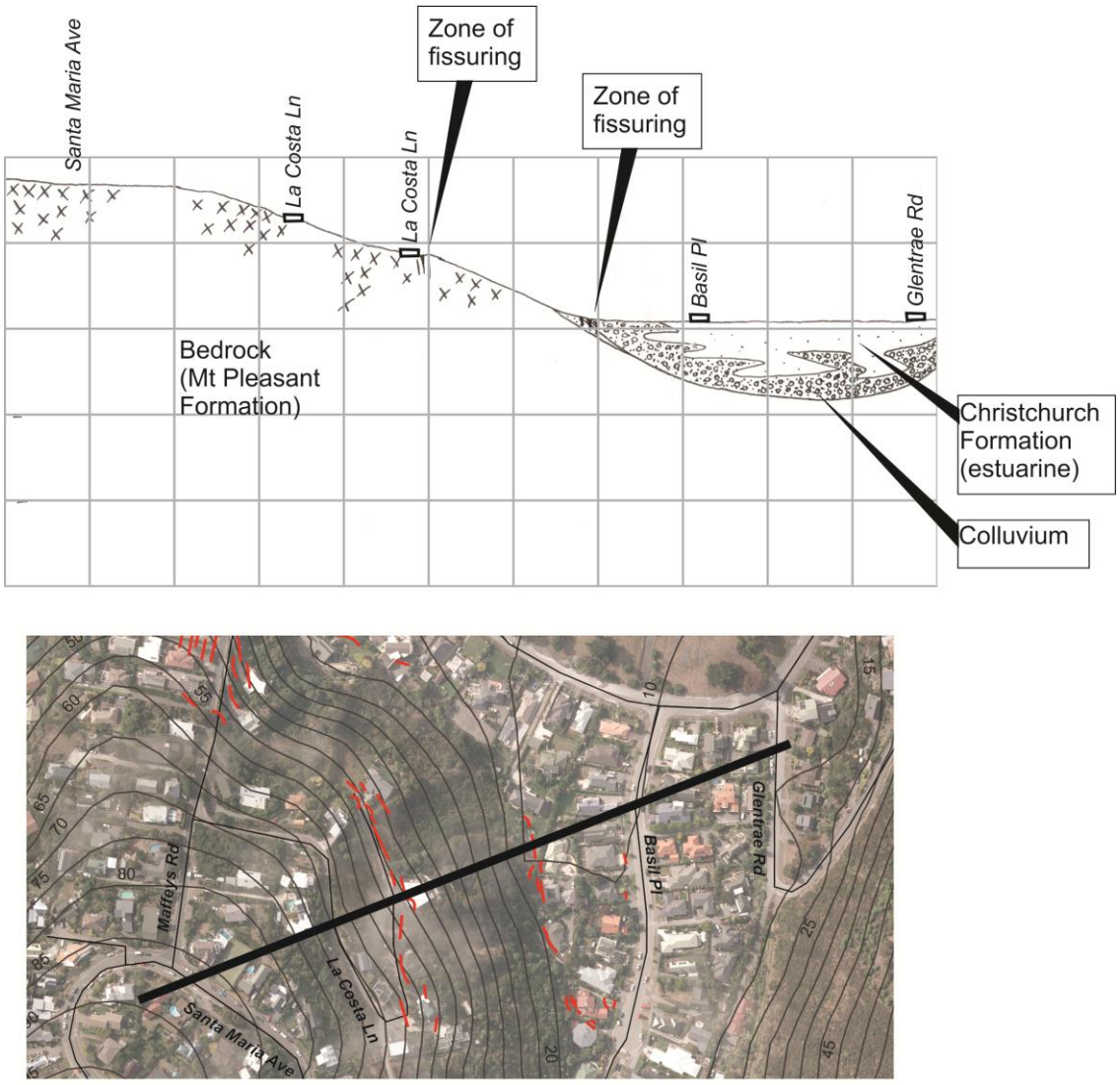

Figure 3.16 Schematic cross section through La Costa Lane fissures. Bedrock and Christchurch Formation mapped based on geological map in Brown and Weeber, 1992. Scale: natural scale.

3.7 Synthesis

1) Three large earthquakes occurred in the Christchurch region from 2010-2011:

    a) The Darfield Earthquake, September 4 2010, on the Greendale Fault west of Christchurch. M7.1, dextral strike-slip mechanism.
    b) The Christchurch Earthquake, February 22 2011. Fault located beneath the Christchurch Port Hills. M6.2, oblique thrust mechanism.
    c) June 13 aftershock, June 13, 2011. Fault located towards the eastern end of the Port Hills, M 6.0.

2) While some fissuring and spring emergence was recorded in the Port Hills following the Darfield Earthquake, the majority of the geotechnical damage occurred during and immediately after the Christchurch Earthquake. Extended fissure traces formed in loess foot-slope positions of the north-facing valleys of the Port Hills, with some fissures continuing for several hundred metres.
3) There are five main valley sites of post-earthquake fissuring in the north-facing valleys of the Port Hills. These sites, from west to east, are Bowenvale Valley, Hillsborough Valley, Huntlywood Terrace–Lucas Lane, Bridal Path Road, and Maffeys Road–La Costa Lane.
4) The fissure traces are normally roughly contour-parallel, and appear to coincide with the boundary between the hill-mantling loess deposits and the colluvial valley fill.
5) One feature of the fissuring has been the contemporaneous formation of new springs and seepages in some of the valley floors. The two prevailing locations where springs formed were the western side of the valley opposite Bridle Path Road, alongside Tunnel Road, and around the entrance to the Hillsborough Valley.

4 Case Study: Hillsborough Valley

As outlined in Chapter 3, ground fissuring in the foot-slopes of the Port Hills occurred in several of the north-facing valley walls, and affected numerous Christchurch properties. This chapter looks in depth at one of these valleys, that below Mount Vernon, containing Albert Terrace, Vernon Terrace and Rapaki Road (Figure 3.8) which developed fissures on both sides of the valley during the Christchurch Earthquake in February, 2011.

4.1 Description of fissuring and compression zones

The fissuring on either side of the Hillsborough Valley has been mapped through properties from Albert Terrace to Ramahana Road on the western side, and between Vernon Terrace and Rapaki Road on the eastern side. The fissure traces run in a roughly contour-parallel orientation, each extending for a distance of 500-600m, as shown in Figure 4.1.

In general, the fissure traces appear remarkably similar at any given location along the fissure trace. There is always an amount of lateral extension, in the order of 0.10-0.20 m, and usually some vertical movement, whereby the down-slope side of the fissure trace has dropped by a varying amount, usually between 0.05-0.15 m. Two instances of discrepancy to this were found: when tracing a smaller, subsidiary fissure through the property at 62 Albert Terrace, there was a short approximately 2 m section of fissure where the down-slope side was higher with respect to the up-slope side by approximately 0.10 m. This was not observed at any other site along the western fissure trace. A second area with similar “graben”-style blocks observed by GHD field geologists in the vicinity of 44a Rapaki Road. Figure 4.2 shows a more typical example of the fissure trace, where it passes through 3 Glenview Terrace.

The fissure traces on either side of the valley appeared at similar heights (Figure 4.3), beginning on the western side at the 20 m contour near the southern end of the valley, rising slightly reach the 30 m contour by Glenview Terrace on the west and around 40 Rapaki Road on the east, and then continuing at this elevation with only minor height fluctuations in the order of 5-10 m and a slight gradual decrease in elevation towards the 20 m contour again at their ends near Centaurus Road.

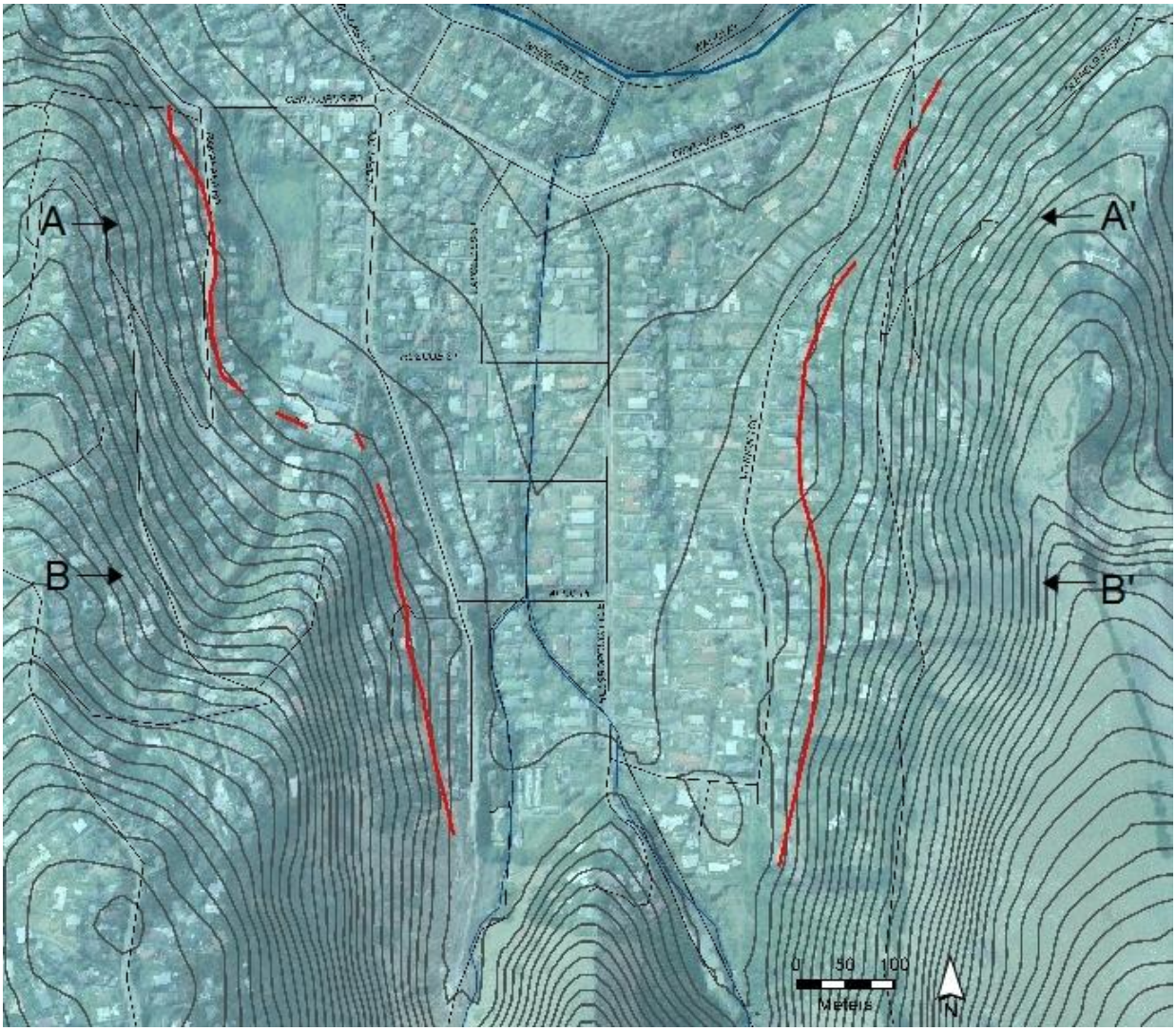

Figure 4.1 Simplified fissure traces on either side of the Hillsborough Valley, shown in red. Topography shown by 15 m D.E.M. from LiDAR data, and 5 m interpolated contours. A-A' and B-B' indicate profile locations, as seen in Figure 4.4.

Figure 4.2 Two photos of the tension crack passing through yard of 3 Glenview Terrace, A4 clipboard for scale in left hand image. Vertical displacement in right hand image is ~0.20 m, and horizontal ~0.15 m

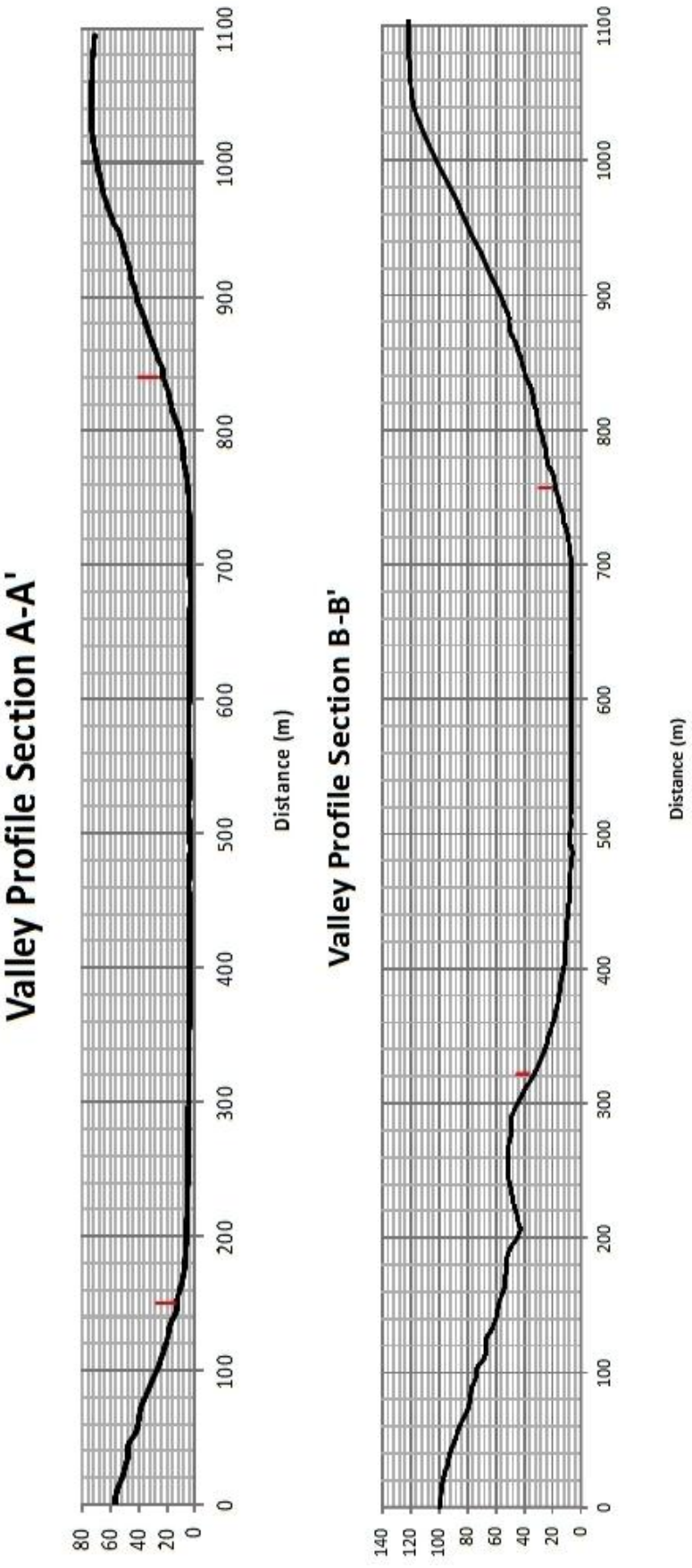

Figure 4.3 Profile sections of the Hillsborough Terrace valley, with location of main fissure trace shown by red dash. Profile endpoints shown in Figure 4.2. Left-axis shows height in metres above sea level.

Along both segments of the fissure trace in the Hillsborough Valley, it passed across several paved driveways. These sections often showed the movement more clearly than the grassed sections, many of which became rapidly overgrown. In the sealed section of Glenview Terrace there were six individual traces of the fissure. In the upper part of the road the fissure trace was evident as linear pot-holing, with substantial cavity formation beneath the sealed surface (Figure 4.4). This cavity formation implied that water was flowing into the fissures at these locations, and passing through cracks in the loess, carrying fines in suspension. It was interesting to note that at a driveway several metres along from the pot-holes site, the fissure appeared to be providing an exit point for the water with its suspended load; in the driveway of 2 Glenview Terrace the fissure traces were observed to be seeping water and suspended loess sediment (Figure 4.5).

Figure 4.4 Tension crack passing beneath roadway of Glenview Terrace. Cavity beneath road of substantial volume showed loess material was being excavated by water flow. Pencil for scale.

Figure 4.5 Tension cracks passing through driveway of 2 Glenview Terrace. Water was emerging from the cracks at this location, and carrying loess sediment.

It was realised fairly soon after the formation of the fissures in February 2011, that, if left without remediation, they could pose a serious landslide hazard, particularly during the coming winter when heavy rainfall could enter the cracks and lead to extensive tunnel-gully formation or land-sliding. Under the direction of David Bell from Bell Geoconsulting Ltd and James Molloy from GHD, acting for the Port Hills Geotechnical Group, the residents of Vernon Terrace worked together to fill the largest of the fissures over the course of a weekend. They used a 1:6 mixture of bentonite clay (a clay formed by the alteration of volcanic ash, which swells to many times its original volume on contact with water to produce a soft gel (Bell 2007)) and SAP-20 gravel (well-graded, locally-sourced, greywacke gravel with all grains being less than 20 mm diameter). The use of low-permeability bentonite clay was intended to prevent further infiltration of rainwater into the cracks, and as it is a swelling clay, on contact with infiltrating surface water it expanded to fill the fissures over a few days.

The residents of the western streets of the valley did not accomplish a community remediation effort; however individual houses were advised to fill the cracks in a similar manner. Members of the 400-level Engineering Geology class at the University of Canterbury provided assistance to the owner of 3 Glenview Terrace in the infilling of fissuring through his property. Figure 4.7 shows a photo taken shortly after the remedial work was conducted at the Glenview Terrace property. It was noted that there had been a small amount of settling (up to

30 mm) in one area over a distance of less than one metre (Figure 4.7). The outcome of this is discussed further in Chapter 4.3.

In June, 2011, Christchurch City Council and the New Zealand Government produced a two-page guide for filling cracks on the Port Hills. The fact sheet provided information on procurement of bentonite powder and SAP-20 gravel, as well as providing detailed diagrams and practical information on the crack-filling process (Figure 4.6).

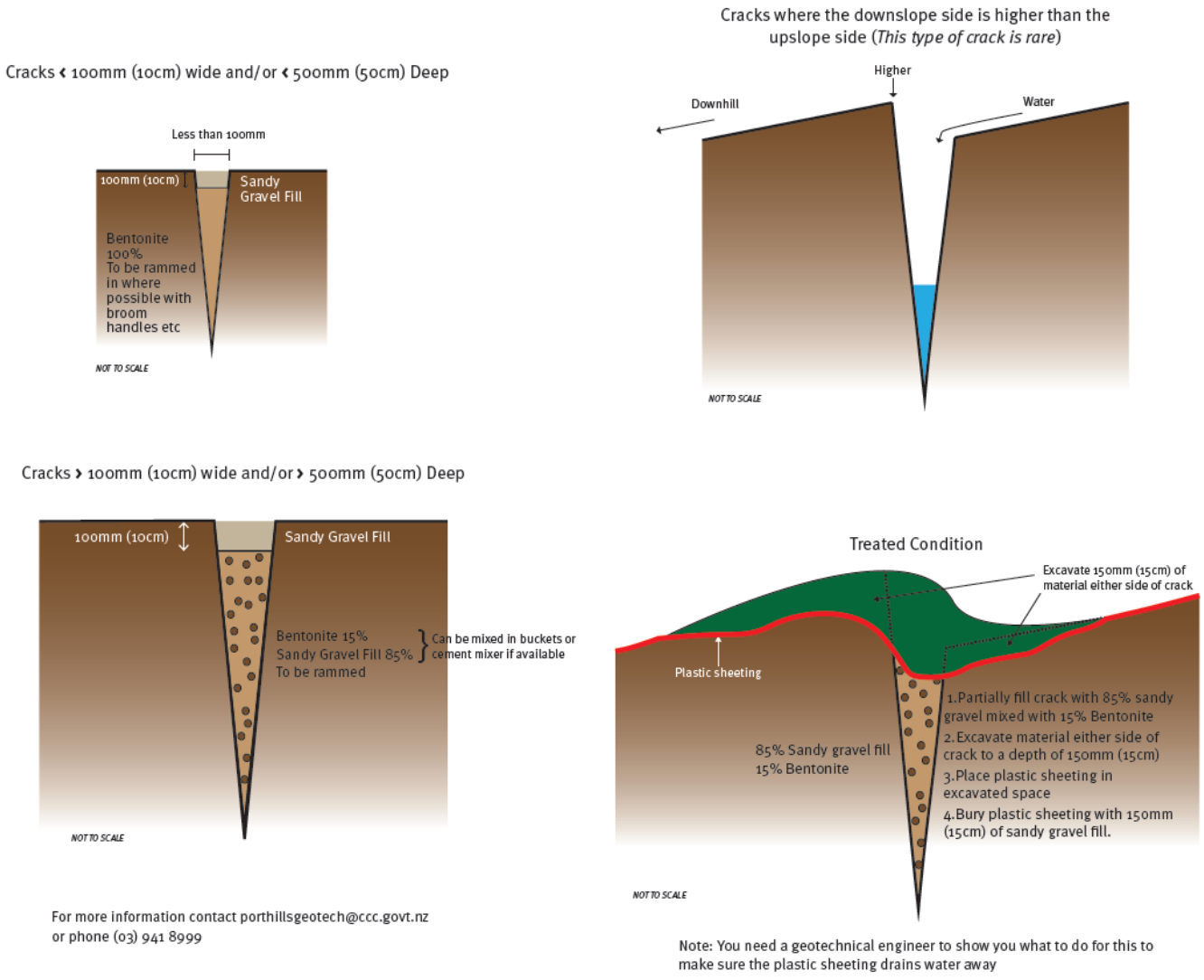

Figure 4.6 Christchurch City Council fact sheet diagrams on the filling of tension cracks. Christchurch City Council, 2011.

Figure 4.7 Fissure at 3 Glenview Terrace, following remediation infilling with bentonite and SAP-20 gravel. This photo shows the approximately 30 mm subsidence of the fill that was observed on this 30 June 2011 site visit

The initial geotechnical hypothesis on the formation of the fissures was that they were the head-scarps of deep-seated landslides (Dellow et al. 2011a; Dellow et al. 2011b; Hancox et al. 2011), with Dellow et al. (2011a) suggesting that the Vernon Terrace fissures formed on a possible pre-historic landslide head-scarp. This hypothesis was encouraged by the appearance of compression features in the valley floor. These features were often visible in driveways on the eastern side of Albert Terrace, and the western side of Vernon Terrace. In Vernon Terrace in particular, the compression was very distinct, and the features were apparent in most driveways, in a linear fashion, directly below the fissuring (Figure 4.10). The compression showed up to 0.20 m of lateral movement, evident as fracturing and overlapping in sealed sections. In most of the east-west streets, lateral compression could be seen in kerbing on the roadside. In Figure 4.8 a plastic outlet pipe in Roscoe Street has created a weaker zone in the concrete kerbing, which has encouraged compression to be focused in that location.
Liquefaction was not reported in the sediment in the Hillsborough Valley, which contains peat swamp material, although some houses in the centre of the valley were severely damaged, some by possible lateral spreading of the banks of the central drain system (Figure 4.9), indicating the intense ground motion experienced in that area.

Figure 4.8 Kerbing in Roscoe Street. Such evidence of lateral compression was observed in kerbing at many sites in east-west running streets in the valley floor.

Figure 4.9 Damage to house at 5 Leonard Place. House was located centrally in valley, alongside the channelled stream, and experienced the worst damage after the Darfield Earthquake.

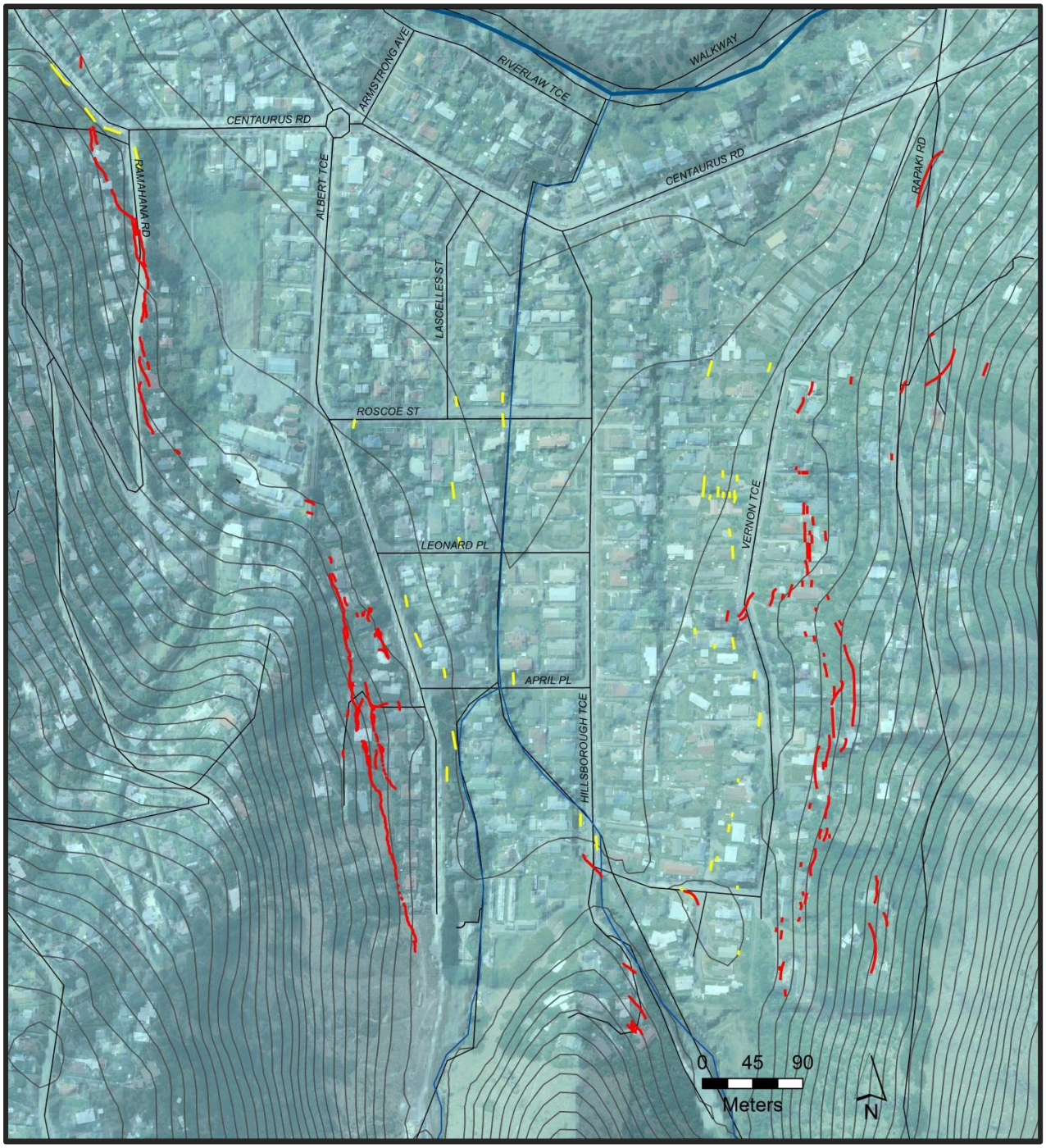

Figure 4.10 Areas of obvious compression in the Hillsborough Terrace valley. Compression features, usually parallel to the fissure trace above, are shown in yellow.

4.2 Mapping the Hillsborough Valley Albert Terrace-Ramahana Road fissure trace

Initial site inspections at 3 Glenview Terrace noted that the fissuring passed from this property into the neighbouring section at 1 Glenview Terrace, where they continued directly beneath the house, which was rendered structurally unsound after the Christchurch Earthquake. It was not until later that the lateral extent of the fissures was fully realised.The author undertook detailed mapping of the fissure trace (Figure 4.11), and in attempting to locate the end of the fissure trace, was able to follow it for approximately 600 m, from Centaurus Road in the north, to the end of Albert Terrace in the south (Figure 4.12).

While none of the fissures on either side of the valley are perfectly continuous traces, those on the western side are slightly more continuous than those on the eastern side. While mapping the western fissures the author was able to distinctly observe one larger, more dominant fissure which continued for most of the distance from Centaurus Road to the end of Albert Terrace. In looking at the mapped fissures from the eastern side (mapped by GHD) it is clear that these fissures are of a more discontinuous nature, as well as having a wider coverage of the hillside between the highest and lowest extent of the subsidiary fissures; at its widest, the eastern fissure zone is up to 120 m wide, compared with a maximum width of 70 m on the western side.

Figure 4.11 (over page) Mapped fissure trace from Ramahana Road to Albert Terrace.

DETAILED TENSION CRACK MAPPING,
RAMAHANA RD – ALBERT TCE, HUNTSBURY, CHRISTCHURCH.

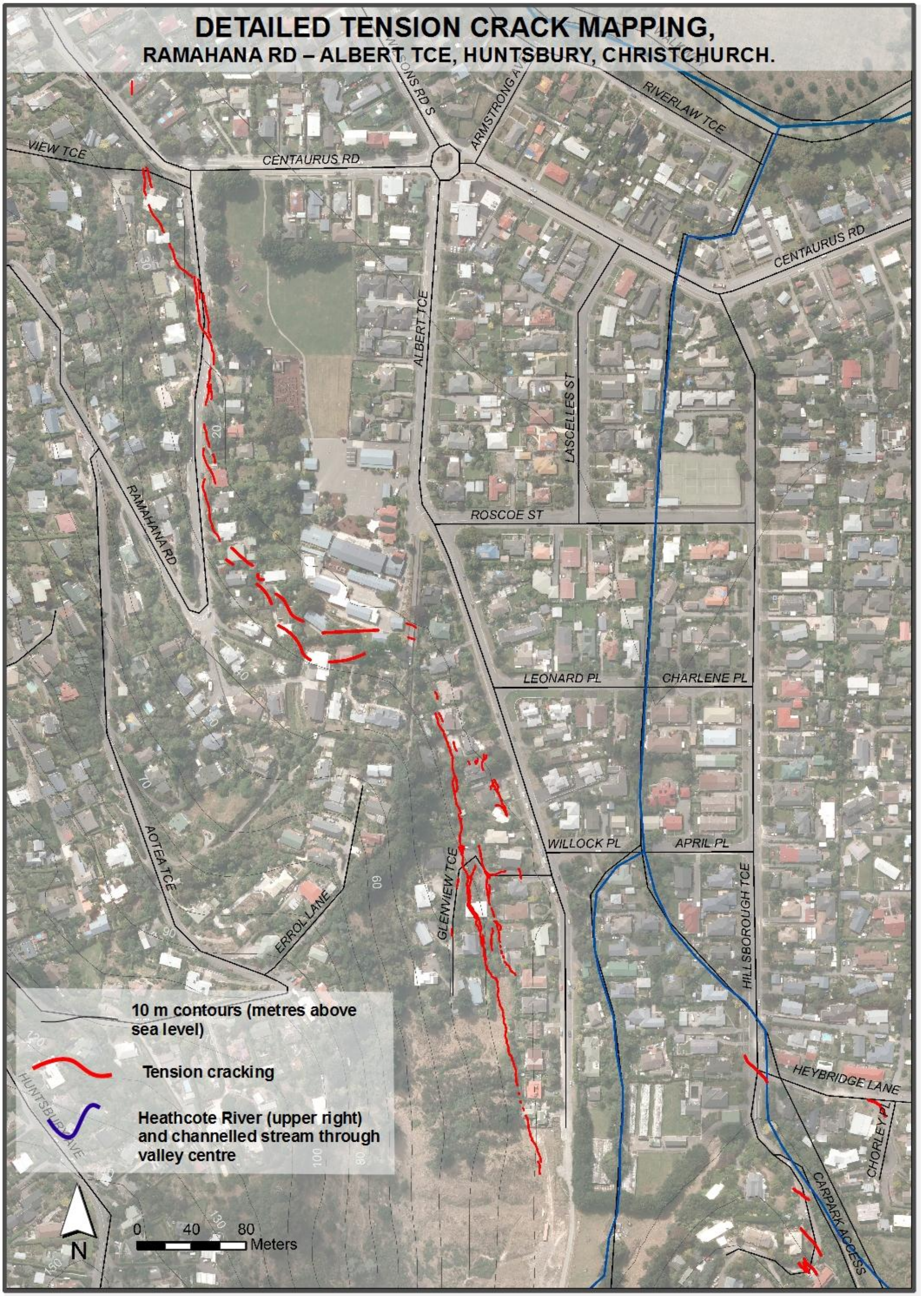

a)

b)

Figure 4.12 Photographs taken at either end of the fissure trace. (a) The author alongside the fissure trace as it crosses Ramahana Road, 50 m south of the Centaurus Road intersection. Photo: J. Claridge. (b) The fissure trace ended in empty sections to the south of Albert Terrace.

The fissure trace varied in appearance along its length, sometimes tapering out completely for a short distance, only to reappear in the next property. While there was one more dominant fissure trace, which was notably the larger and more continuous, there were nearly always subsidiary fissures to this main trace, usually occurring up to 20 m down slope from the main trace (Figure 4.13).

Figure 4.13 Subsidiary fissure trace apparent as approximately 30 mm cracking in kerbing of Glenview Terrace, 20 m up-slope from intersection with Albert Terrace.

Dimensions of the fissure varied along its length, with both the horizontal and vertical offsets being up to 0.30m, although normally in the order of 0.10 m, with vertical offsets being smaller than their horizontal counterparts. Ascertaining the depth of a fissure posed difficulties as the loose loess had often fallen in on itself, effectively blocking the base of the fissure; however in some cases it was possible to extend a rigid tape measure into the fissure by over 1 m, and occasionally to depths of greater than 5 m.

Figure Figure 4.14 provides a detailed cross section of the western Hillsborough Valley fissure system. The reader is referred to Figure 3.9 and related discussion for a detailed cross-section drawn east to west through the Hillsborough Valley. It was decided to produce the cross-section in Figure 4.14 with a down-ridge orientation, and two bends, thus enabling it to

begin at the Huntsbury Reservoir site on the western ridge of the Hillsborough Valley, pass through the area of fissuring and spring behaviour at Centaurus Road, and continue towards the Heathcote River, where riverbank lateral spreading was observed.

The cross section shows the beginnings of the shearing that was observed below the Huntsbury Reservoir, though it does not attempt to provide possible linking between this fracturing and the fissure and springs below. The fissuring at Centaurus Road is some 10 m in elevation lower than that in the central of the Hillsborough Valley fissures, however it is still apparent that the fissuring is occurring in the foot-slope positions of the hillside in this location, as opposed to the Maffeys Road-La Costa Lane fissures, which occur at higher elevations on the hillside.

Compressional features were observed on Centaurus Road, which in this instance coincided with the seepages, emerging from driveways on the southern side of the road. These, as well as the flowing springs (discussed in more detail in Section 4.7) have also been located on the cross section. The area the cross section passes through at Centaurus Road is unusual in that it is the only site where spring flow and fissuring have been in such close proximity, in fact, the springs below 211 Centaurus Road appear to be emerging from within a fissure itself.

The Heathcote River is some 600 m from Centaurus Road, and is underlain by approximately 50 m of Christchurch Formation silts and sands (Brown & Weeber 1994). At this distance and with such different subsurface circumstances the lateral spreading observed near the Heathcote River does not appear to be related to the fissuring and compression movement near Centaurus Road.

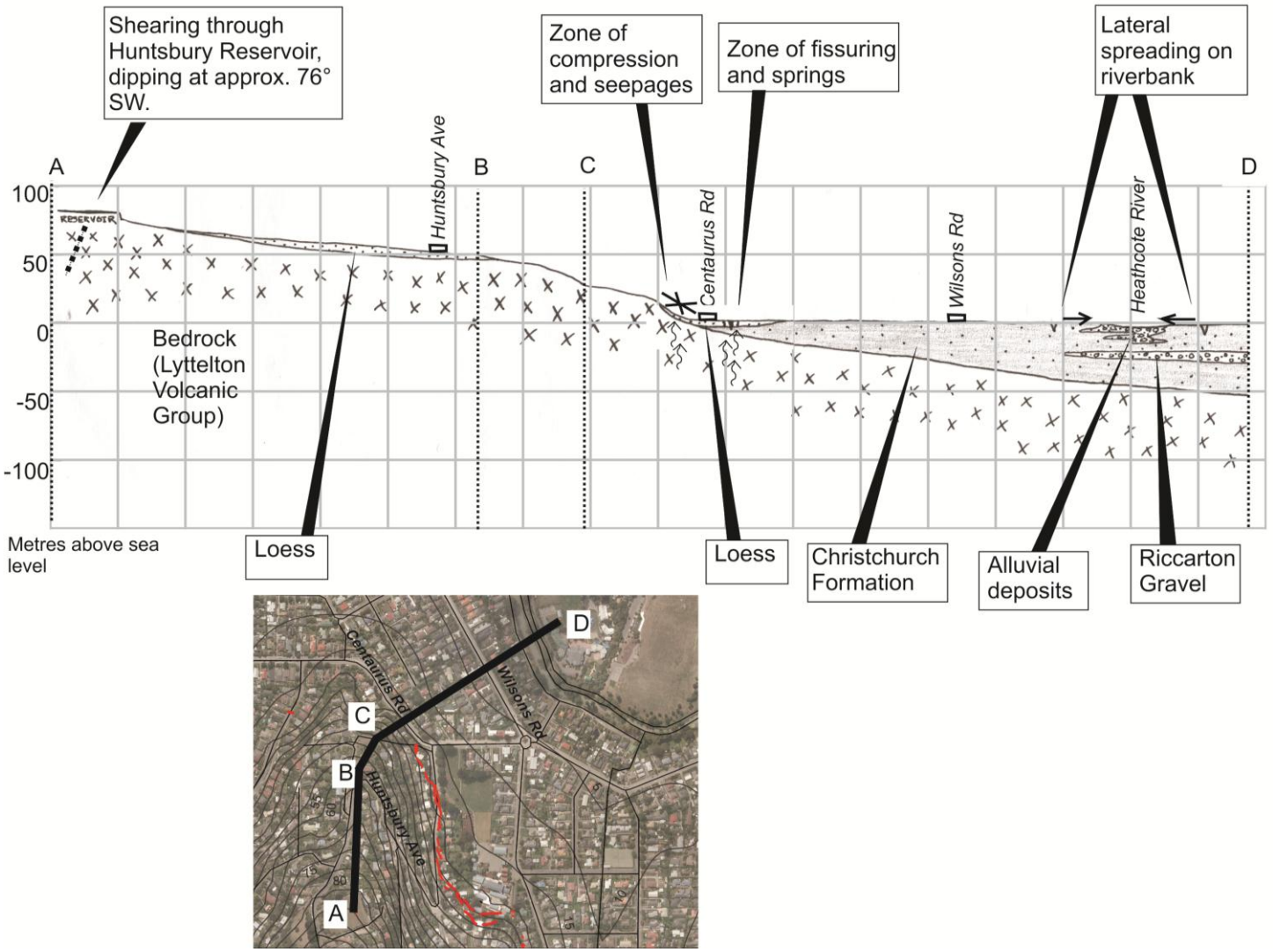

Figure 4.14 Schematic cross section from Huntsbury Reservoir, through fissuring and spring appearance at Centaurus Road, to Heathcote River.

4.3 Case study focus location: 1 and 3 Glenview Terrace, Huntsbury

Detailed mapping and field investigation has been undertaken at two properties, 1 and 3 Glenview Terrace, Huntsbury. On these sites, fissures were recorded in greater detail and push-tube soil samples were taken for laboratory analysis from an excavation site at 3 Glenview Terrace. Initial inspection of 3 Glenview Terrace took place after the owner of the property, who was concerned about the appearance of open fissures crossing his yard after the Christchurch Earthquake, brought it to the attention of the Port Hills Geotechical Group. The fissuring at 3 Glenview Terrace became the main site of investigation for this study, as it provided a typical case of the fissuring, as well as some of the more defined vertical and horizontal offsets, and one of few locations where evidence of the direction of movement of the down-thrown side was observed – a measureable offset feature indicating a fissure opening orientation of 046°. A detailed engineering geological sketch plan of these two properties is provided in Figure 4.15.

The effects of the June Earthquake were initially considered to be minimal in the Glenview Terrace area, with the owners reporting no changes to the tension cracks in their properties. Following a heavy (for Christchurch) snowfall on 25 July 2011, the subsequent melt-water was observed to flow into open tension cracks which had not undergone remedial infilling work or put in place measures to prevent surface water entrance. This was noted by the owners of 3 Glenview Terrace, where constant flows of melt-water were experienced for several days following the snowfall. Five days after the snowfall, on 30 July 2011, the owner of 3 Glenview Terrace reported the sudden appearance of a large cavity, of approximately $1m^3$, in his back garden, directly over one of the fissure traces (Figure 4.16).

Figure 4.15(over page) Engineering geology sketch plan of 1 and 3 Glenview Terrace, Huntsbury.

ENGINEERING GEOLOGY SKETCH PLAN

1 and 3 Glenview Terrace

NORTH

FISSURE CONTINUES TO NORTH

Profile Section A - A'

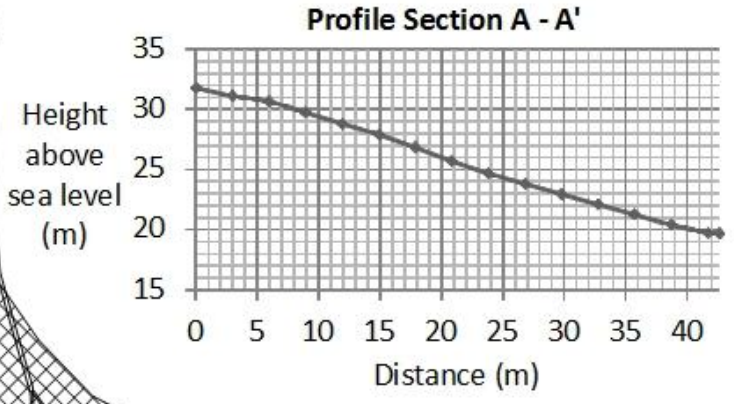

SUBSIDENCE/FILL FAILURE BENEATH ROAD
Larger hole 0.40m deep,
Smaller hole 0.10m deep,
2.2m apart.

Glenview Terrace SEALED R.O.W.

PAVED AREA

TIERED GARDEN LEVELS

FISSURE MEASUREMENTS:
Width: 0.05m
Depth: 0.60m
Drop(East): 0.05m

FENCE

MASS CONCRETE RETAINING WALL
2m high (approx.)

HOUSE FOOTPRINT
Lot 8
DP 22939
1 Glenview Tce.

FISSURE MEASUREMENTS:
Width: 0.05m
Drop(East): 0.05m

FISSURES PASS BENEATH HOUSE
location inferred from entry/exit locations.

FISSURE MEASUREMENTS:
Width: 0.30m
Drop(East): 0.10m
Depth: 0.25m

TUNNEL GULLIES
Three exit points visible, gullies extend ≥0.7m into bank, taper with depth.

FISSURE MEASUREMENTS:
Width: 0.10m
Drop(East): 0.05m

TREES

SHRUBS

A

A'

SUBSIDENCE CAVITY
Subsidence post-June earthquake and snow. Cavity volume approx. 1m³, depth 0.70m.

ACCESS PATHWAY/STAIRS

DRAINS

FISSURE MEASUREMENTS:
Width: 0.20m
Drop(East): 0.10m
Depth: 0.50m

STEEP LOESS EMBANKMENT
approx. location only

HOUSE FOOTPRINT
Lot 7
DP 22939
3 Glenview Tce

FISSURE MEASUREMENTS:
Width: 0.10m
Drop(East): 0.20m

WOODEN RAMP TO GARAGE

FISSURE MEASUREMENTS:
Width: 0.10m
Drop(East): 0.30m

FISSURE OPENING DIRECTION:
036° (approx.)

0 Metres 10

FISSURE CONTINUES TO SOUTH

a)

b)

Figure 4.16 The cavity at 3 Glenview Terrace, on July 30th, 2011. Broken drain has been removed back to junction with white pipe shown. Small section of orange dazzle on grass at edge of hole corresponds to dazzle in Figure 4.7. (a) Facing west, fissure trace crossing left to right. (b) Facing north-west, with arrows delineating in-filled fissure trace.

Upon visiting the site on 30 July 2011, it was noted that there was a breakage in a storm water drain, coincident with the location of the cavity, which was allowing snowmelt to flow directly into the fissure. While it is unknown whether this breakage occurred after the Christchurch Earthquake or the June Earthquake, it is most likely that it was initiated in February, and exacerbated in June, but had not been detected.

After studying original drainage plans of the property, it was decided that the storm water drain was collecting melt water from the roof of the house, and directing it towards a large sump in the North-eastern corner of the section, before being intercepted by the fissure. It was observed that the melt water would flow from the broken end of the pipe, into the cavity, and disappear from view. On this occasion while on site for approximately one hour, "gurgling" sounds were heard from the cavity, which gave the impression of there being another hollow space underground into which the water was flowing at intervals of a few minutes. At this time it was unknown as to where the volume of loess had been removed and as to where the water was being drained.

Two days later, on 1 August 2011, the property was again inspected at the request of the owner. Previously he had been advised to excavate the cavity to attempt to locate its base, before filling with suitable materials. Upon attempting this excavation, he exposed a subterranean tunnel-gully (Figure 4.17) on the northern side of the hole, at a depth of approximately 0.60 m below the ground surface. The gully was tall and narrow, tapering at the top to a hairline crack which continued up most of the distance to the ground surface before becoming too small to locate. Its height was approximately 0.20 m, and width, 0.05 m at its base (Figure 4.18). The inner sides of the gully showed undeniable evidence of the regular passage of water, being particularly smoothed over in places. Fine root systems had entered the tunnel, further indicating that this was a regular passage-way for water, as well as providing proof that it had been in place for some time.

The cavity clearly required immediate attention to prevent further inflow of water. The owner had already prevented further flow from the storm water pipe by using flexible piping around the cavity. He was advised to fill the cavity using a similar method to that already initially successful on the other fissures across his property.

Figure 4.17 Subterranean tunnel-gully exposed in north wall of excavation at 3 Glenview Terrace.

The base of the excavated cavity, up to a depth of 250 mm, and a short distance into the exposed tunnel-gully, was in-filled with a mixture of loess and hydrated lime at a ratio of 20:1. This mixture was manually compacted in several layers in order to provide a non-erodible base layer, as per the studies on Port Hills loess stabilisation by Bell et al. (1986), Bell (1981), Glassey (1986), and Yetton (1986). This base layer was followed by a water-retarding mixture of bentonite clay and SAP-20 gravel up to within 150 mm of the ground surface. This was the same combination that was used to fill the tension cracks elsewhere. The hole was topped with a layer of concrete which served as a stable base for the drainpipe when it was re-piped across the fissure at a later date. A schematic diagram of the excavation is shown in Figure 4.18.

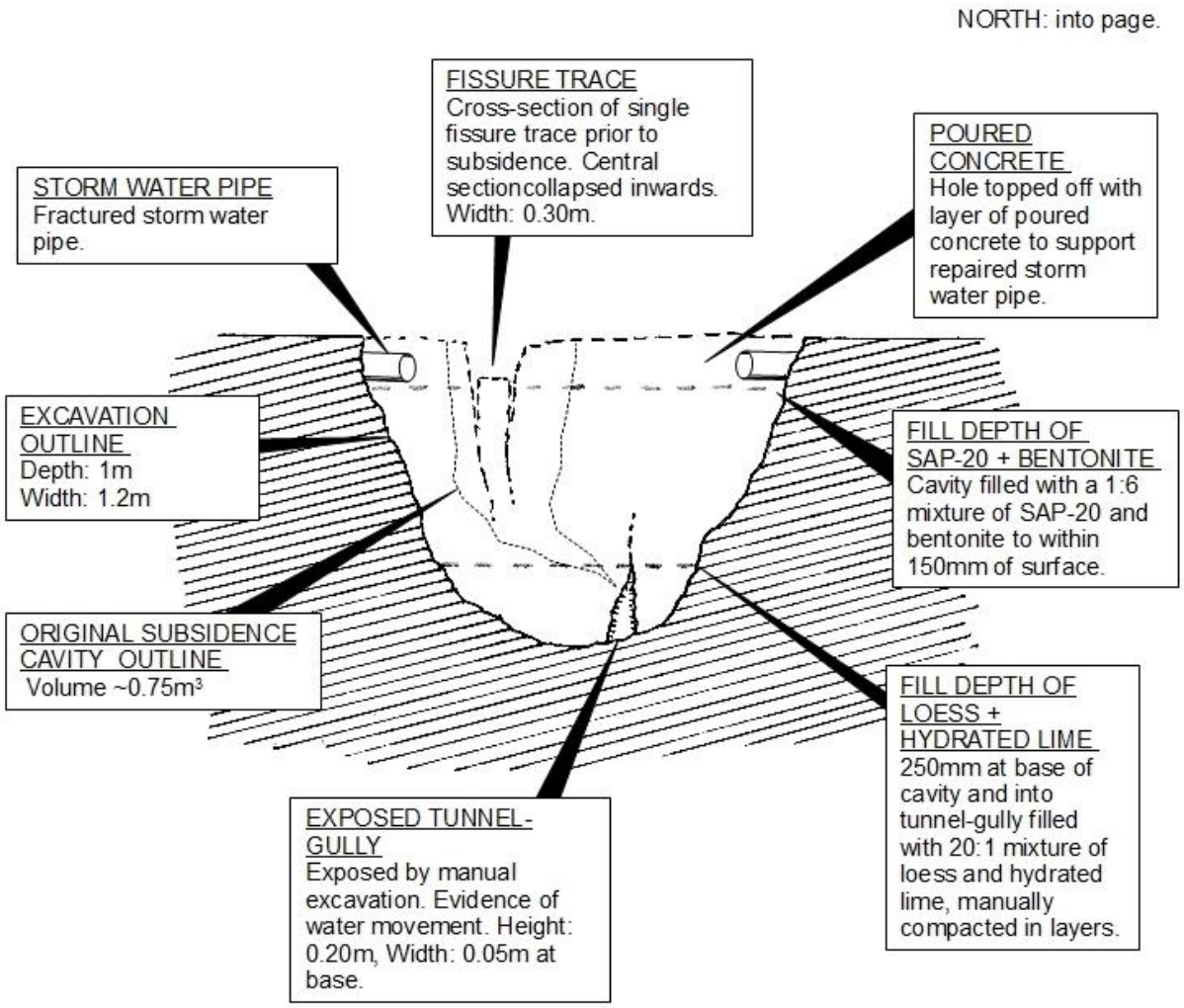

Figure 4.18 Schematic diagram of cross-section through subsidence cavity at 3 Glenview Tce and subsequent excavation showing fissuring and relationship to subterranean tunnel-gully system. Storm water pipe flow is from left to right across the diagram.

While conducting engineering geological site investigations at 3 Glenview Terrace, it was observed that the section had already experienced tunnel-gullying in the loess material. Three exit-holes were found at the north-eastern corner of the house, at the base of the steps leading to the back of the section. Their location is mapped in Figure 4.15. The tunnel-gullies extended up to 0.60 m into the loess bank before tapering closed. It is thought probable that these exit-holes would extend upwards into the loess bank as smaller fissures within the loess, allowing the passage of groundwater. As water exited the bank, over time it has gradually carried greater quantities of loess, forming the enlarged exit holes as seen in Figure 4.19. Tunnel gullying was also observed in the empty sections at the southern end of Albert Terrace, and it may be assumed therefore that this occurrence is prevalent over the hillside in this area.

Figure 4.19 Exit-hole of one of three tunnel-gullies observed at 3 Glenview Terrace.Wooden posts have a width of 12 cm.

4.4 Case study focus location: 40 Rapaki Road

Detailed mapping and field investigation of the Vernon Terrace-Rapaki Road fissure has been undertaken by the author at 40 Rapaki Road which was visited on May 13th, 2012. Fissures throughout the section were recorded in greater detail, and push-tube soil samples were taken for laboratory analysis. The site offered an ideal case study as it was located almost directly opposite 1 and 3 Glenview Terrace on the other side of the valley.

Figure 4.20 Fissure trace through 40 Rapaki Road at the point of greatest offset.

The owners of the property had elected not to fill their fissures for insurance purposes, and had prevented water infiltration by means of tarpaulin covers. This meant that the fissures were retained in an almost as-formed condition, with very little soil collapse or grass growth. The lack of water infiltration also meant, however, that the ground directly below the tarpaulins was,

although not completely dry, distinctly drier than the surrounding area. It was also a fairly large section, thus offering a good distance (approximately 60 m) of the fissure trace for observation.

The main fissure ran in a straight line through the property of 40 Rapaki Road, on an orientation of approximately 320°. There were three subsidiary fissures, at a higher elevation than the main fissure, all trending sub-parallel to the main fissure. These were up to 8 m long, and were distinctly thinner and showed less movement than the main fissure. The main fissure was 0.12 m wide at its widest point, and also had a maximum drop to the west of 0.12 m, however these measurements were not taken from the same location along the fissure. Depth was measured using a metal tape, and was found to be 0.70 m at the deepest point. Depth was harder to ascertain in many places as fragments of the sides of the cracks had a tendency to fall inwards. A detailed engineering geology sketch plan of the site at 40 Rapaki Road is shown in .

Measurements of the horizontal width, vertical offset and depth of the fissure were taken at multiple sites along the length of the fissure (Figure 4.22). Depth was harder to measure in all places, as the fissures were sometimes slightly curved below ground, and the dry loess of the sides had a tendency to fall inwards. Using a rigid tape measure it was possible, however, to get a good indication of the open fracture depth. This varied greatly across the section at 40 Rapaki Road, with the greatest measurement recorded being 0.70 m, while just 10 m away the fissure tapered closed and for a short distance had no measureable depth. The width of the fissure trace at 40 Rapaki Road was narrower than that observed on the opposite side of the valley at 3 Glenview Terrace. The average width was 70 mm, and the average drop (to the west) was 60 mm.

Figure 4.22 Measuring the vertical offset of the main fissure at 40 Rapaki Road.

Figure 4.21 (over page) Engineering geology sketch plan of 40 Rapaki Road, Huntsbury.

ENGINEERING GEOLOGY SKETCH PLAN

40 Rapaki Road

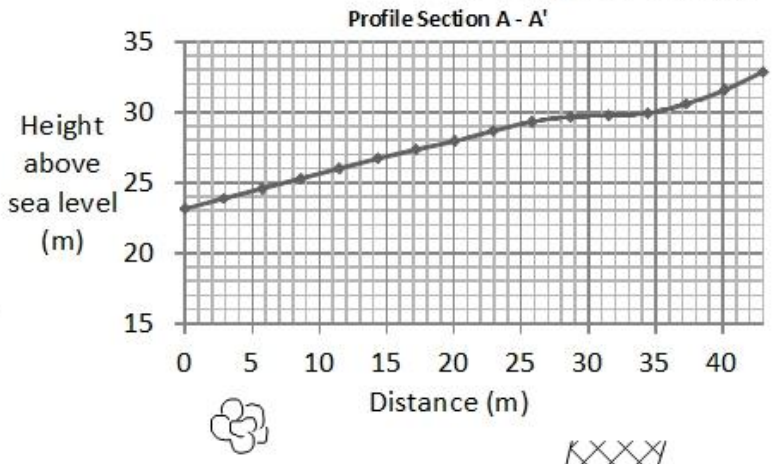

NORTH

FISSURE CONTINUES TO NORTH

FENCE

SHRUBS

TREES

SAMPLE LOCATION
Excavated around fissure to depth of 0.60m

FISSURE MEASUREMENTS:
Width: 0.10m
Drop(West): 0.05m
Depth: 0.40m

FISSURE MEASUREMENTS:
Width: 0.11m
Drop(West): 0.05m
Depth: 0.70m

FISSURE MEASUREMENTS:
Width: 0.12m
Drop(West): 0.09m
Depth: 0.60m

FISSURE MEASUREMENTS:
Width: 0.12m
Drop(West): 0.05m
Depth: 0.65m

FISSURE MEASUREMENTS:
Width: 0.01m
Drop(West): 0.01m
Depth: 0.00m

FISSURE MEASUREMENTS:
Width: 0.05m
Drop(West): 0.00m
Depth: 0.30m

FISSURE MEASUREMENTS:
Width: 0.08m
Drop(West): 0.12m
Depth: 0.28m

FISSURE MEASUREMENTS:
Width: 0.03m
Drop(West): 0.12m
Depth: 0.28m

FISSURE MEASUREMENTS:
Width: 0.05m
Drop(West): 0.05m
Depth: 0.48m

CONCRETE RETAINING / FACING WALL
<1m high (approx.)

HOUSE FOOTPRINT
Lot 4
DP 9173
40 Rapaki Rd.

FISSURE MEASUREMENTS:
Length: 5.40m
Width: 0.05m
Drop(West): 0.07m

FISSURE CONTINUES TO SOUTH

ACCESS PATHWAY/STAIRS

SHARED DRIVEWAY
Off Rapaki Road

A

A'

0 Metres 10

4.5 Laboratory Analysis

4.5.1 On-site data collection methods

Loess samples were collected from 3 Glenview Terrace on 1 August 2011. A push-tube sampler was used to collect four short (pinhole) tubes, and four long (density) tubes from a depth of 0.70 m and 1.50 m from within the post-snowfall excavated cavity. Some bulk loess material was also collected. All samples were double-bagged in air-tight "snap-lock" bags to ensure their water-tightness. The samples were then used in a series of laboratory tests including laser particle sizing, water content and shear box testing.

The engineering geological field description of the Glenview Terrace loess is as follows (based on the Bell and Pettinga (1983) method of presentation of geological data):

Moist, compact, light yellowish brown, massive, silty fine sand with some clay, USCS: ML.

The same push-tube collection and double-bagging method was used to collect loess samples from 40 Rapaki Road on May 13th, 2012. A push-tube sampler was used to collect four short (pinhole) tubes, and four long (density) tubes from a depth of 0.50 m from the largest portion of the fissure, after some further excavation to enable access to a greater depth (Figure 4.23). Bulk loess material was collected from this site as well.

The engineering geological field description of the Rapaki Road loess is as follows (based on the Bell and Pettinga (1983) method of presentation of geological data):

Dry-moist, compact, light yellowish brown, massive, silty fine sand with some clay, USCS: ML.

Figure 4.23 Excavating the fissure at 40 Rapaki Road to enable push-tube samples to be taken from a depth of 0.50 m.

4.5.2 Loess laser-sizing analysis

Approximately 1 cm^3 samples were taken from the loess collected from 0.70 m and 1.50 m depth from the 3 Glenview Terrace site, and from the loess collected from 0.50 m depth at the 40 Rapaki Road site. The procedure followed was the standard laboratory procedure established though previous experimental work at University of Canterbury, and is outlined in Appendix 2. The samples were left at the in-situ water content and Calgon was added to these samples in vials, and left to saturate overnight. To ensure that the samples used for grain size analysis were representative of the total sample, the total sample was thoroughly mixed before testing.

Three trials were performed on the Glenview 0.70 m sample, which produced a mean particle diameter of 64.1 μm, and four trials were performed on the 1.50 m sample, giving a mean particle diameter of 68.6 μm. Three trials were also performed on the Rapaki 0.50 m sample. The results of each of the trials were statistically consistent within their margins of error.

Cumulative log plots of the particle diameter consistently show a small quantity of fines ranging in diameter up to 20 μm, followed by an incremental curve from 20 μm, peaking at roughly 60 μm, and tapering to 200 μm. On all the outputs this was followed by a second, smaller curve, potentially resultant from fragments of organic matter that were visible in the sample, however, it was brought to the attention of the author by members of the Geological Science department that the laser sizing machine has been prone to producing this second curve.

The laser results for the three loess samples show that the grain size of the loess is very similar at each of the locations, on both sides of the Hillsborough valley, although the Rapaki Road sample has a slightly lower clay content, and slightly higher medium-sand content than the Glenview Terrace loess. All of the samples are poorly graded, with silt and fine sand making up 85% of the soil. All loess samples had approximately 50 % silt and 35 % fine sand, 5 % clay and 10 % medium sand-sized particles. According to Alley (1966), Crampton (1985), Yetton (1986), Port Hills loess tends to have between 65-80 % silt-sized particles, so these figures are consistent with their findings, however their clay content estimates were 11-25 %, showing that the loess in the Hillsborough Valley area has a lower than normal clay content.

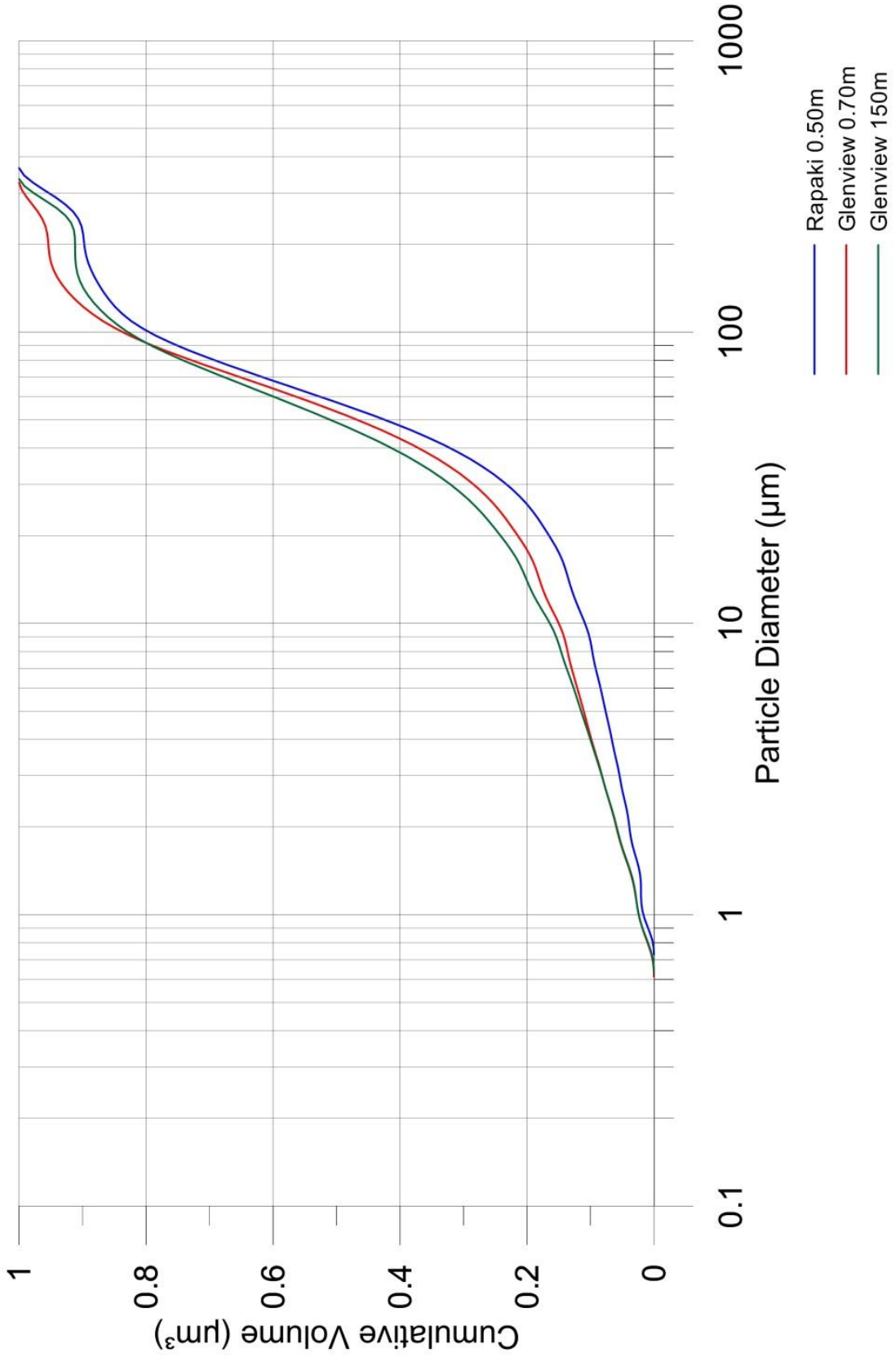

Figure 4.24 Particle size distribution plot for loess samples from 40 Rapaki Road and 3 Glenview Terrace.

4.5.3 Shear-box testing

The direct shear-box was used on loess samples from Glenview Terrace to ascertain the shear strength of the disturbed and remoulded loess from the site. This testing was undertaken with the goal of establishing the geotechnical properties of the loess in order to see whether they corroborate with loess from other Port Hills sites (thus enabling data from previous investigations to be used), and also to provide data for use as input parameters for modelling the failure potential of the soil.

The basic concept of the direct shear-box is the measurement of the shear strength (τ) of a soil by causing failure along a pre-determined horizontal plane whilst subjecting the sample to a load applied normal to that plane (σ_n). By carrying out three or more tests at different normal pressures, a shear strength envelope can be derived, based on the Mohr-Coulomb failure criterion and the effective stress theory for saturated soils, given by the following equation:

$$\tau \leq c' + \sigma'_n \tan \emptyset'$$

where τ on any plane in a soil is less than or equal to the sum of the effective cohesion (c') and the tangent of the internal angle of friction (ϕ') (Terzaghi et al. 1996; Powrie 2004).

The method used was a standard direct shear-box test, using equipment similar to that in Figure 4.25, whereby the shear force and strain at any point during the experiment are calculated by transducers connected to a computer (Smith & Smith 1998). It was decided to conduct the experiments without the use of a water bath in the shear-box (used to prevent samples from drying during the experimental process).

Experimental studies have shown (Lutenegger & Hallberg 1988) that as the moisture content of loess increases, its shear strength decreases towards zero at a liquidity index value of 1. This was corroborated in the laboratory analysis of loess in this study when a water bath was used in the first (trial) run of the shear-box, and it was found that the capillary suction of the loess meant it rapidly absorbed a large quantity of water, inducing an almost immediate reduction in cohesion and the natural peak shear strength of the soil was not reached.

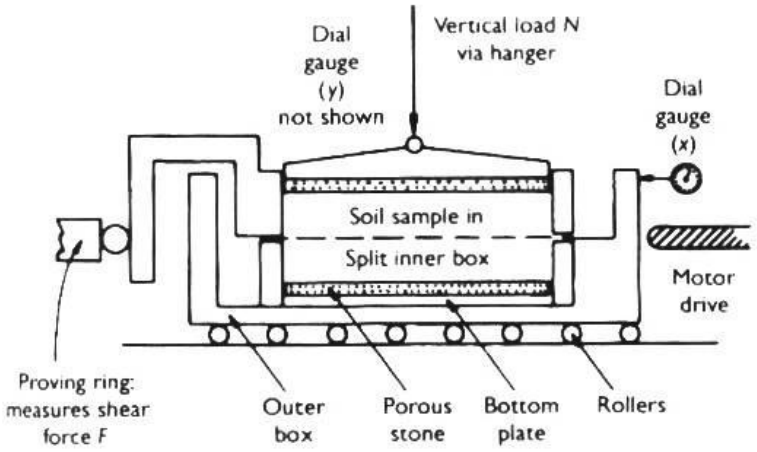

Figure 4.25 Standard shearbox apparatus. After Powrie (2004), p. 81.

Three sets of experiments were carried out: two on samples from 40 Rapaki Road, taken from a depth of 0.50 m, and one on samples from Glenview Terrace, taken from a depth of 1.50 m. Properties of the Rapaki Road and Glenview Terrace loess samples used in the shear strength calculations are summarised in Table 4.1. These values were calculated using samples collected by the push-tube method, following standard methods described in NZGS 4402 Part 1 (1980) Test 1 p.15-17.

Table 4.1 Properties of loess from 40 Rapaki Road and 3 Glenview Terrace.

	Moisture content (%)	**Wet bulk density ($kg.m^{-3}$)**	**Dry bulk density ($kg.m^{-3}$)**
Rapaki Road	6.83	1885	1631
Glenview Terrace	13.5	1995	1858

The first group from 40 Rapaki Road were manually compacted (Figure 4.26) into four rings, and even compaction to near that given in Table 4.1 was estimated through retaining similar mass values. The experiment was carried out using four hanging masses of 1 kg, 2 kg, 3 kg, and 6 kg which equated to overburden pressure depths of 0.76 m, 1.44 m, 2.11 m and 4.14 m respectively for the 1885 $kg.m^3$ density loess.

Figure 4.26 Manual compaction (left) of the loess samples where consistency was achieved by ensuring similarity of mass of samples, and (right) finished sample in ring ready for shearing analysis.

The second group of Rapaki Road loess samples were compacted using the New Zealand Standard Compaction Test 4.1.1 (Standards Association of New Zealand 1986) using a Proctor mould as a means of comparison to establish the validity of the initial tests. The test uses a cylindrical metal apparatus, within which the soil is compacted in three layers using a hammer which is released from a constant height, 27 times for each layer (Figure 4.27). The method followed is a variation on the Proctor Test, a laboratory test described by Das (2002) and McNally (1998) which was developed by R.R. Proctor in the 1930s. Their tests found that with increasing moisture content, the compaction and strength of the loess also increases, up to a maximum dry density of 1.814 $t.m^{-3}$ (which may exceed the original strength of the unexcavated loess), and optimum water content of 13 %, after which the compaction and strength of the loess will decrease if further water is added.

To reach optimum water content, dry loess was mixed with a calculated volume of water to achieve water content of 13%, however, later tests showed water content was 14.3%, likely due to there being some residual moisture within the loess in the beginning. Three tests were conducted on these Proctor-compacted samples from Rapaki Road, using hanging masses of 1 kg, 2 kg and 3 kg, with corresponding overburden pressure depths being the same as above.

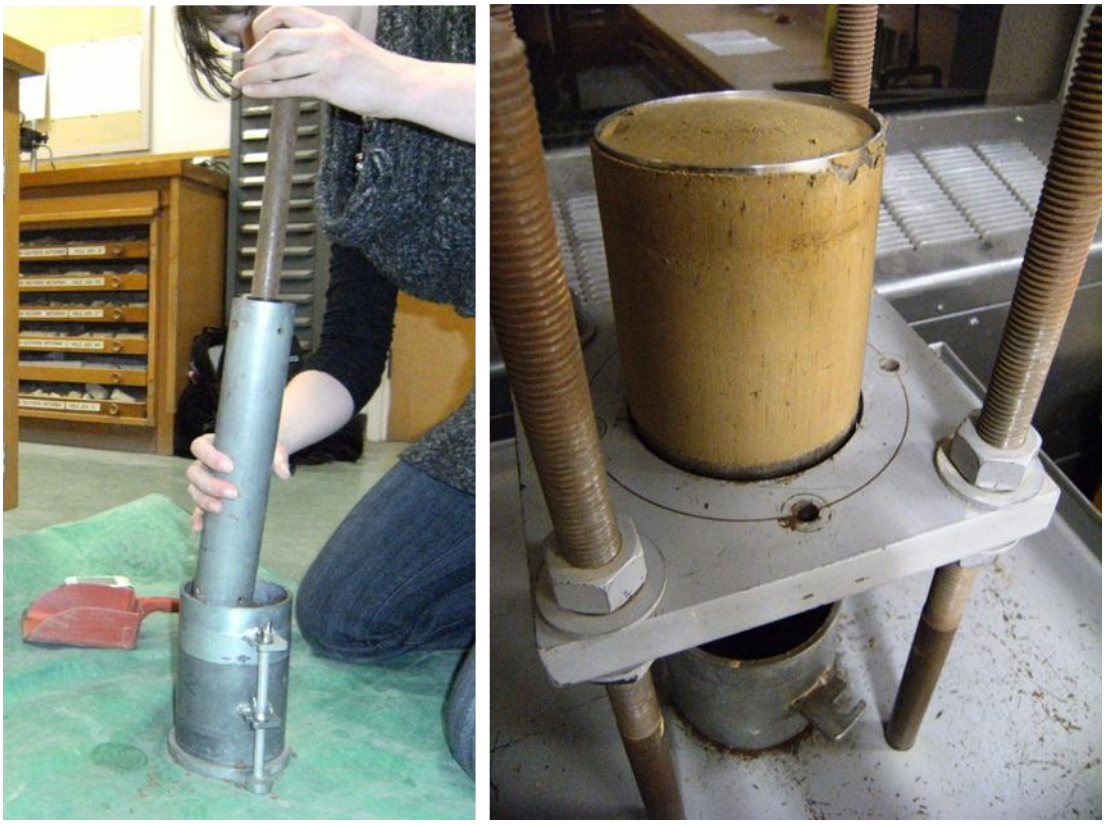

Figure 4.27 (left) Compacting three layers of loess within the Proctor mould, using 27 vertical blows of the hammer. (right) Compacted loess being extruded from mould into rings for shear strength analysis.

The third group of samples, taken from 3 Glenview Terrace, were also manually compacted in the fashion of the first group from 40 Rapaki Road. These experiments were also conducted using four hanging masses of 1 kg, 2 kg, 3 kg, and 6 kg which equated to overburden pressure depths of 0.72 m, 1.36 m, 2.00 m and 3.91 m respectively for the 1995 kg.m^3 density loess.

Most samples produced a slightly convex shear plane (Figure 4.28), although removal of the top layer of loess to observe the plane proved difficult. Figure 4.28 shows a sheared sample of Glenview Terrace loess. The direct shear test data was collected by the computer in the form of shear stress over time (equivalent to displacement), and the graphs thus produced are shown in Figure 4.29, Figure 4.30, and Figure 4.31.

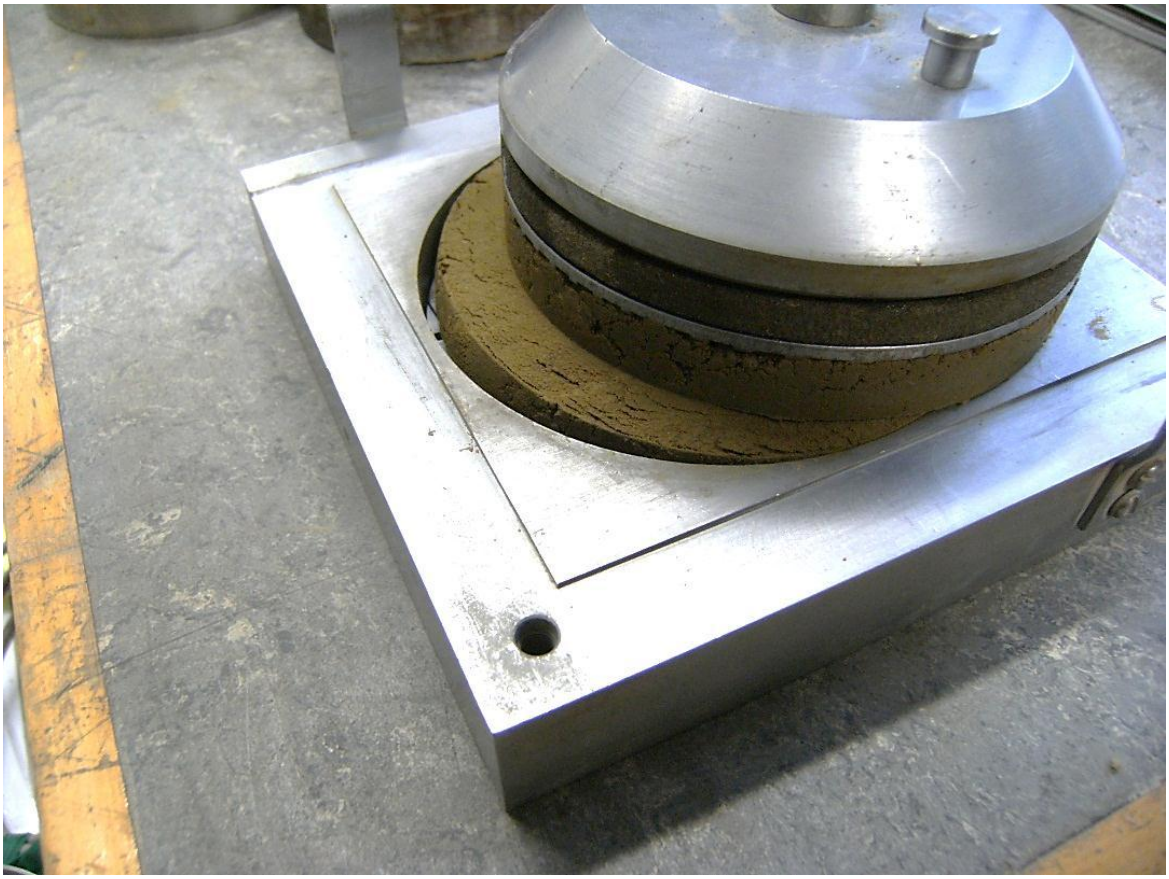

Figure 4.28 Completed shear of Glenview Terrace loess.

The normal stresses (σ_n in Pa) are calculated by adding the force from the hanging masses to the additional (1.29 kg) weight of the top plates, all multiplied by the force of gravity and divided by the area of the sample (7.85×10^{-3} m^2). These normal stress values are then plotted (Figure 4.32, Figure 4.33, and Figure 4.34) against peak shear stress values, to carry out a Mohr analysis on the loess. Peak shear stress is calculated as being the result of dividing the peak force applied by the shear test apparatus by the surface area of the sample. Using these results the cohesion and internal friction angle for each of the loess samples were able to be calculated. Final results are provided in Table 4.2 and Table 4.3

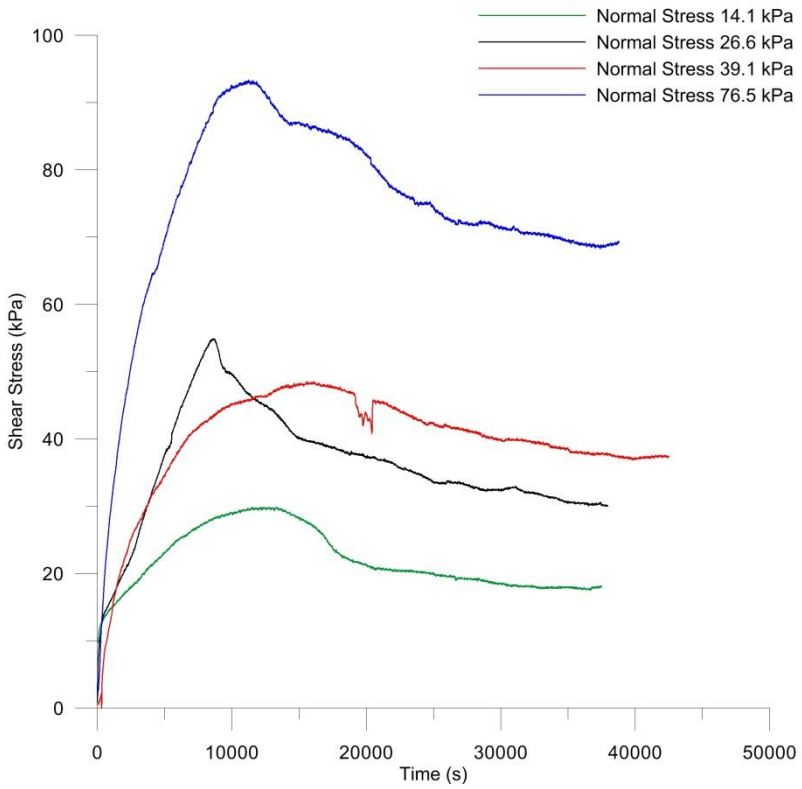

Figure 4.29 Glenview Terrace loess shear stress over time at different applied normal stresses.

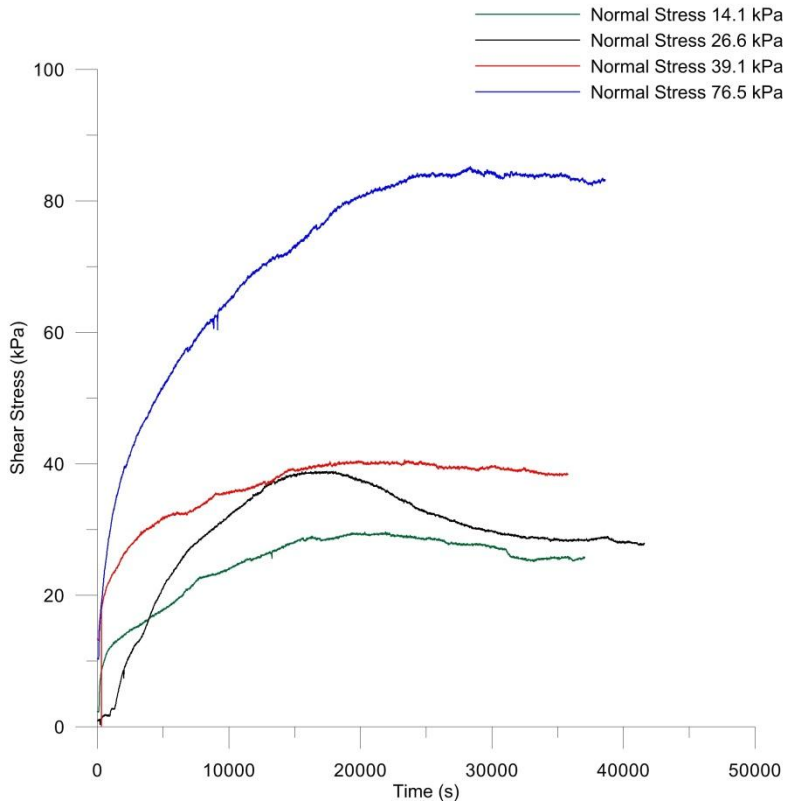

Figure 4.30 Rapaki Road loess shear stress over time at different applied normal stresses.

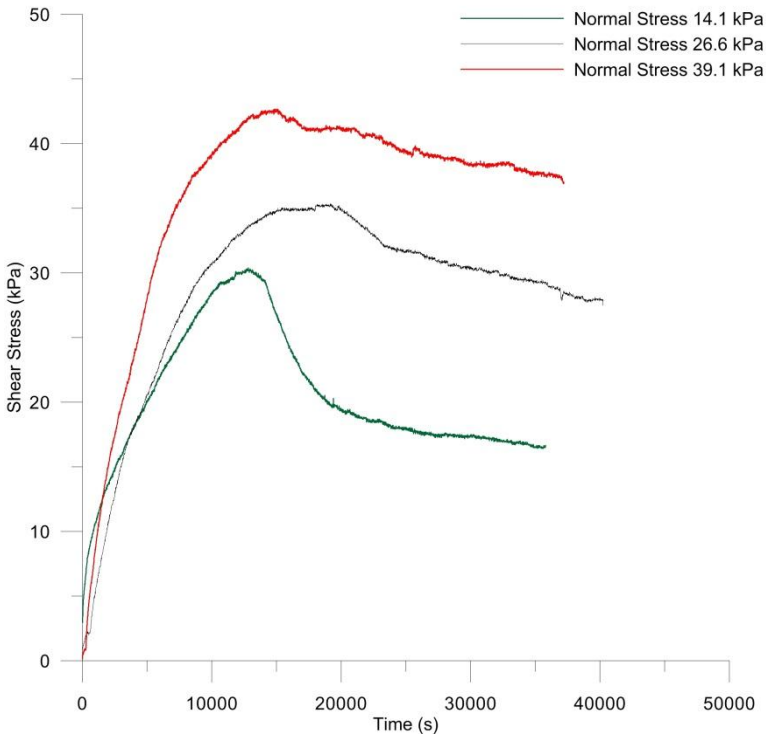

Figure 4.31 Rapaki Road loess shear stress over time at different applied normal stresses, loess at standard compaction.

The loess soil strength is estimated from using the data above through use of the Mohr-Coulomb failure condition, whereby when the state of stress on the soil falls along the line plotted in Figure 4.32, Figure 4.33, and Figure 4.34, the soil will fail. Above this line is an impossible state of stress, and below this line are stress states where the soil will not fail (Smith & Smith 1998). From these plots the values for cohesion, c (kPa) and the internal friction angle, ϕ (degrees) were established. The c values for the 40 Rapaki Road, 3 Glenview Terrace and compacted 40 Rapaki Road loess samples were 13.4 kPa, 19.7 kPa and 28.6 kPa, respectively. The corresponding ϕ values were 42.0 °, 43.4 °, and 18.4 °. Goldwater (1990) stated that c and ϕ values for Port Hills loess are usually 0-20 kPa, and approximately 30 °. The figures from the experiments in this study are roughly similar to those of Goldwater, but there is a wider range of variability.

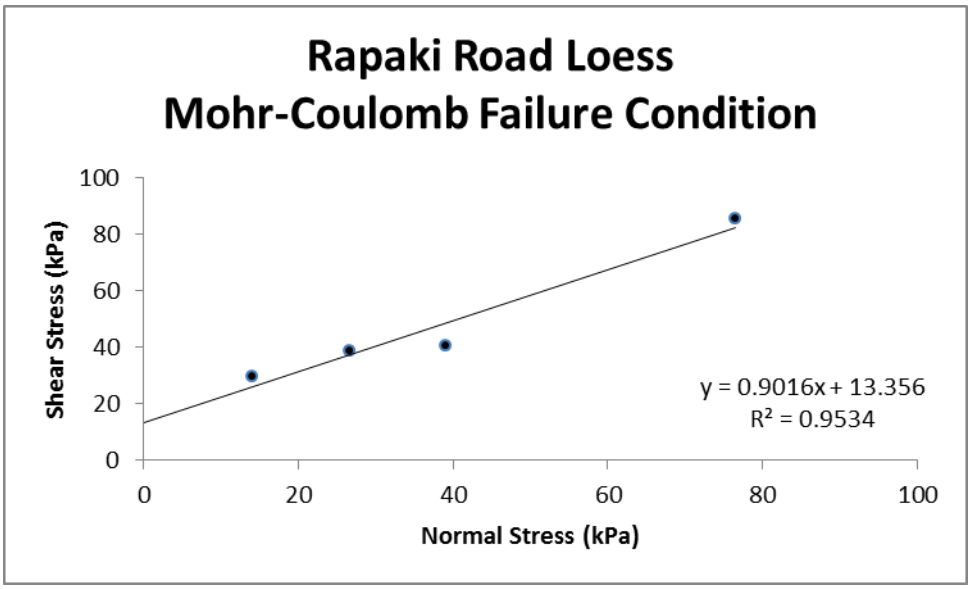

Figure 4.32 Normal vs. shear stress plot for loess samples from 0.5 m depth at 40 Rapaki Road.

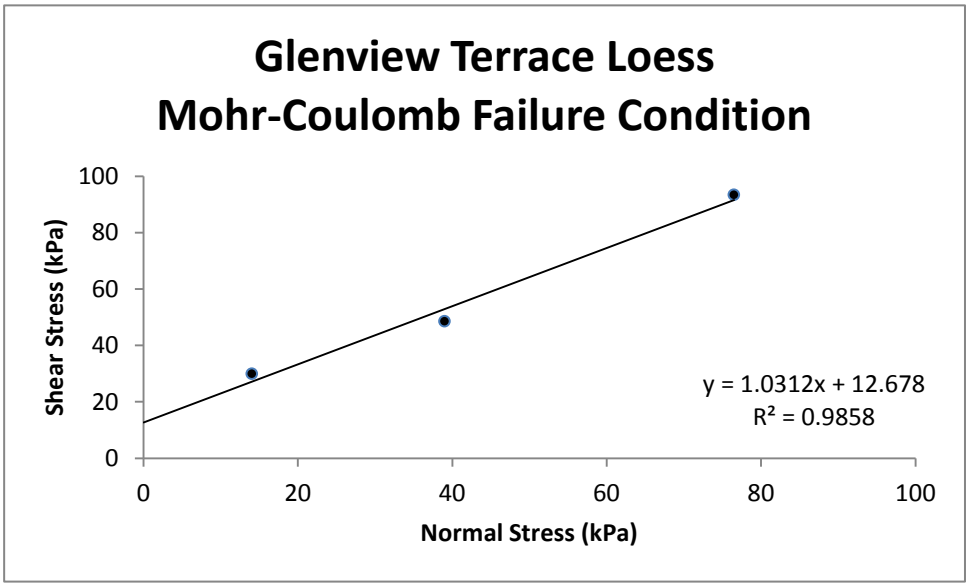

Figure 4.33 Normal vs. shear stress plot for loess samples from 1.5 m depth at 3 Glenview Terrace.

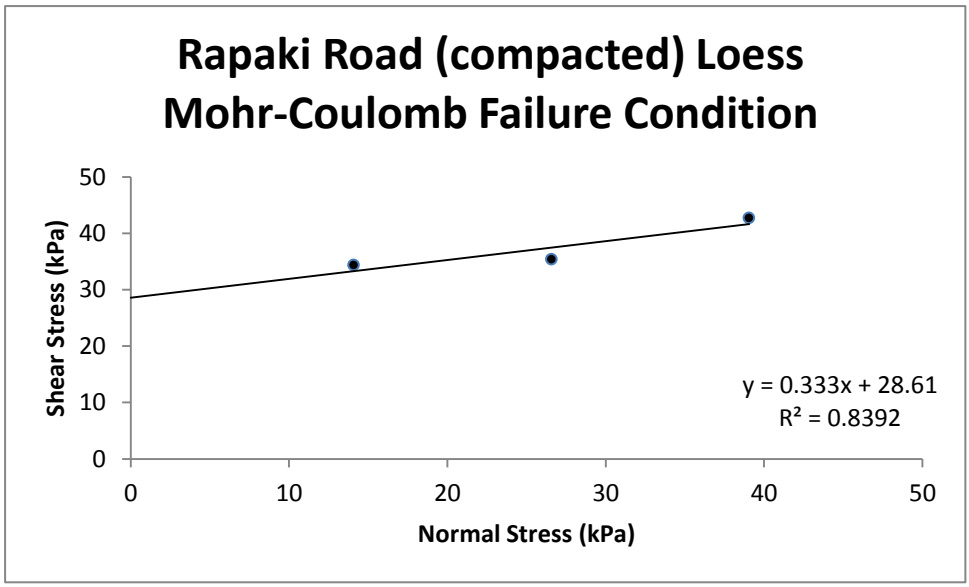

Figure 4.34 Normal vs. shear stress plot for compacted loess samples from 0.5 m depth at 40 Rapaki Road.

Table 4.2 Results of shear strength analysis of Rapaki Road and Glenview Terrace loess.

Sample	Mass of sample (g)	Mass of weight applying normal force (kg)	Peak force on sample (N)	Peak Shear Stress, τ (kPa)	Peak Normal Stress, σ_n (kPa)	Effective Overburden Depth (m)	Cohesion, c (kPa)	Angle of internal friction, ϕ (°)
R1	212.5	1	232.5	29.6	14.1	0.76	13.4	42.0
R3	220.4	2	305.2	38.9	26.6	1.44		
R2	211.8	3	318.9	40.6	39.1	2.11		
R4	216.8	6	669.3	85.2	76.5	4.14		
G1	337.0	1	234.7	29.9	14.1	0.72	19.7	43.4
G4	334.2	2	431.2	54.9	26.6	1.36		
G2	326.5	3	380.9	48.5	39.1	2.00		
G3	320.0	6	733.3	93.4	76.5	3.91		

Table 4.3 Results of shear strength analysis of Rapaki Road loess (Procter compacted).

Sample	Mass of weight applying normal force (kg)	Peak force on sample (N)	Peak Shear Stress, τ (kPa)	Peak Normal Stress, σ_n (kPa)	Cohesion, c (kPa)	Angle of internal friction, ϕ (°)
RP1	1	269.8	34.4	14.1	28.6	18.4
RP2	2	277.7	35.4	26.6		
RP3	3	335.1	42.7	39.1		

The loess samples from the Rapaki Road site in the not Procter compacted test (Figure 4.30) behaved very plastically, with little or no peak strength visible in the plots as the test went almost directly to residual strength. This was further evidenced by its low calculated cohesion value of 13.4 kPa. In the laser-sizing analysis (Chapter 4.5.2), the Rapaki Road loess was shown to have a slightly lower clay fraction than the Glenview Terrace loess, which could have produced lower cohesion. Furthermore, the Rapaki Road samples in Table 4.2 have lower masses than the Glenview Terrace samples to which the same test was applied. This shows that the Rapaki Road samples which were tested in the shear box had a lower density than the Glenview Terrace samples, and this would also have reduced the peak shear strength in the test. Results from the two non-Procter compacted trials gave cohesion results which compared favourably with those of other authors, such as Goldwater (1990), however with angles of internal friction of 42° and 43° for the Rapaki Road and Glenview Terrace sites, respectively, which are more than 10 degrees higher than the value of 28° which Goldwater (1990) and Bell (2012, pers. comm.) agree to be more appropriate for Port Hills loess. This may be due to experimental method, or abnormalities of the Hillsborough Valley loess itself.

The samples which had undergone Procter compaction showed a marked difference in Mohr-Coulomb parameters, with a cohesion of 28.6 kPa, and an internal friction angle of 18.4°, shown visually in Figure 4.34. The trend line of this plot is noticeably nearer the horizontal than those of Figures 4.32 and 4.33, demonstrating the effect that the Procter compaction had on the loess sample. The cohesion value of 28.6 kPa is markedly higher than the norm for Port Hills loess, which was calculated by Goldwater (1990) to be between 0 – 20 kPa. As well as this high cohesion value, the Procter compaction resulted in a very low angle of internal friction (18.4°, where Golderwater's work showed 28° to be the norm). These results were unexpected, and may be due to the test method used, and the manner in which the recompacting of the loess would have likely destroyed some of the natural electrostatic bonds. Based on these outcomes, and in comparing them to the work of others such as Goldwater (1990), it is concluded that

Procter compaction of loess soils is not necessary in shear strength analysis, and may in fact produce erroneous results.

In the process of carrying out the above procedure, assumptions were made in order to simplify calculations. These assumptions included:

- Loess samples are understood to be identical between each of their trials under different weights, i.e. the hanging weights are the only independent variable.
- The density of the loess is assumed to be homogenous, and was calculated using push-tube loess samples where a volume was able to be measured.
- Vertical force applied by the weights under gravity represents the normal load on the plane of failure – since the shear plane direction is necessarily horizontal (Smith & Smith 1998).

Error analysis for the experiment was not carried out, as the errors inherent to the apparatus used were unknown. This makes the validity of the experiment questionable since error margins are not reported with the findings, but since the readings were taken directly by computer, mechanical errors should be minimal. Computational errors could have been introduced through human fault, although as most calculations were computerised, and rounding was kept to a minimum, these should also be negligible. For greater accuracy of the experiment, it would have been ideal to have larger quantities of loess available to conduct further trials, and to have all trials performed at standard compaction. Ideally, *in situ* borehole shear tests would be conducted in the field, as the shear strength of loess is dependent on its structure.

4.6 Resistivity Survey: Centaurus Park

A resistivity survey was carried out across Centaurus Park, near the intersection of Ramahana Road and Centaurus Road. Resistivity was selected as the geophysical method of choice due to its ability to differentiate between soil types of different conductivity values, and it was anticipated that the loess or loess colluvium on that site would have a distinctly different signature to the bedrock below. It was intended that the survey would pick up the bedrock interface and/or signs of spring or fissure formation, however the length of the line and spacing of electrodes (and thus, the depth of penetration) was limited by housing and paving in the area.

Based on approximate values from Sharma (1986), it was expected that any igneous bedrock would show up as highly resistive, with values of higher than 100 Ωm, potentially up to 10 000

or 100 000 Ωm, while a clayey silt would be much more conductive, being likely to have values within the range of 1-100 Ωm.

In a resistivity survey, a direct current is injected into the ground by means of metal electrodes which are inserted a short distance into the topsoil. Electrical geophysical investigation methods are particularly sensitive to water content and water quality (Nobes 2003), and as such resistivity was selected as the method of choice for this investigation.

4.6.1 Methods

The resistivity survey was conducted in July 2012 at Centaurus Park. The maximum line length possible was 96 m due to the presence of houses and paved roadways in the area, and it was not possible to pass the survey directly across the Ramahana Road fissures. It was decided to align the survey approximately perpendicular to the fissure trace, thus running on a diagonal through the park (this also enabled greater use of the available space). The weather in previous days had been wet, and on the day of the survey there was occasional light rain, meaning the topsoil was saturated and ideal for conducting electricity. An area of boggy ground was noted near the centre of the survey, extending between electrodes 33 and 45 (Figure 4.35).

A 64-electrode configuration was employed, with electrodes being inserted into the ground every 1.5 m for a distance of 96 m. The hole into which each electrode was inserted was saturated with salt-water prior to insertion of the electrode to ensure greater surface connectivity.

Using a Wenner array setup, the computer programme RES2DINV was used to automatically determine a two-dimensional resistivity model for the subsurface, based on an inverted triangular arrangement of rectangular blocks which are combined with the data points in the pseudosection collected by the computer.

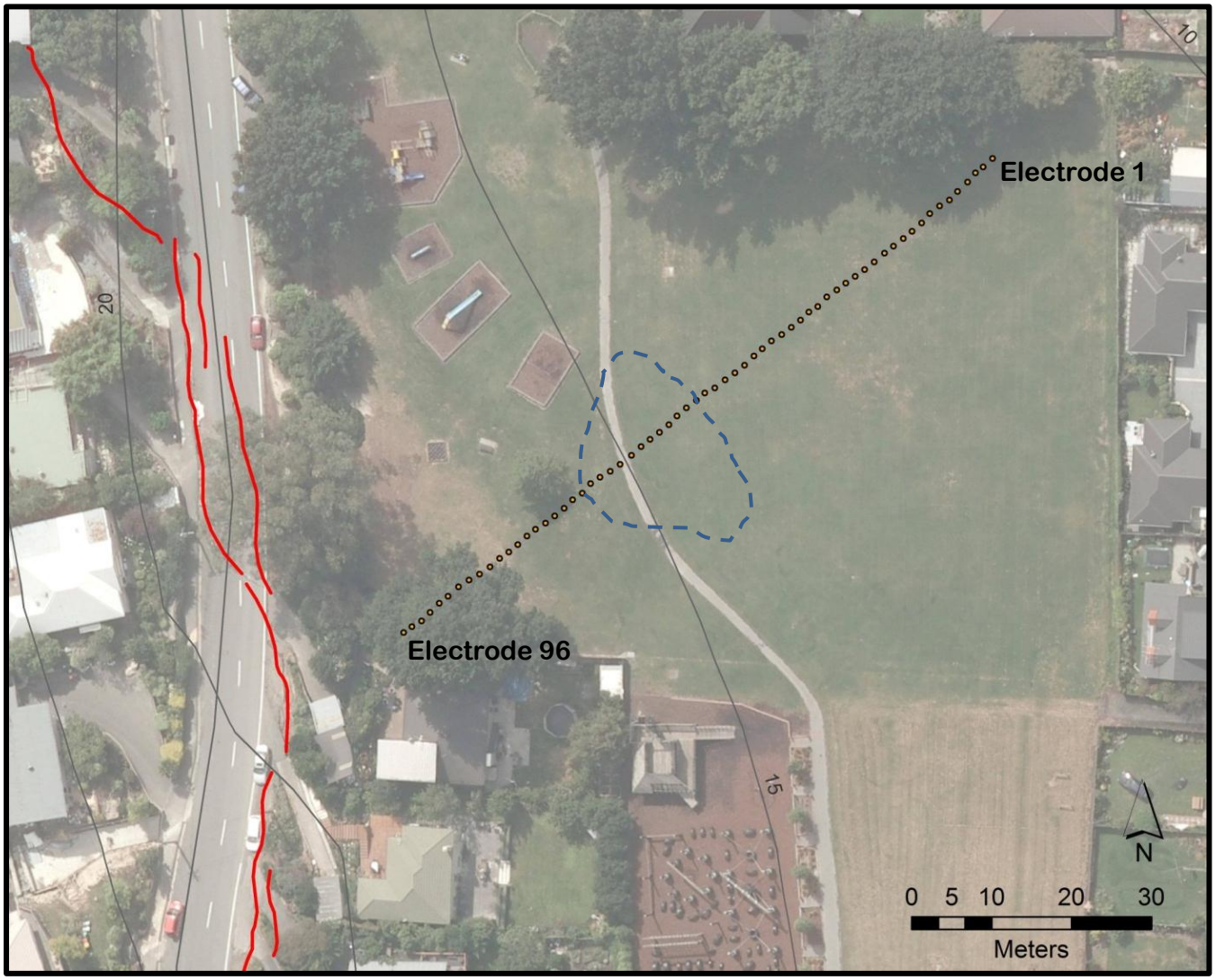

Figure 4.35 Centaurus Park resistivity survey electrode placing with upper right end being the start of the line. Red lines are mapped fissure traces crossing Ramahana Road. Area defined by dashed blue line shows location of boggy ground. Thin grey lines show five metre contours of elevation above sea level.

4.6.2 Results

The outputs from the survey were processed by Matt Cockcroft (University of Canterbury), and the resultant plots are shown in Figure 4.36, Figure 4.37 and Figure 4.38. The first plot uses theory based on the smoothness-constrained least-squares method, and the subsequent plots show further processing using both default settings and combined inversion methods, both with and without defined models.

The cross-sectional plots show a zone of high resistivity in the centre of the model at the 48 m mark which curves around to the south-west end at depth. There is a zone of low

resistivity along the base of the cross section, as well as near the surface on the south-western side where the ground line heads up slope. Resistivity values vary in range from approximately 0.5 ohm.m to a high resistivity of approximately 500-5000 ohm.m.

4.6.3 Discussion

The zone of high resisitivity in the centre of the model does not correspond with the location of the concrete path which crosses the survey site (Figure 4.35), but rather falls to the north-west of the path, coinciding with the area of boggy ground. It was expected that this area would have a low resistivity value, making this an unusual outcome. There is, however, an area of low resistivity 1-2 m below the surface in the centre of the section, which does satisfactorily coincide with the water-logged area.

The central zone of high resistivity trends towards the south-west. This may coincide with the subsurface geology, perhaps indicating a band of colluvial material within the clayey-loess. This area may also correspond to subsurface compression features related to the fissuring above, although it is unknown how this movement may affect the resistivity values of a soil. The section of low resistivity at the bottom of the cross-section is likely indicative of higher ground water levels. This is consistent with the appearance of springs in the area (see Section 4.7), indicating the presence of a high water table.

The survey extended to a depth of less than 10 m, and as a result did not extend deep enough to establish the depth to the bedrock interface. If reached, this would likely have shown on the sections as an area of distinctly lower resistivity than the rest of the section, beginning at greater than 10 m depth.

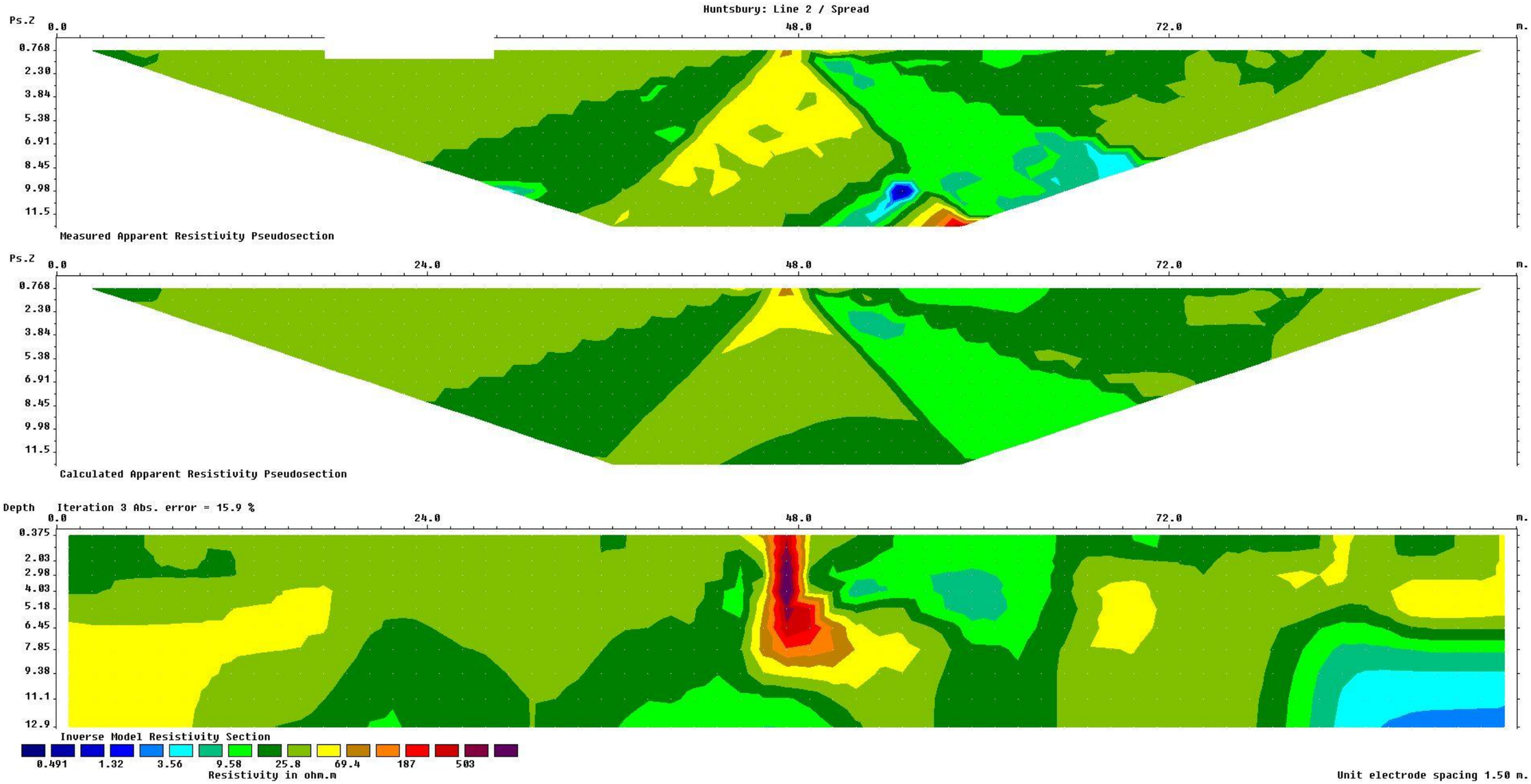

Figure 4.36 First processing of resistivity outputs showing inversion approximation based on least squares inversion.

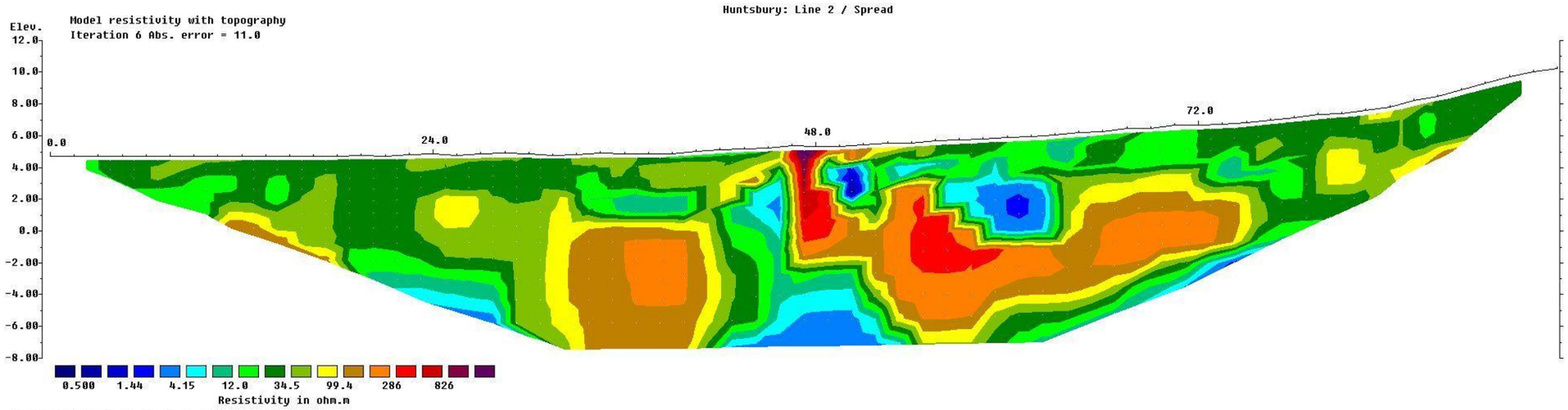

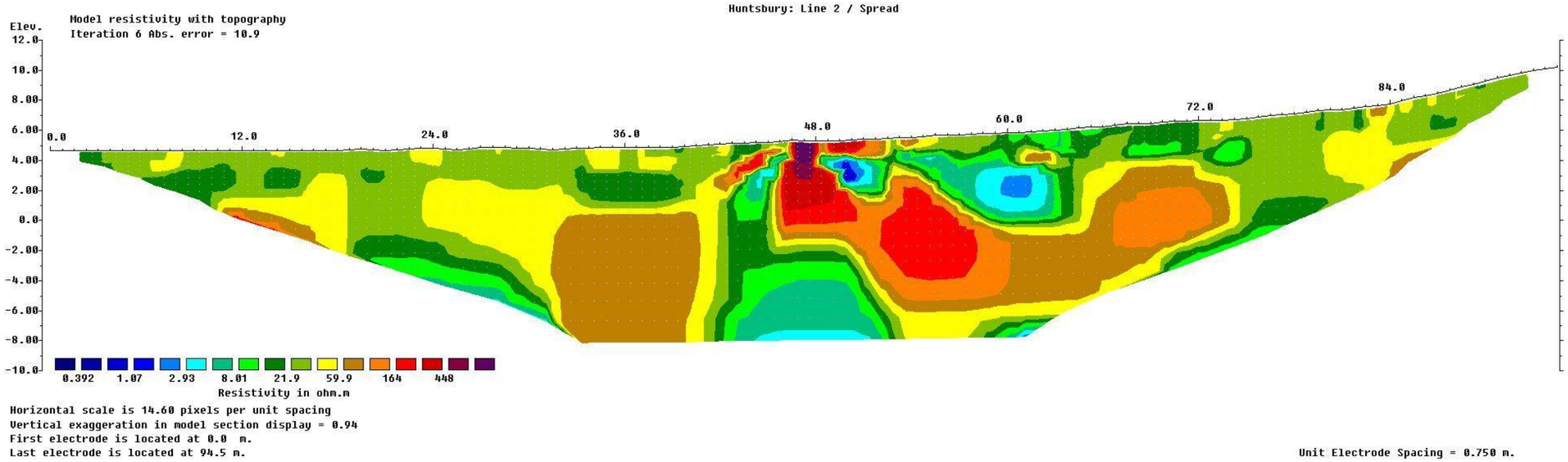

Figure 4.37 Processed resistivity outputs with the upper image showing combined inversion with no model refined, and the lower image showing combined inversion with model refined.

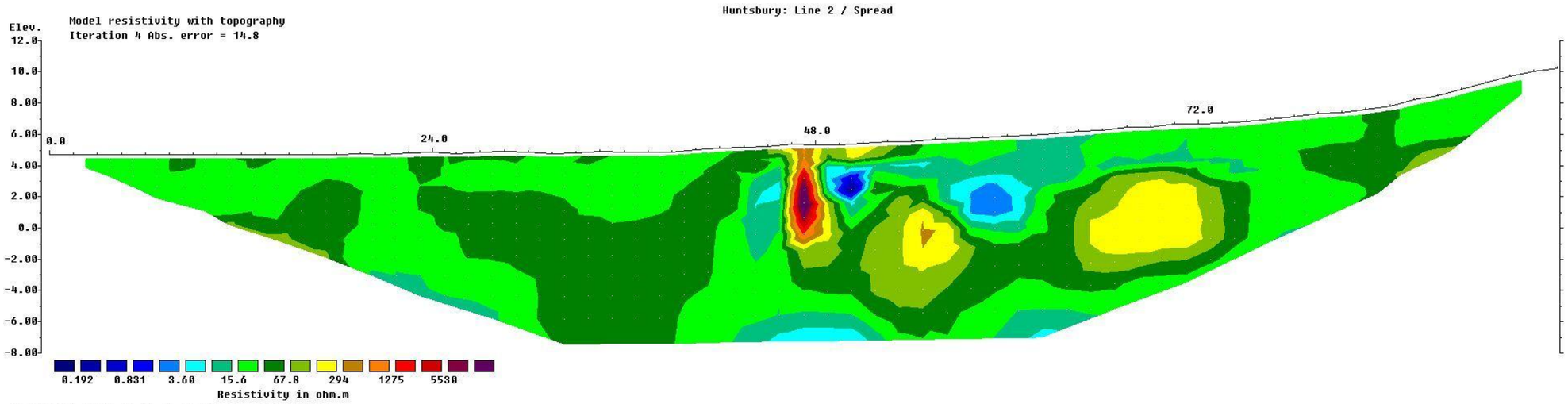

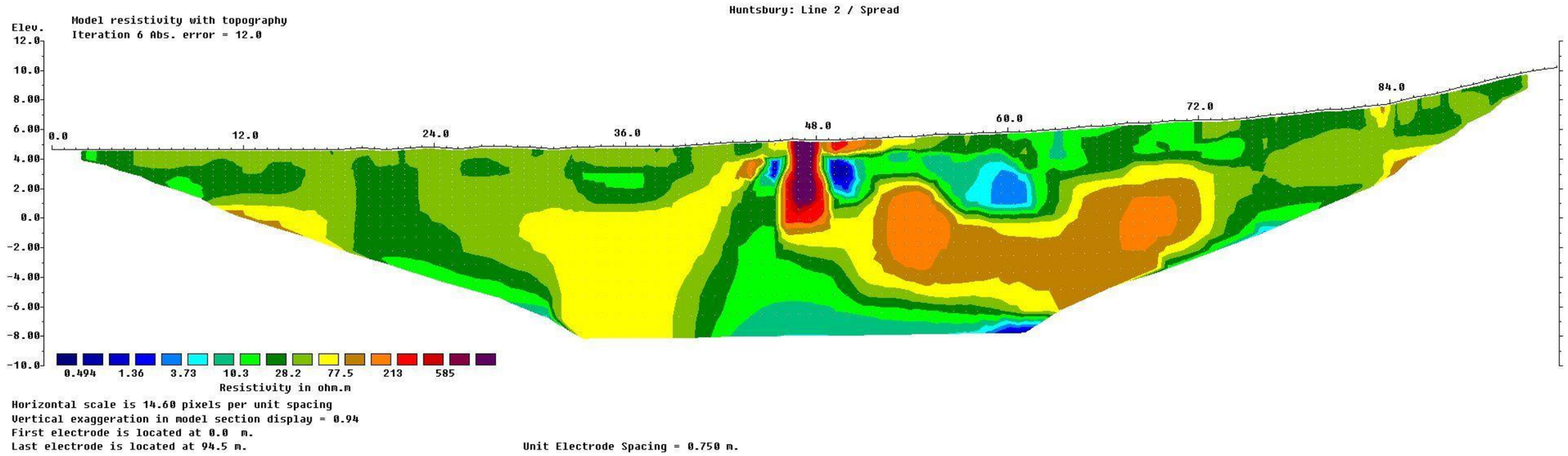

Figure 4.38 Processed resistivity outputs with left upper image showing default settings with no model refined, and lower image showing default settings with no model refined.

4.7 Groundwater

Changes in the amount, direction, and rate of water flow in streams and in fluid pressure in the subsurface following large earthquakes have been well documented, and history has shown that it is relatively common for new springs to form, old springs to disappear or change in their discharge volume, or water levels to fluctuate by several metres, sometimes permanently (Manga & Wang 2007). It is not surprising, therefore that such changes were observed in many locations around Christchurch following the Darfield Earthquake, Christchurch Earthquake and June Earthquake, as well as the smaller aftershocks. Manga and Wang (2007) explain how hydrologic responses occur as a result of changes to fluid pressure and hydrologic properties such as permeability within the ground as a result of a buildup of *strain*.

Sometimes changes to ground water level as measured in wells remain as quasi-permanent changes, the effect only diminishing slightly over time. These can often be explained (see Figure 4.39) by coseismic static strain created by an earthquake, whereby water level rises in zones of contraction, and falls in regions of dilation (Jonsson et al. 2003; Manga & Wang 2007).

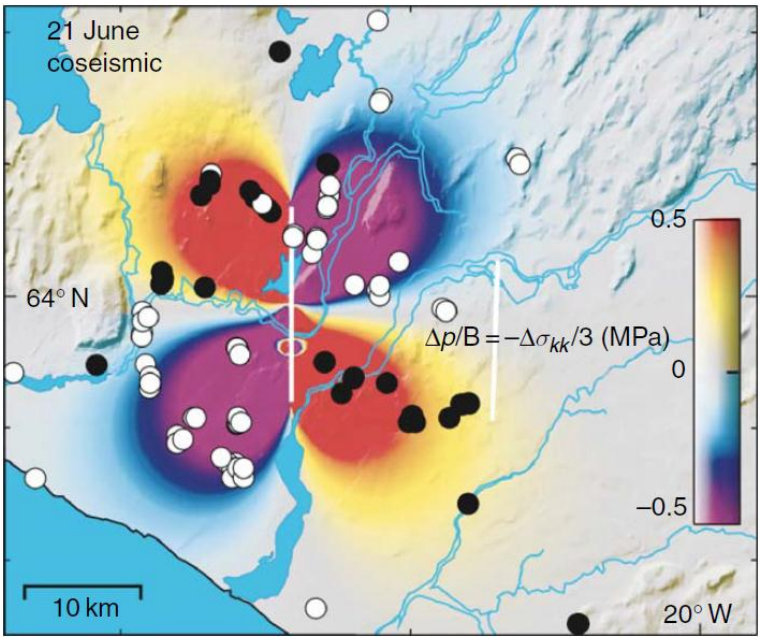

Figure 4.39 Predicted (colour map) and observed (circles) co-seismic water-level changes following a M6.5 dextral strike-slip earthquake in Iceland, 2000. Black and white circles indicate water level increases and decreases, respectively. The white line shows the mapped surface rupture. After Jonsson et al. (2003).

4.7.1 Observations in the Hillsborough Valley

Following the September 2010 Darfield earthquake some changes were observed in spring behaviour in the Port Hills area. After the Christchurch Earthquake, many of these changes were exacerbated, and new changes were observed such as the formation of new springs, seepages and groundwater level alterations. The Hillsborough Valley area has experienced the formation of at least two dozen new springs, many of which are still flowing at the present time (August, 2012) and do not appear to be greatly affected by season or rainfall, other than with an increase in surface ponding. Residents in the area have suffered from unusable yards due to bog, and have reported health impacts due to fungus and mould growth in their homes.

The springs are located in three main groups; one at the end of the western fissure, where Ramahana Road meets Centaurus Road; another along the eastern side of Albert Terrace, about half-way into the valley by Leonard Place; and the third about half-way down Vernon Terrace, on the western side of the road. Figure 4.40 provides a summary of the location and extent of the ground water problems in the Hillsborough Valley area.

Some of the more prominent spring behaviour has been observed in a group of properties along Centaurus Road, near the intersection of Ramahana Road. The heightened water flow in this area affects at least 11 properties, with at least three affected by considerable spring-flow, and the remainder by persistent water seepage. The property at 211 Centaurus Road has had four sump pumps working constantly since the Darfield Earthquake, discharging approximately 9000 litres of water per day. This property has the unique circumstance of being affected by both fissuring and spring behaviour, as beneath the house there is an approximately 5 m long fissure trace, being the far northern end of the Ramahana Road-Albert Terrace fissure system (see schematic cross section of the hillside from the Huntsbury Reservoir, through the Centaurus Road springs and fissures, to the Heathcote River in Figure 4.14, page 80). It is from this fissure trace that the spring is flowing. Neighbouring properties have also experienced the formation of flowing springs, as well as water ponding issues. Across the road at 216 and 220 Centaurus Road, seepage is visible emerging from driveways (Figure 4.41).

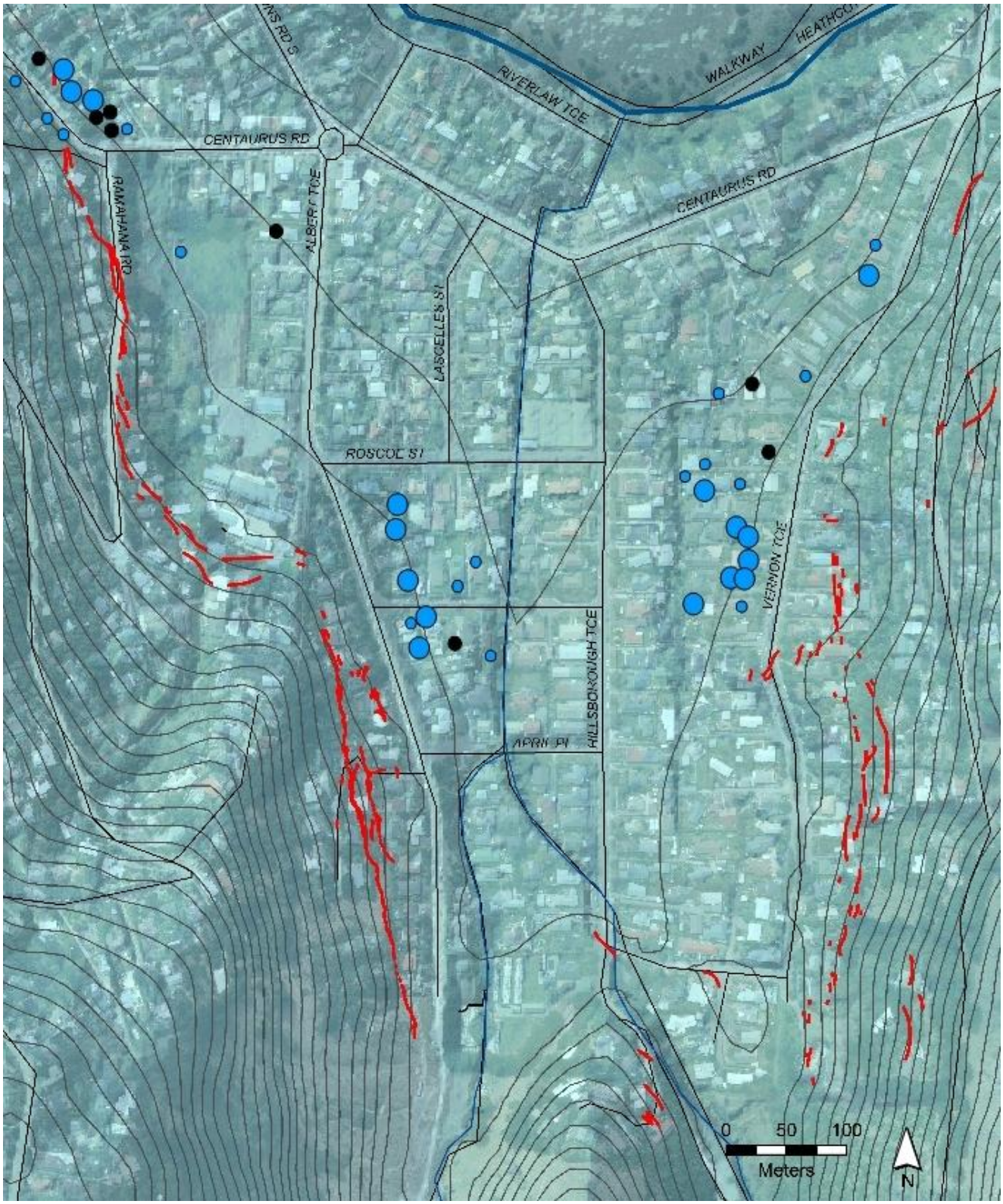

Figure 4.40 Map of known locations of springs, seepage and/or ponding issues in the Hillsborough Terrace valley area. Large blue dots show sites of flowing springs, small blue dots are areas of persistent seepage or boggy ground, and black dots show sites where ground water issues were reported but the extent is unknown by the author. Red lines indicate the fissure trace. Spring data from H. Rutter (Aqualinc, 2012) and the author's own observations.

(a)

(b)

Figure 4.41 Seepage through cracks in paving at base of driveways of 216 (a) and 220 (b) Centaurus Road. Over the substantial length of time that the seepage has been in existence, moss growth has made the paved surfaces slippery.

The second of the three groups of springs is located half-way down Albert Terrace, on the eastern side of the road, around the intersection of Leonard Place. At this site there are five properties where there are still persistently flowing springs, and at least five others which are affected by seepage and ponding. Residents of Leonard Place and Albert Terrace have reported

substantial water ponding and overland flow during and immediately following rain events. One resident reported an unusual occurrence outside 2a Leonard Place: *"a small drain that flows out into the roadside gutter spasmodically and for no discernible reason gushes water for 5-6 minutes. This occurs irrespective of whether it has rained or been dry for days"*. Several of these houses have instigated daily pumping or siphoning of the water off their sections, with 31 Albert Terrace pumping 3000-3500 litres of water off their section every day. Residents of this group of properties report that the water issues started following the Christchurch Earthquake, and have been prevalent since, irrespective of seasons or rainfall.

The third of the spring clusters is located on the western side of Vernon Terrace, roughly level with the Albert Terrace-Leonard Place group of springs on the other side of the valley. This group contains at least seven constantly flowing springs, and at least five nearby sites are experiencing severe seepage/drainage problems. Multiple residents in this group reported the formation of "pools" or small "lakes" on their properties, with one stating the depth of water was sufficient to be a drowning hazard for young children. Rainfall does have an impact on this spring area, as at least one pool site is said to dry out in extended dry weather, and others distinctly worsen after rainfall, implying that the ponding is the combined effect of both a raised water table, and constant spring flow. Residents first reported the appearance of springs in this area following the Darfield Earthquake, with the Christchurch and June Earthquakes each exacerbating the problem.

There are two spring/seepage sites which do not appear to be part of the three main groups; at Centaurus Park, and at 8 and 10 Vernon Terrace. In the centre of Centaurus Park (at the intersection of Ramahana Road and Centaurus Road) there is a distinctly boggy section of ground which was noticed by the author while conducting a resistivity survey in the area (See Chapter 4.6). The appearance of a spring has also been reported on the neighbouring property at 4 Albert Terrace. Two springs were reported directly opposite this location, on Vernon Terrace, at 8 and 10. Residents of 10 Vernon Terrace report that they are pumping over 240 l of water per hour from beneath one of their bedrooms.

Water collected from springs in the Hillsborough Valley has been analysed Aqualinc Research Ltd, who have been investigating the changes to groundwater in the Hillsborough Valley area following the earthquakes. Piper plots of the chemical constituents of the water (Figure 4.42)has shown that water from the Vernon Terrace, Centaurus Road and Leonard Place springs has a mineral content consistent with that typical of water which has been sourced from within the volcanic rocks of the Port Hills. This water was compared to water collected from Riccarton Mall, and from a laundry tap at 10 Vernon Terrace, both of which were sourced from

Canterbury Plains aquifers, and possessed a distinctly different chemical signature (H.Rutter, Aqualinc Research Ltd, pers. comm., 2012).

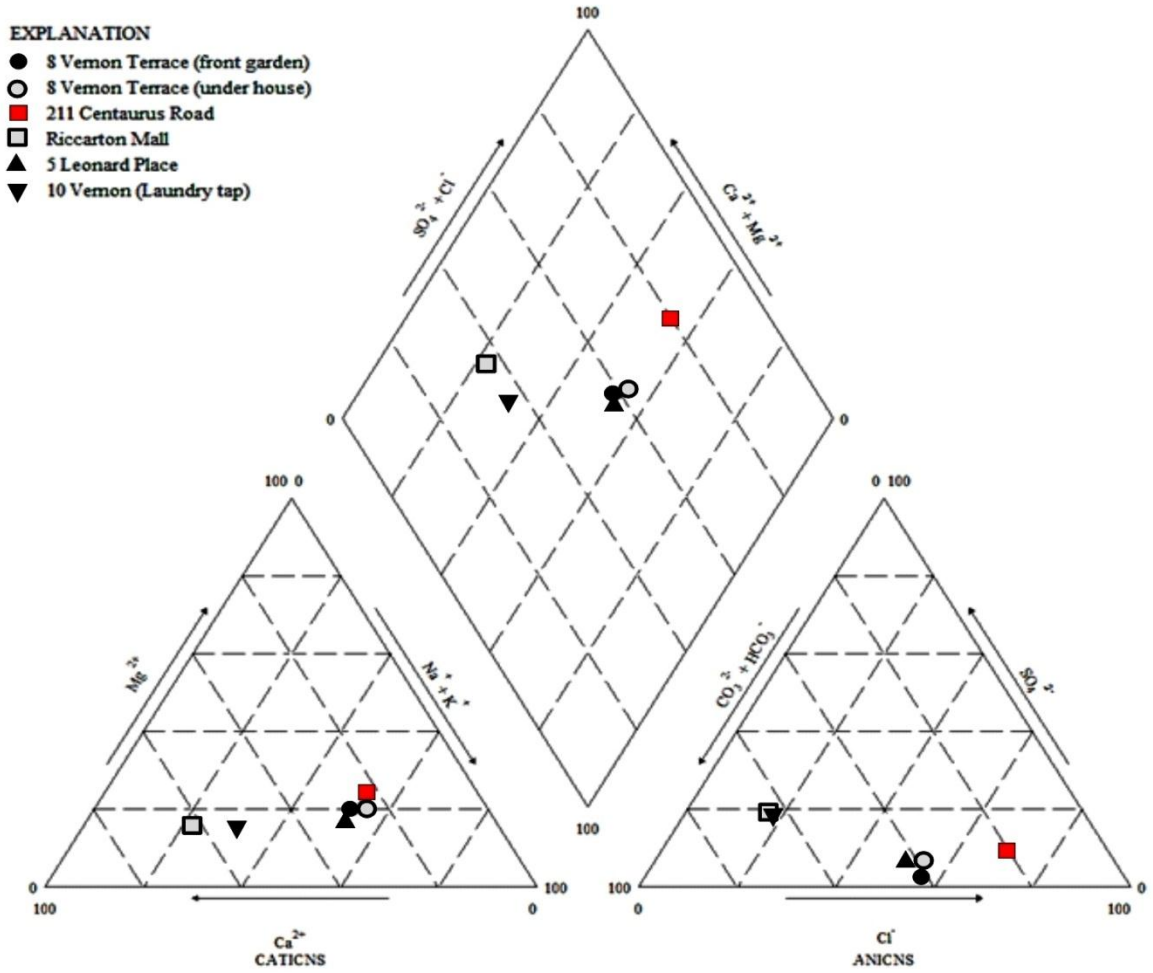

Figure 4.42 Piper plots of chemical analysis of spring water from Vernon Terrace, Centaurus Road and Leonard Place, showing significantly different chemical composition to water sourced from Canterbury Plains aquifers collected at Riccarton Mall and from a tap at 10 Vernon Terrace. After H. Rutter, Aqualinc Research Ltd, pers. comm. 2012).

4.7.2 Discussion

The three main groups of spring/seepage occurrence in the Hillsborough Valley area all occur down slope from the mapped fissure traces in the foot hills. The Hillsborough Valley contains many more post-earthquake springs than other north-facing valleys of the Port Hills (H.Rutter, Aqualinc Research Ltd, pers. comm., 2012), even those with similar loess fissuring.

The Centaurus Road and Vernon Terrace spring clusters emerged following the Darfield Earthquake, and were exacerbated by the subsequent earthquakes. Residents reported that the

Albert Terrace spring cluster was first observed only after the Christchurch Earthquake, although land damage was reported in the area alongside the central valley drain in September which led to at least two houses being uninhabitable.

From studies of the map produced in Figure 4.40, it is apparent that the springs are located towards the northern end of each distinct section of fissure trace. The Vernon Terrace springs occur at the end of the section of hillside with the most fissuring, although some fissuring does continue further north, perhaps being the cause for the spring behaviour at 8 and 10 Vernon Terrace. On the western side there are two groups of springs, the one on Albert Terrace occurs at the "dog-leg" in the fissure zone, and the one on Centaurus Road occurs at the far end of the fissuring, and actually coincides with the fissure trace in 211 Centaurus Road. This layout indicates that there is a correlation between the locations of the springs and the locations of the fissures. It is uncertain whether one caused the other, or whether they are both outcomes of a higher-level, as yet undefined, geotechnical occurrence.

4.8 Synthesis

1) Fissuring on either side of the Hillsborough Valley has been mapped through properties from Albert Terrace to Ramahana Road on the western side, and between Vernon Terrace and Rapaki Road on the eastern side. The fissure traces run in a roughly contour-parallel orientation, each extending for a distance of 500-600m.

2) Fissure lateral extension tends to be in the order of 0.10-0.20 m. Vertical movement is usually shown by the down-slope side of the fissure trace having dropped by between 0.05-0.15 m.
3) Linear pot-holing, with substantial cavity formation beneath sealed road surfaces implies that water was flowing into the fissures at these locations, and passing through cracks in the loess, carrying fines in suspension.
4) Fissures were filled using a 1:6 mixture of bentonite clay and SAP-20 gravel.
5) Evidence of lateral compression was apparent in the valley floor topographically down slope from the fissures.
6) Fissures on 1 and 3 Glenview Terrace on the west of the valley as well as 40 Rapaki Road on the east of the valley were mapped in greater detail, showing offset measurements and fissure orientation.
7) Following heavy snowfall in Christchurch the subsequent melt-water caused a large collapse of loess at 3 Glenview Terrace, as the fissure system appeared to link up to subterranean tunnel gullying. Remedial measures were undertaken at this site.

8) The laser results for the three loess samples show that the grain size of the loess is very similar at each of the locations on both sides of the valley, although the Rapaki Road sample has a slightly lower clay content, and slightly higher medium-sand content than the Glenview Terrace loess. All of the samples are poorly graded, with silt and fine sand making up 85% of the soil. At approximately 5 %, the loess in the Hillsborough Valley area has a lower clay content than is typical for the Port Hills.

9) The direct shear-box was used on loess samples from Glenview Terrace to ascertain the shear strength of the disturbed and remoulded loess from the site. The c values for the 40 Rapaki Road, 3 Glenview Terrace and compacted 40 Rapaki Road loess samples were 13.4 kPa, 19.7 kPa and 28.6 kPa, respectively. The corresponding ϕ values were 42.0 °, 43.4 °, and 18.4 °.

10) A resistivity survey was carried out across Centaurus Park, near the intersection of Ramahana Road and Centaurus Road. The survey length was 96 m, which provided a depth of penetration of approximately 10 m in the centre, which was not long enough to establish the location of the subsurface bedrock interface. The survey did show an area of low resistivity at the base of the section, which likely corresponds to a zone of saturated clayey loess/loess colluvium, indicating a high water table in the area, and thus consistent with the appearances of local springs.

11) The Hillsborough Valley area has experienced the formation of at least two dozen new springs, many of which are still flowing at the present time (August, 2012) and do not appear to be greatly affected by season or rainfall. The springs are located towards the northern end of each distinct section of fissure trace and chemical analysis shows that they are sourced from the Port Hills volcanics.

5 Fissuring Mechanisms

5.1 The Five Possible Fissuring Mechanisms

Throughout the course of this study, several possible interpretations of the mechanisms behind the formation of the fissuring have been proposed, and to date are still not conclusive. It may be a positive thing that the debate on the cause of the fissuring has continued, as, until the mechanisms are thoroughly understood, land developers must err towards caution when considering properties which may be subject to fissuring. At the time of writing, there have been further reports of erosion cavities forming on the fissures, similar to that of 3 Glenview Terrace, but this time on Vernon Terrace. While the fissures continue to surprise geotechnical experts, it would seem only prudent to be cautious when applying definitive mechanism models to their behaviour.

This chapter introduces and analyses five possible interpretations of the fissuring. While any of these has the potential to explain the fissures, alone none of these are able to fully explain every observation that has been made. It appears, therefore, that the mechanism behind the fissuring is a result of the cumulative effects of a combination of the following five fissuring interpretations.

Based on the study in this thesis, the Port Hills fissuring may be sub-divided into three categories (summarised in Table 5.1), each characterised by distinctive features of the fissures, called hereafter Category A, Category B, and Category C. For a location map the reader is referred to Figure 3.5. Category A, typified by Bowenvale Valley, Hillsborough Valley, and Huntlywood Ave includes fissures which display evidence of, spring formation, tunnel-gullying, and lateral spreading-like behaviour or quasi-toppling. These fissures are several metres down-slope of the loess-bedrock interface, and are in valleys containing a loess-colluvium fill. Category B is typified by the Bridle Path Road fissures and the lower fissures at La Costa Lane, which are also several metres down-slope from bedrock outcrops, but, particularly in the case of Bridle Path Road fissures, are in a much wider valley than those in the first category. The valley contains estuarine silty sediments which liquefied during the earthquake, and springs were formed, at a distance of several hundred metres from the fissures, on the far side of the valley. Category C is that of the fissures at La Costa Lane and Maffeys Road, which occurred at higher elevations than the fissures in the preceding categories, being almost coincident with bedrock outcropping. This category may also include the fractures observed at Whitewash Head.

Table 5.1 Summary table of the three fissure categories, their typical characteristics, and the fissure sites in each category.

	Typical Characteristics	Fissure Sites
Category A	Spring formation, Tunnel gullying, Fissures near the loess-colluvium boundary, Compression features, Elevation of 20-30 m Fissures mirrored on opposite sides of valleys	Bowenvale Valley, Hillsborough Valley, Huntlywood Avenue
Category B	Spring formation Fissures near the loess-colluvium boundary Liquefaction in valley floors Fissures not mirrored on opposite side of valley Elevation 10-20 m	Bridle Path Road, Basil Place
Category C	Fissures near loess-bedrock boundary Elevation 30-50 m Fissures not mirrored on opposite side of valley	La Costa Lane Maffeys Road Whitewash Head

Geotechnical mechanisms involved in the formation of the fissures at each of the sites in these categories are likely to be subtly different, each involving an individual combination of the possible interpretations discussed below.

5.2 Mechanism One: Incipient landsliding

Incipient, large-scale landsliding has been one of the preferred interpretations of the fissuring since shortly after the Christchurch Earthquake. The landsliding hypotheses implies that the fissures are head-scarp tension cracks, with small amounts of vertical displacement, and related compressional features near the toe areas (Dellow et al. 2011a; Dellow et al. 2011b; Hancox et al. 2011). Typically, as shown in Figure 5.1 and Figure 5.2, shallow landslide features such as these have a distinct head-scarp on the upslope side, immediately followed by a zone of depression or subsidence, then a zone of bulging towards the toe which is usually observed as distinct compressional folding/brittle fracturing of the ground surface at the base of the slide area. Landslides of this nature may also produce seepages or springs near the toe bulges of the slide, if, for example, an aquifer stratum was forced upwards towards the bottom of the slide, causing it to break the surface.

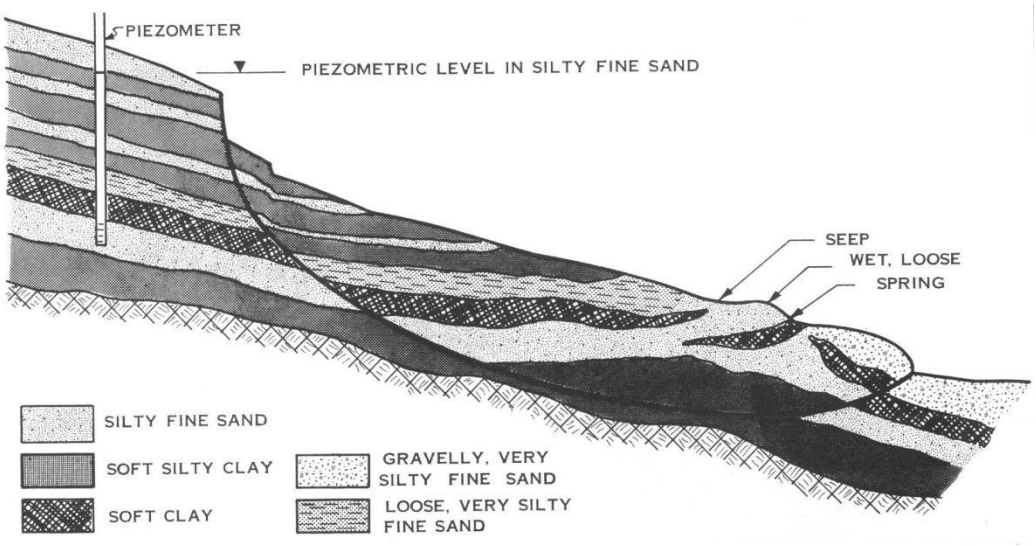

Figure 5.1 Typical geologic cross section through the centre of a landslide. From Keaton and DeGraff (1996).

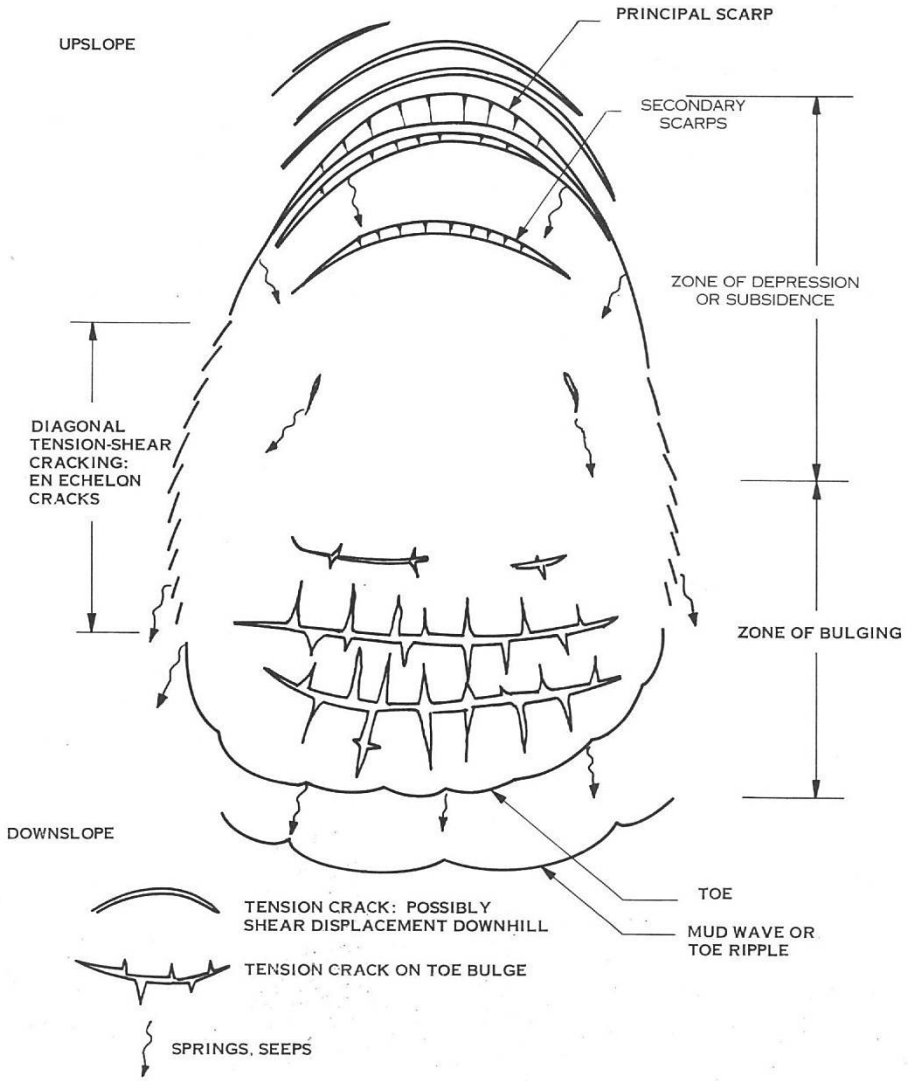

Figure 5.2 Typical cracks, bulges, scarps, and springs of a landslide in plan view. From Sowers and Royster (1978).

The landslide hypothesis does provide a suitable explanation for the appearance of the fissuring; the, albeit long, linear fissures could be interpreted as head scarp features, and the occurrence of springs and compression features in the valley floors correlate with this assumption. As explained above, spring formation near the toe of the slope is also typical of many landslides, however it would be less likely that springs from a surface landslide would be sourced from the depths required for the water to gain the chemical signature of the volcanic bedrock, they would more likely be sourced from surface water infiltration and be subject to seasonal and rainfall influences.

There are several other factors which do not correlate particularly well with the theory of landsliding, such as the length and linearity of the fissures and the lack of shear cracking (as shown in Figure 5.2) between the ends of the fissures and the compression zones. Also, there is no apparent large-scale bulging of the toe at any of the sites (other than the "concertina-style" compression of roads and pavements). Such bulging may not be apparent in the initial incipient landslide stages, and would likely require technical land surveying to recognise. Geotechnical firms who have conducted bore logs in the fissuring areas have not reported the appearance of a shear zone or basal slide plane which would be expected to connect the upper fissuring with the toe compression features, should they be found to be landslides. Factors against such a theory include the linearity of the fissures, as they would be expected to curve down slope towards the ends should they be a landslide headscarp feature. Furthermore the lack of evidence of a basal shear plane, or of diagonal tensional shear cracking (Figure 5.2), or *en echelon* cracking, down the hillsides between the outer edges of the fissures and the compression features in the valley below is inconsistent with a landslide theory.

5.3 Mechanism Two: Bedrock fracturing

A second interpretation of the fissuring and related spring behaviour in the Port Hills is that they occurred as a result of complex tectonically-induced movement within the bedrock of the Port Hills. This hypothesis is able to be linked to the other possible mechanisms behind the fissuring, but largely stands alone, as the other interpretations are more focussed on the behaviour of near-surface soils and rocks, and whereas this interpretation takes into account the proximity and movement of the fault line beneath the Port Hills, and the affect this may have had on the terrain immediately above. This hypothesis is that high vertical ground acceleration in the area of the fissuring lead to topographically-controlled fissuring, requiring relatively dry loess to behave in a brittle manner in response to propagation of forces from bedrock.

Two main models of the location of the fault responsible for the Christchurch Earthquake have been postulated to date. These are summarised as a single-fault model, as proposed by both Kaiser et al. (2012) and Beaven et al. (2011), and as a two-fault model, as proposed by Eliot et al. (2012) and Beavan et al. (2011) whereby the fault branches at around the Hillsborough Valley area, with one segment trending north north-east, and the other continuing straight. Figure 5.3 overlays a map of the modelled fault location and slip magnitude, as published by Kaiser et al. (2012), above a street map of Christchurch, and the fissure traces as mapped by the author. The resultant image shows that the top edge of the fault, albeit at a depth of approximately one kilometre, visibly coincides with the locations of Category A fissures (that is, those of Bowenvale Valley, Hillsborough Valley and the Huntlywood Terrace area) which are aligned directly above the top edge of the fault plane. Figure 5.4 provides a more detailed view of the Hillsborough Valley area, relating the modelled fault positioning from Kaiser et al. with the fissuring in this area, as well as the location of the Hillsborough Reservoir and the springs and compression features. In this image it is particularly clear that the Huntsbury Reservoir and "dog-leg" bend in the Ramahana Road-Albert Terrace fault traces coincide with the location (at depth) of the top edge of the fault plane.

In their 2011 paper, Beaven et al. provided a satellite-produced image of the observed vertical ground displacement. Figure 5.5 shows this image, with fissure traces overlaid by the author. Red areas to the north and west of the Port Hills show areas of vertical displacement away from the satellite, and blue areas in the Port Hills and the Avon-Heathcote Estuary area show areas of vertical displacement towards the satellite. As with Figure 5.3, a correlation is visible between the locations of Category A of fissures, and, in this case, the location

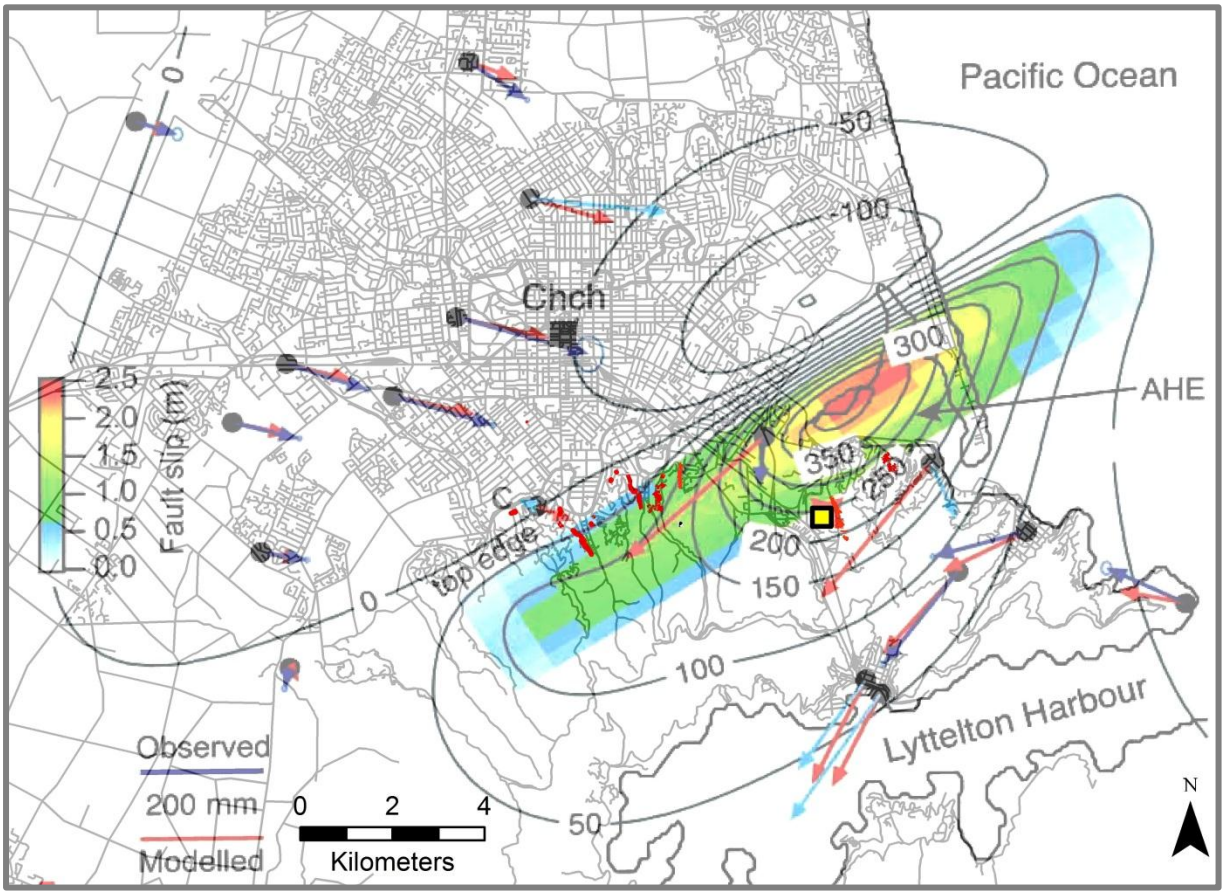

Figure 5.3 Modelled fault location and slip magnitude with overlaid fissure trace locations (red, near centre). The fault is shown dipping to the southeast with its top edge at 1km depth. Filled black circles show the near-field GPS stations contributing to the solution with observed (blue arrows with 95% confidence uncertainty ellipses) and modelled (red arrows) displacements. The yellow and black square shows the epicentre as located using data available in March 2011. The black contours show uplift and subsidence in millimetres as predicted by the model. Overlay fault location of single fault model, after Kaiser et al. 2012.

of the boundary between land that largely moved upwards, and land that largely moved downwards. With no gradual colour change between positive and negative vertical displacement, the colour scheme utilised by Beaven et al. (2011) makes it appear as though there were few areas of little or no vertical change. In doing this, however, it does help to delineate the relatively linear, regular boundary between the two displacement directions. This linear boundary prompted Beaven et al.'s proposition of there being two fault traces at angles to each other – one branching off northwards where the linear displacement boundary makes a distinct bend, near the area of Hillsborough Valley (Figure 5.5).

When plotted from a "bird's-eye" perspective, it is clear that the sub-crop of the fault responsible for the Christchurch Earthquake corresponds with the alignment of Category A fissures. In order to further visualise this relationship, the author generated a three-dimensional model of the fault plane beneath the Port Hills using ArcScene 10 software by ArcGIS.

Measurements for the size and orientation of the fault plane were taken from Kaiser et al. (2012), where it was described as a simple single-fault model. Using the ArcScene software it was possible to "fly" around the image, in order to gain insight into the spatial relationship between the fault location and the ground surface above. Three still images of the model, taken from different perspectives, are shown in Figure 5.6. The model clearly showed the fault plane beginning well below the Port Hills (at a depth of 1000 m), and, according to data in Brown and Weeber (1991), this would put it below the level of the volcanic rock, in the lithified sediments below, making it an inherited structure from the Cretaceous, or earlier. The model also makes it visibly clear that with a width of 7000 m, and a dip angle of 69°, the fault plane would extend to depths below the ground in the vicinity of 8000 m.

Study of the three dimensional modelling shown in Figure 5.6, together with the "bird's-eye" view maps in Figures 5.3 – 5.5, strongly suggest that movement of the upper edge of the fault plane, at even 1000 m below the ground surface, may have caused related fracturing propagating to the surface within the Port Hills volcanic bedrock. With areas of the Port Hills increasing in elevation by up to a metre relative to areas of Christchurch City (Beavan et al. 2011), it would seem logical that fracturing may occur within brittle rocks which straddle the boundary between up-thrown and down-thrown land. This hypothesis provides a possible explanation for the occurrence of the springs, as newly-generated fracture sets would provide enduring conduits for groundwater to reach the surface. The formation of the fracture set through the Huntsbury Reservoir and surrounding area provides circumstantial evidence that some bedrock fracturing did occur within the volcanic rocks of the Port Hills, and these fractures certainly provided a conduit for water as the reservoir was drained. Whether they did form as a result of complex fracture sets propagating to the surface from 1000 m deep fault movement is unproven, however certainly warrants further investigation, as part of a separate study.

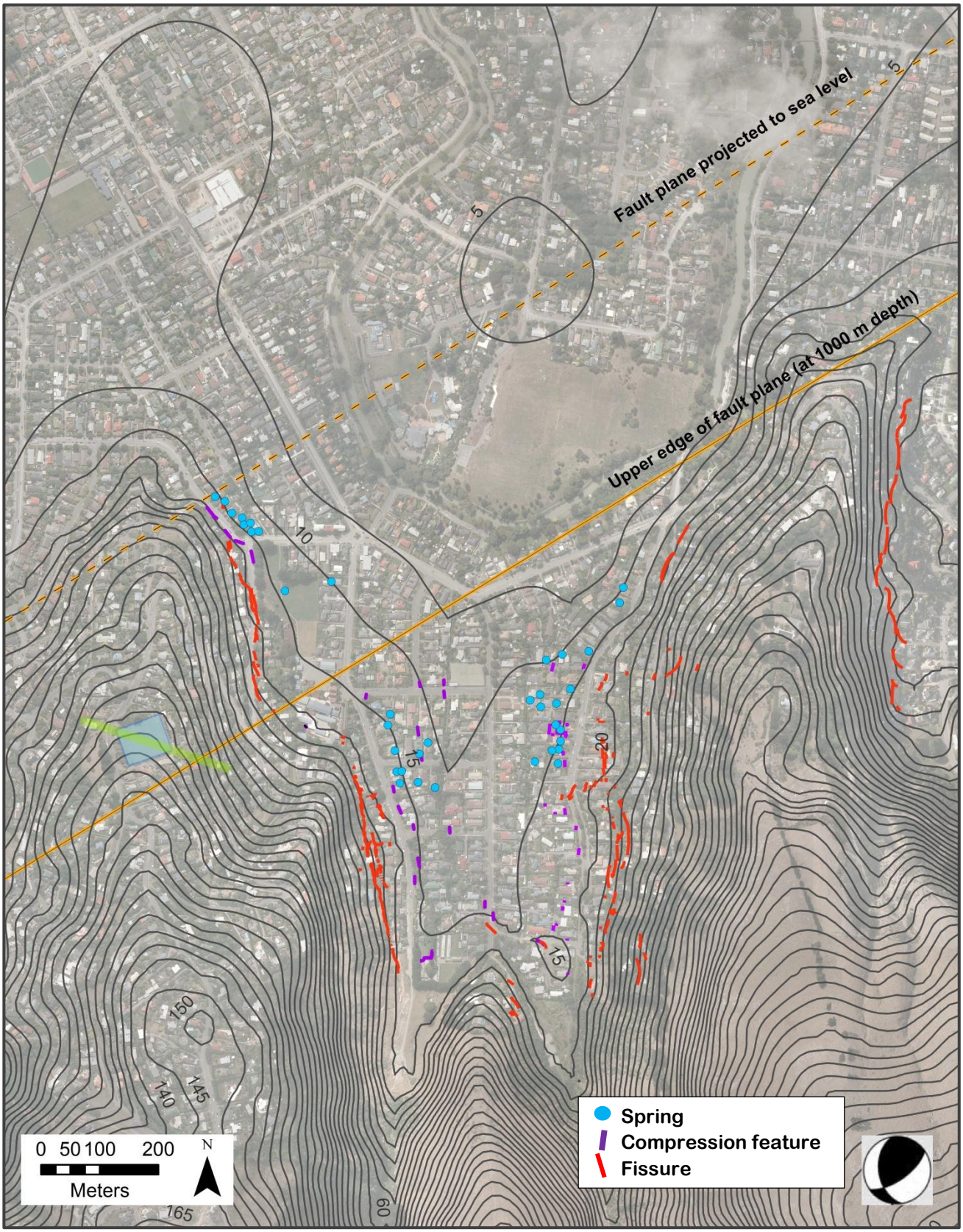

Figure 5.4 Map showing location of upper edge of fault plane, at a depth of 1000 m, where it passes beneath the Hillsborough Valley area, as well as the location of the projected sea-level expression of the fault. Huntsbury Reservoir outlined with blue square, and green line showing orientation of shearing. Beachball diagram of fault mechanism shown in lower right corner, and fault plotted using data from Kaiser et al. (2012).

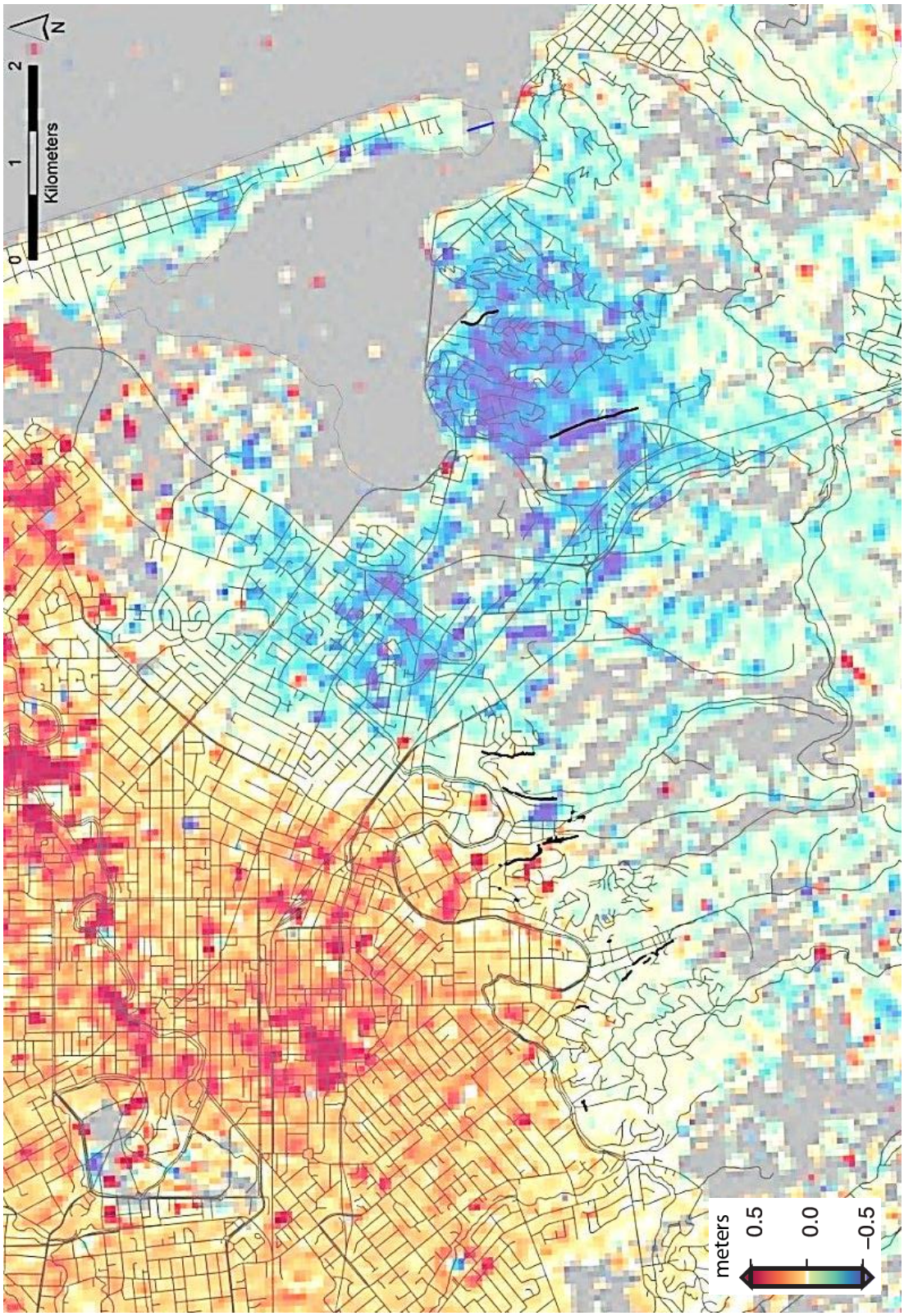

Figure 5.5 Fissure traces (black) and Christchurch road centrelines overlaid with observed ground displacement, with red denoting displacement away from the satellite, and blue denoting movement towards the satellite. Note the distinct boundary between areas of upwards and downwards directed displacement, which coincides with Category A fissures. After Beavan et al. (2011).

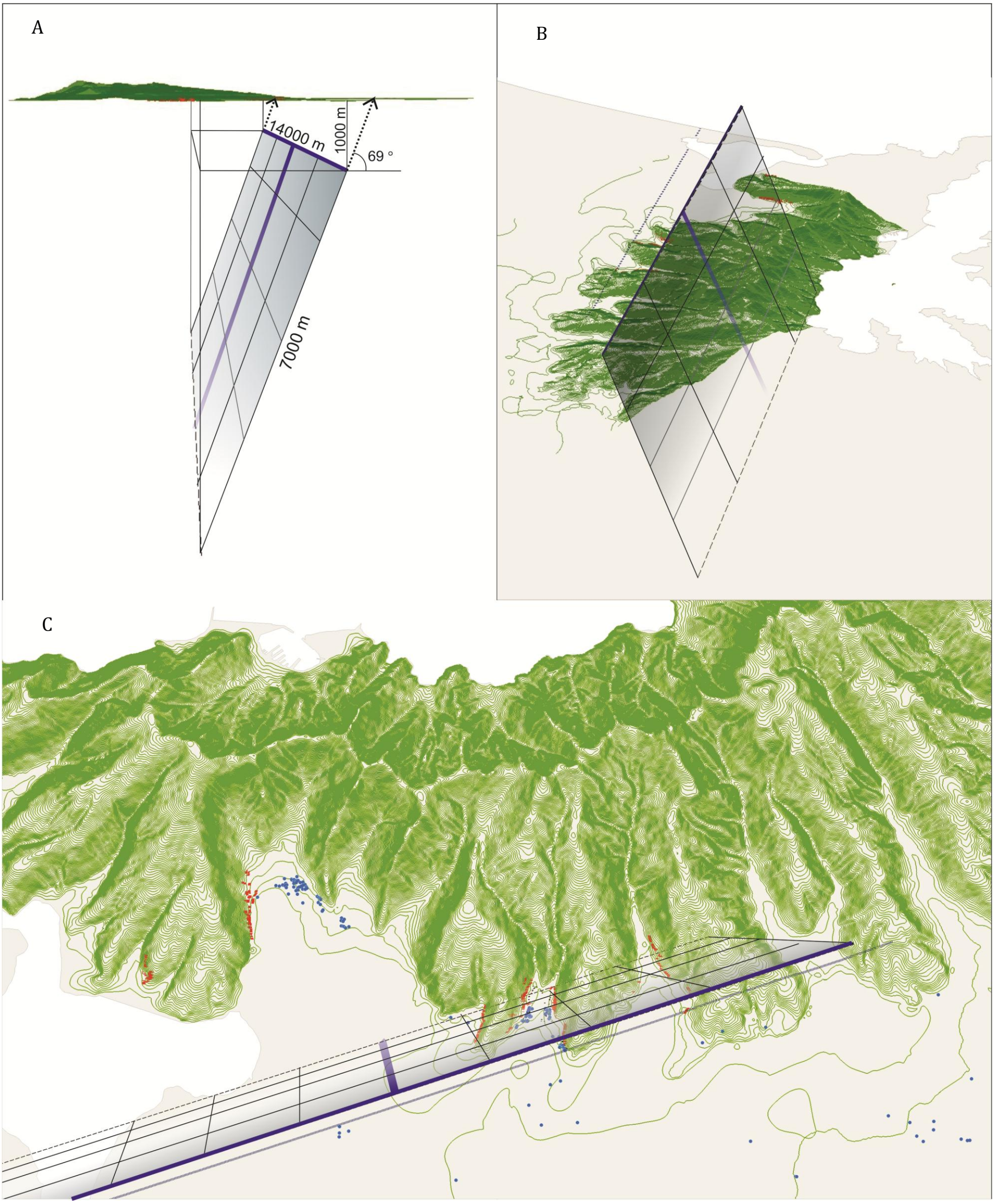

Figure 5.6 Modelled location of fault plane of the Christchurch Earthquake of 22 February 2011, based on data from Kaiser et al. (2012). Fault strike = 58°; dip = 69° SE. Model shows the top edge of the fault plane as a thick blue line at 1 km below the surface, with an approximate surface expression as a thin blue line, separate to the fault plane. Fissures are marked in red, and springs as blue dots. (A) Facing due west, looking along fault trace, below the Port Hills. (B) Facing east and looking obliquely down at fault trace. (C) Facing south and looking obliquely down fault trace.

5.4 Mechanism Three: Toppling failure

Toppling failures in rock or soil bodies occur when there are steeply dipping joint sets, which split apart, causing the front sections to fall outwards. It is proposed that this phenomenon may be used as a corollary to the formation of the Port Hills fissures, which may be described as "quasi-toppling", being similar to the state of a soil or rock mass which is in the early stages of a toppling failure.

According to Bell (1999), soil toppling failures usually have a single, nearly vertical, head scarp, with subsidiary cracks running parallel to this. The body of the failure is comprised of a unit or units which have tilted away from the crown (Figure 5.7), forming the principal head scarp. If the columnar sections are of sufficient length, *block flexure toppling* can occur, in which accumulated motions through several joints combine to a pseudo-continuous curve down slope, ultimately forming limited tension cracks in the typically vertical head scarp (Hoek & Bray 1981). Lutenegger and Hallberg (1988) described the phenomenon occurring in road cuttings whereby, when the lateral support is removed, the loess was observed to "topple in cohesive blocks", and Lohnes and Handy (1968) describe the use of an inclined, unsupported body of gelatine (Section 2.5.2) to simulate the toppling process and the formation of fissures by this means.

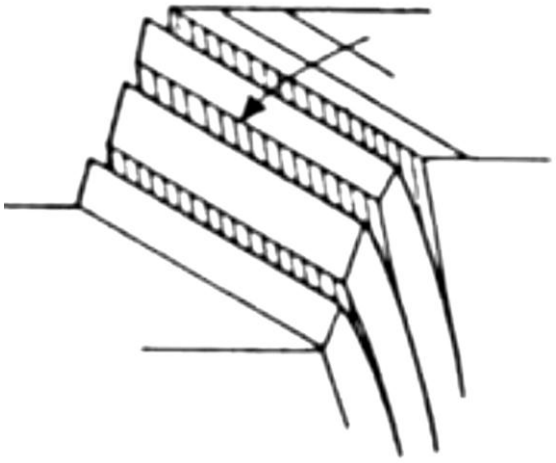

Figure 5.7 Toppling failure caused by steeply dipping joints.(Hoek & Bray 1981).

It is proposed that the sub-vertical columns inherent of the fracturing within the Port Hills loess discussed earlier in the thesis, may have split apart from each other, in a similar way to that discussed by Lutenegger and Hallberg. Figure 5.8 provides a block diagram sketch of the

possible subsurface structure of the loess based on observations made at 3 Glenview Terrace, showing sub-vertical columns within the loess splitting apart. Rather than there being a road cut to remove lateral support, as described by Lutenegger and Hallberg (1988), in the case of the Port Hills fissures, the lateral support would have been provided by sediments in the valley floors, many of which liquefied during the Christchurch Earthquake, thus effectively temporarily removing lateral support.

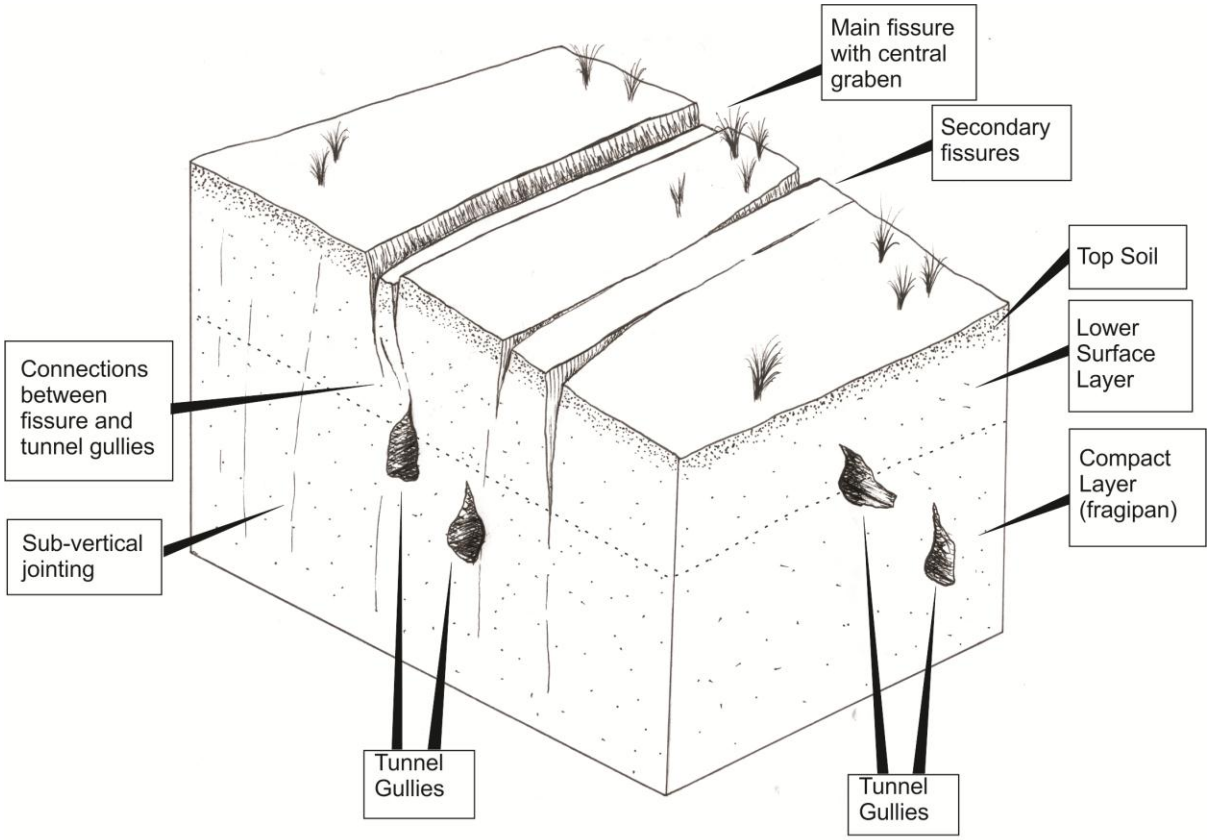

Figure 5.8 Schematic block diagram of fissured section of loess showing toppling within sub-vertical jointing of the loess body, and interactions of fissures with tunnel gullies. Scale: depth of land block shown approximately 2 m.

5.5 Mechanism Four: Trampoline effect

Scientists at GNS Science have reported observing evidence of the phenomenon known as the "trampoline effect" in Christchurch (GNS Science 2011). The trampoline effect occurs as a result of the extraordinary vertical ground accelerations which cause weaker upper sedimentary layers to travel farther upward than the more competent lower layers. This causes the layers to

separate at the crest of the passing earthquake wave, then "slap" into each other when the lower layers begin to rise with the next wave and collide with the upper layers which are still falling under gravity (Aoi et al. 2008; GNS Science 2011) (Figure 5.9). Aoi et al. (2008) hypothesised that when the trampoline effect takes place the sediment material is subjected to dilational strain when undergoing downward acceleration such that the bulk tensile strength of the near-surface material is reached. This, they hypothesise, would lead to these layers losing their cohesion through the development of tensile cracks and fractures.

As the sedimentary layers "slap" into one another, the impact energy travels back up to the surface, being felt as additional intensity of the shaking. GNS Science (2011) explain that this process can contribute to the generation of liquefaction as large amounts of water is forced up to the surface as the layers collide.

Being located along the front of the Port Hills, directly above the fault responsible for the Christchurch Earthquake, these areas were subjected to the extraordinary accelerations that are required to produce the trampoline effect. The trampoline effect would provide a logical mechanism for the fissuring, in that it provides explanation for the occurrence of the fissuring as a result of loss of cohesion in the loess as it undergoes dilational strain as explained by Aoi et al. (2008). The liquefaction in the valley floors is also explained by this interpretation.

While the trampoline mechanism does appear to provide a suitable interpretation of the fissuring, there are at least four fracture observations which, in this first study, for which it does not provide an explanation:

- The fact that some of the fissuring in Vernon Terrace began to form in September 2010, as ground acceleration from the Darfield Earthquake in the vicinity of the fissuring was not of the levels required to produce the trampoline effect.
- It is uncertain whether the shearing observed in bedrock below the Huntsbury reservoir is related to the fissuring. If this was so, the trampoline effect method of fissure production does not provide any link to this shearing, in particular the apparent correlation between the Albert Terrace–Ramahana Road dog-leg.
- Several residents of the Hillsborough Valley area who were affected by spring flow reported that their springs were unaffected by rainfall, and that the water flow has not abated since the series of earthquakes (greater than one year ago at the time of writing). This is not clearly explained by the trampoline effect theory, as this would induce immediate post-earthquake liquefaction and potentially spring flow, but not necessarily the continued flow that has been observed.

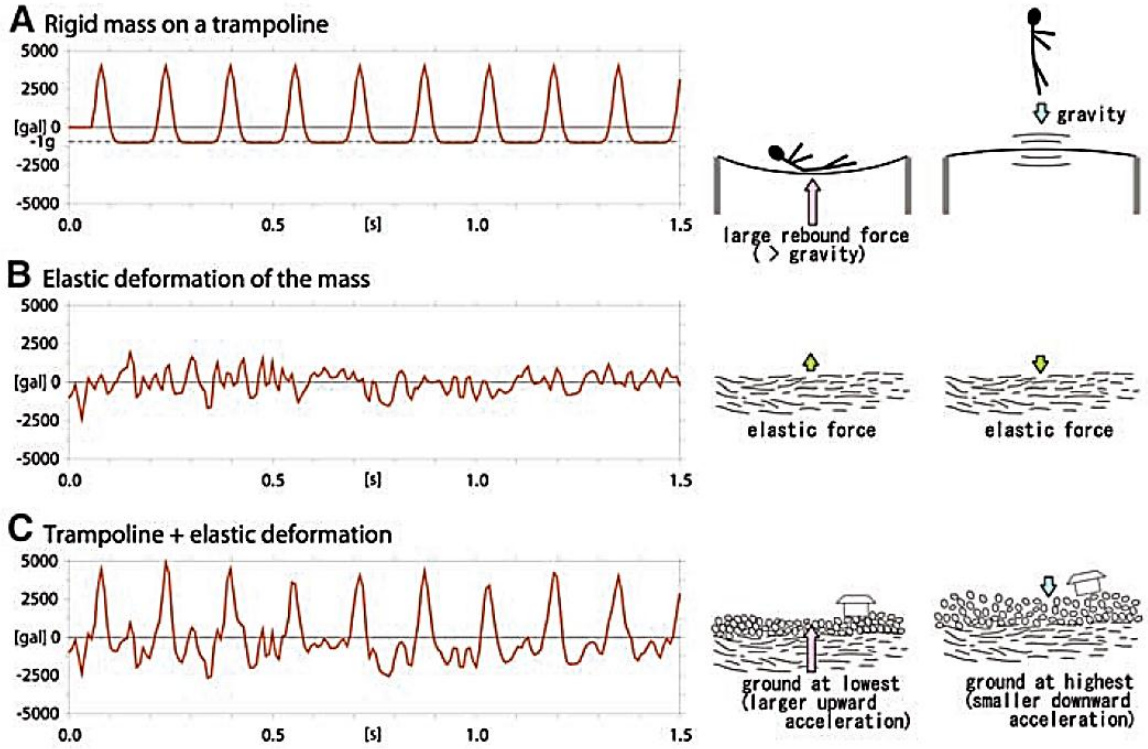

Figure 5.9 Plots of acceleration (gal) against time (s) of vertically accelerated objects. (A) Simplified model of the motion of a non-deformable mass bouncing on a trampoline. (B) Elastic deformation of a deformable mass, represented by a selected part of a downhole seismic record. (C) Simulated motion of a deformable mass bouncing on a trampoline, obtained as the sum of (A) and (B). From Aoi et al. (2008).

5.6 Mechanism Five: Lateral spreading

The phenomenon of riverbank lateral spreading during earthquakes has provided a useful corollary to the development of the fissurs, and with some minor adaptations in application, may be used as an interpretation of the mechanism behind the fissuring.

Lateral spreading occurs when an imbalance of forces acting on a soil mass beside a river channel results in movement of the soil, as a cohesive body, towards the centre of the river, leaving distinctive, river-parallel fissures along the banks of the river. The phenomenon (diagrammatically depicted in Figure 5.10) occurs due to the fact that the density of the water in the river channel is lower than the bulk density of the soil on the river bank, and when the shaking effects of an earthquake produce instability in the soil, lateral spreading can occur (Hentlass & O'Grady 1997).

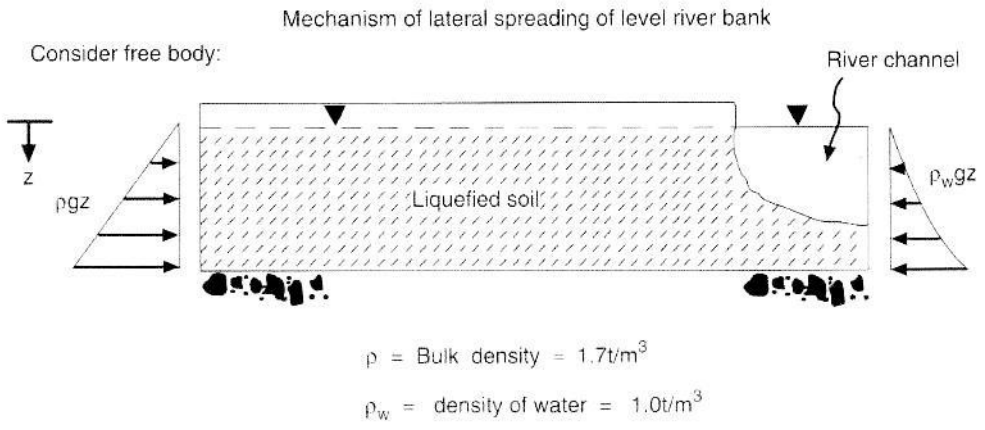

Figure 5.10 Diagram showing imbalance of forces acting on soil mass beside river channel, resulting in lateral spreading, such as that observed beside the Avon and Heathcote Rivers in Christchurch. After Hentlass and O'Grady (1997).

The theory of lateral spreading as a driving mechanism behind the formation of the fissures results from the fact that liquefaction occurred in several of the valley floors (particularly in the Heathcote Valley), which, it is postulated, would produce the same imbalance of forces, and loss of lateral support against the valley flanks as in the case of a soil mass beside a river channel during an earthquake. Following the loss of lateral support in this this manner, the style of movement of a cohesive body of soil on the flanks of the hill could be described by either the incipient landsliding mechanism theory, or the toppling failure mechanism theory.

Dellow et al. (2011a) hypothesise that the Vernon Terrace fissuring is caused by the saturated marginal marine sediments in the valley floor having liquefied during the Christchurch Earthquake, and thus having removed the buttress support to the toe of what they believe to be an incipient landslide. They argue that the fissures continued to develop in the Vernon Terrace area as the strength recovery of the sediments occurred over a period of days, if not weeks, and that the inferred loss of strength in the toe buttress materials may also explain the movement observed at Vernon Terrace after the Darfield Earthquake.

5.7 Intra-loess water coursing and tunnel gullying

Intra-loess water coursing and tunnel gullying is hypothesised to be an instrumental factor in the fissure formation in the Port Hills. It is considered unlikely that water coursing or tunnel gullying acted as causative, triggering mechanisms for the fissuring, however the presence of water is believed to have exacerbated the soil's propensity to form fissures. This is hypothesised based on both local analysis of the Port Hills loess, as well as evidence from overseas examples of water producing failure in loess soils. Based on these data, the interpretation is proposed that

the Port Hills loess in the vicinity of the fissures was in a state bordering on instability due to saturation by water courses prior to the Christchurch Earthquake, and the added stress from the earthquake itself provided the final action for the soil to ultimately fail.

Having observed the formation of the cavity in the section of 3 Glenview Terrace following large quantities of snow melt having been focused on the area through the broken drain pipe, as well as reading the work of Yetton (1986) on tunnel gullying in the Port Hills, it became apparent that the passage of water has the potential to have an enormous effect on the loess of the Port Hills. This was further shown by the effect of the water bath on the shear-box loess test (Chapter 4.5.3) where it was found that the capillary suction of the loess meant it rapidly absorbed a large quantity of water, inducing an almost immediate reduction in cohesion, and failure of the sample.

In the Albert Terrace area, numerous tunnel-gullies were observed in properties located near to the fissures. These tunnel gullies provide evidence of water coursing through the Port Hills loess. Studies have shown that water flowing through loess will eventually weaken the soil structure, resulting in drastic loss of tensile strength. The example of the Teton Dam, as discussed in Chapter 2.4.4, provides documented evidence of the ability of permeating water to produce failure in loess. In the case of the Teton Dam in the United States, a small leak lead to catastrophic breach of the dam as it lead to severe internal erosion and piping, leading ultimately to failure.

5.8 Mechanism Conclusions

It is believed that the mechanism responsible for causing the fissuring is a complex combination of three of the interpretations described in Section 5.1: the trampoline effect, bedrock fracturing, and lateral spreading. These three mechanisms can be applied in varying degrees to each of the fissuring sites in categories A, B, and C, in order to provide explanation for the observations made at each. The toppling mechanism hypothesis usefully describes the soil movement as a consequence of the aforementioned three causative mechanisms, and provides insight into the movement of the loess. Intra-loess water coursing and tunnel gullying is thought to have encouraged and exacerbated the fissuring, while not being the driving force *per se*. Incipient landsliding is considered to be the least likely of the five possible fissuring interpretations, however continued infiltration of water into the fissures may have the potential to generate such failures.

5.8.1 Category A Fissures

In the fissures of Category A (that is, those of Bowenvale Valley, Hillsborough Valley, and Huntlywood Avenue), the discussions provided in Section 5.1.2 show that with the proximity to the underground fault trace in these areas, it is logical that deep bedrock fracturing could have propagated upwards from the fault, into the volcanic rocks of the Port Hills. This would have produced conduits for deeply-sourced groundwater to travel to the surface, observed as both springs and an area of high conductivity in the resistivity survey. This deep bedrock fracturing is thought to have taken place during the Christchurch Earthquake, and would have occurred at the same time as the up to 2.2 g vertical acceleration was causing the surface sediments to separate and rift via the trampoline effect.

Working in conjunction with the trampoline effect and the bedrock fracturing would have been lateral spreading. In the case of Category A fissures, liquefaction was not apparent in the valley floors, but under the influence of the trampoline effect, lateral support would have been removed from the valley walls. This, as discussed in Section 5.1.6, would have induced an imbalance of horizontal forces, causing the valley sides to form fissures like those formed parallel to river banks in the typical case of lateral spreading. These blocks of loess soil can be modelled as having moved in a quasi-toppling failure, whereby the inherent steeply-dipping jointing within the loess acted to facilitate the quasi-toppling movement.

The fact that in the Hillsborough Valley there were pre-existing tunnel gullies across the hillside, in the same sites and at the same elevation as the fissures, would have caused the loess to be pre-weakened in the area where gullies interact with joints, thus exacerbating the likelihood of fissuring at the contour-parallel altitudes where they formed.

5.8.2 Category B Fissures

The fissures from Category B, that is, those along Bridle Path Road, and those in the lower section of La Costa Lane, can also be attributed to the combined mechanism of the trampoline effect, bedrock fracturing, and lateral spreading. The main difference with this category of fissure is that the bedrock fracturing likely has less of an impact due to the valley being a greater distance from the Christchurch Earthquake fault (see Figure 5.6, B and C), thus not straddling (and accommodating the stresses between) the area of land between the uplifted hills and the downthrown city area. While the bedrock fracturing has likely had less of an impact on the fissures in Category B, the phenomenon of lateral spreading has had a much stronger influence in this region, and is considered to be the main driving force behind the fissuring along Bridle Path Road. This is due to the presence of Christchurch Formation silts and sands in the Bridle

Path Road valley floor, which were observed to liquefy during the Christchurch Earthquake, as a result of the 2.2 g vertical ground acceleration that was felt in the area. This liquefaction would have resulted in immediate loss of lateral support to the valley walls, resulting in their moving westwards into the valley, leaving the discontinuous fissure zone.

Toppling failure can still be used as a corollary to the movement of the loess immediately adjacent to Category B fissures, however this description is perhaps less pertinent for this category as it is for Category A fissures. This is due to the large influence of the lateral spreading mechanism at this site, which alone is able to show how the fissures developed, based on the imbalance of forces, as shown in Figure 5.10.

Tunnel gullying has been reported in many locations over the Port Hills though (Yetton 1986), and while tunnel gullying was not observed at the Bridle Path Road site it would be unusual for this area to be entirely free from any erosional drainage of this nature., making the chance of there having been pre-weakened sections of loess lower than in Category A fissures, but still distinct.

5.8.3 Category C Fissures

Category C fissures, that is, those along La Costa Lane and Maffeys Road, appears to have formed under slightly different mechanisms from the other two categories, due to its elevation and proximity to outcropping bedrock. This has led to the conclusion that these fissures are not formed by the same lateral spreading-style mechanism as the other two categories, rather, that their formation is predominantly due to a toppling-style failure, brought about by intense vertical ground acceleration forces in the area, and still related (though to a lesser extent) to the fault-triggered fracturing within the bedrock, and the trampoline effect causing loss of lateral support from the valley sediments.

The quasi-toppling nature of Category C fissures is a likely mechanism hypothesis due to the steeper gradient of the hillside (see cross section in Figure 3.16), making the situation similar to that described by Lohnes et al. (1968) whereby in a road cut in loess, toppling failure can occur in the batter face as the lateral support is removed. In the case of the La Costa Lane and Maffeys Road fissures, the loss of lateral support came not from cutting a batter face, but rather from the high intensity shaking effects of the earthquake. The toppling movement would have taken place along the sub-vertical fracture planes inherent to the loess of the Port Hills.

As with the other fissure categories, it is considered unlikely that Category C fissures are evidence of incipient landsliding in the area, as there have been no apparent basal sliding planes, or in this case, no evidence of compression features in the valley floor. It is important,

however that remediation of the Category C fissures is undertaken, preventing surface water infiltration into the fissures, as continued infiltration of water into the loess fractures via the fissures could lead to failure in the area as the strength of the loess is weakened.

5.8.4 Summary

The application of the three fissuring mechanisms of bedrock fracturing, the trampoline effect, and lateral spreading in varying degrees to each of the three fissuring categories has been undertaken using data from investigations conducted throughout this thesis work, and from an understanding of the properties of loess as developed from research into loess soils and failure mechanisms worldwide. In the course of the investigations of this thesis, numerous observations were made of the Port Hills loess, and the manner in which it behaved during the Christchurch Earthquake of 22 February 2011.

Table 5.2 provides a summary figure where the most salient of the observed and investigated features of the loess are listed, and the five possible fissuring interpretations outlined in Chapter 5.1 are compared to the observations, in order to quickly ascertain which of the mechanism interpretations is able to provide explanation for which of the listed observations. Taking the first line as an example, the table shows that bedrock fracturing (mechanism 2) alone does not suitably explain the tendency for fissures to form near the loess - loess-colluvium boundary. The table shows that the trampoline effect and lateral spreading (mechanisms 5 and 6) are both able to explain this phenomenon (as explained in Section 5.1), and that incipient landsliding, water coursing and toppling failure (mechanisms 1, 3, and 4) would not act as causative means for this observation, do not dissociate with it either.

Table 5.2 Links between observed features of the Port Hills fissuring and the possible interpretations which correlate to the observations. Interpretations are discussed in Chapter 5.1, and are referred to in this table by the numbers 1-6, which correspond to chapter sections 5.1.1 – 5.1.6, respectively.

Observations and Facts of the Fissuring	✔ Interpretations that <u>do</u> correlate with this observation	? Interpretations that may indirectly correlate with this observation	✗ Interpretations that <u>show no correlation</u> with this observation
Fissures tend to occur at the loess-loess colluvium boundary	**5, 6**	**1, 3, 4**	**2**
Zones of compression are apparent at the base of slopes with fissuring	**1, 4, 5, 6**	**3**	**2**
Fissure zones are long, segmentally linear, with slight downslope curves at the ends	**4, 6**	**1, 2, 5**	**3**
Fissures appear to have some correlation with spring/ground water behaviour	**1, 2**	**5, 6**	**3, 4**
Most fissures appeared following the Christchurch Earthquake, and there has been a little continued movement reported	**1, 3, 4, 6**	**2**	**5**
The fissures almost perfectly coincide with the top edge of the Christchurch fault, 1 km below the ground	**2, 5**		**1, 3, 4, 6**
Liquefaction occurred in some valley floors	**1, 4, 5, 6**		**2, 3**
Fissures were observed to connect to pre-existing tunnel-gully features in Albert Terrace	**3, 4**	**1, 5, 6**	**2**
Shearing through the bedrock at Huntsbury Reservoir. Shear zone lines up with dog-leg in Ramahana Road–Albert Terrace fissures	**2**		**1, 3, 4, 5, 6**
Loess features: - tends towards vertical stability - measured unusually low clay content - cohesion average for loess but variable: 13.4 kPa, 19.7 kPa and 28.6 kPa - moisture content average for loess - shear strength average for loess but variable - internal friction angle average for loess but widely variable: 42.0 °, 43.4 °, and 18.4 °	**1, 3, 4, 6**	**5**	**2**
Resistivity did not reach the bedrock interface, however it showed areas of likely saturation due to high ground water level, as well as unusual areas of high resistivity near the centre of the transect.	**1, 2, 3, 6**		**4, 5**
Spring flow does not appear to be affected by season/rainfall influences	**2**		**1, 3, 4, 5, 6**

6 Summary and Conclusions

This final chapter summarises the findings of the thesis, and explains the most important conclusions drawn from the work. It includes a brief section advising on remediation measures, and ends with recommendations for further research work to be undertaken on the topic.

6.2 Summary

Following the Christchurch Earthquake of 22 February 2011, fissuring in the Port Hills caused severe damage to many hill-side properties, with fissures mostly extending segmentally for several hundred metres along foot-slope positions of north-facing valleys of the Port Hills. The fissures are present in nearly all major valleys, occur at similar low altitudes, show a contour-parallel orientation and are often accompanied by both lateral compression/extension features and spring formation in the valley floor below.

This project was undertaken in order to provide explanations for the fissuring behaviour observed in the Port Hills of Christchurch following the series of significant earthquakes which occurred near the city in 2010 and 2011, in particular the Christchurch Earthquake of 22 February 2011. Such explanations would be useful for planners and developers as well as residents currently adversely affected by the fissuring.

The principal objectives of this project, and how they were achieved through the thesis, are outlined below:

> Objective 1: To research local and world-wide loess soils and failures which take place in them, and to confirm whether there are any links between the fissuring behaviour seen in Christchurch and that observed in previously documented locations world-wide.

Chapter two provided an in-depth look at loess soils from around the world, and included a detailed overview of the technical aspects of Port Hills loess. Loess is intrinsically different in different locations, due to the nature of its deposition, being dependent on the composition of its source rocks.

It was found that palaeo-fissuring had been observed on Banks Peninsula by Harris (1983), and that the fissures he found were remarkably similar in form to those which developed during the Christchurch Earthquake, leading to the conclusion that historic earthquakes in the region may have had a similar effect on the loess soils. Loess fissuring was found to have occurred in several locations world-wide, with various causative mechanisms. Landsliding in the loess

plateau of China has resulted in the appearance of many fissures, largely formed as a result of severe rainfall events, although earthquakes were a driving factor also. Geotechnically, oversaturation was found to be the leading cause of loss of strength in loess soils, which in overseas examples tended to lead to rapid failure. In the case of the Teton Dam in the United States, a small leak lead to catastrophic breach of the dam as it lead to severe internal erosion and piping, leading ultimately to failure.

In examining these examples of fissuring and the geotechnical properties of loess it was found that links can definitely be drawn between such examples and the fissuring observed in Christchurch. None of the examples studied provided a perfect corollary to the Christchurch case, but they are still useful, particularly in their methods of investigation, and their remediation techniques, often pertinent facts which can be applied to Christchurch loess are discussed.

> Objective 2: To establish and document the extent of the of the fissure traces on the Port Hills through extensive field investigation and collation of post-earthquake data.

Chapter 3 begins with an overview of the geotechnical damage from the Darfield, Christchurch, and June Earthquakes, with a focus on the nature and occurrence of ground fissuring in five locations: Bowenvale Valley, Hillsborough Valley, Huntlywood Terrace–Lucas Lane, Bridle Path Road, and Maffeys Road–La Costa Lane. Through site investigations at the fissuring locations, and analysis of post-earthquake literature, the fissuring across the Port Hills is described in detail for each location.

The fissure traces at each site are discontinuous segments, which extend in zones of varying width along the hillside, in an approximately contour-parallel orientation, usually at least 20 m overland distance below the base of outcropping bedrock. Nearly every section of fissure trace with measureable extension was found to be accompanied by lateral compression features in the valley floor below. These were observed in sealed roads and kerbing where linear sections had been truncated, “concertina-fashion”. Springs and seepages formed in some locations, contemporaneously with the fissuring and compression features. These were predominantly located on the western side of the Bridle Path Road valley, and around the entrance to the Hillsborough Valley.

> Objective 3: To conduct in-depth study at specific locations, including laboratory analysis of loess taken from fissuring sites to ascertain its geotechnical properties and propensity to form fissures.

Comprehensive investigations into the fissuring were conducted in the Hillsborough Valley area, and Chapter 4 outlines and provides the results of this work. The Hillsborough Valley fissures were mapped through properties from Albert Terrace to Ramahana Road on the western side, and between Vernon Terrace and Rapaki Road on the eastern side. The fissure traces were found to extend in a roughly contour-parallel orientation, 500-600m in length, and fissure lateral extension was in the order of 0.10-0.20 m. Lateral compression was apparent in the valley floor topographically down slope from the fissures. Fissures on 1 and 3 Glenview Terrace on the west of the valley as well as 40 Rapaki Road on the east of the valley were mapped in greater detail, showing offset measurements and fissure orientation. Fissures were filled using a 1:6 mixture of bentonite clay and SAP-20 gravel.

Evidence of the impact of flowing water was observed as linear pot-holing, with substantial cavity formation beneath sealed road surfaces implied that water was flowing into the fissures at these locations, and passing through cracks in the loess, carrying fines in suspension. Following heavy snowfall in Christchurch the subsequent melt-water caused a large collapse of loess at 3 Glenview Terrace, as the fissure system appeared to link up to subterranean tunnel gullying. Remedial measures were undertaken at this site.

The Hillsborough Valley area has experienced the formation of at least two dozen new springs, many of which are still flowing at the present time (August, 2012) and do not appear to be greatly affected by season or rainfall. The springs are located towards the northern end of each distinct section of fissure trace and chemical analysis shows that they are sourced from the Port Hills volcanics.

The laser results for the three loess samples showed that the grain size of the loess is very similar at each of the locations on both sides of the valley, although the Rapaki Road sample has a slightly lower clay content, and slightly higher medium-sand content than the Glenview Terrace loess. All of the samples are poorly graded, with silt and fine sand making up 85% of the soil. At approximately 5 %, the loess in the Hillsborough Valley area has a lower clay content than is typical for the Port Hills.

The direct shear-box was used on loess samples from Glenview Terrace to ascertain the shear strength of the disturbed and remoulded loess from the site. The c values for the 40 Rapaki Road, 3 Glenview Terrace and compacted 40 Rapaki Road loess samples were 13.4 kPa, 19.7 kPa and 28.6 kPa, respectively. The corresponding ϕ values were 42.0 °, 43.4 °, and 18.4 °.

A resistivity survey was carried out across Centaurus Park, near the intersection of Ramahana Road and Centaurus Road. The survey length was 96 m, which provided a depth of

penetration of approximately 10 m in the centre, which was not long enough to establish the location of the subsurface bedrock interface. The survey did show an area of low resistivity at the base of the section, which likely corresponds to a zone of saturated clayey loess/loess colluvium, indicating a high water table in the area, and thus consistent with the appearances of local springs.

> Objective 4: To establish working hypotheses on the geotechnical mechanisms responsible for the formation of the fissures, as well as exploring their geotechnical implications and possible remediation measure. A preferred mechanism for loess fissuring is presented, along with recommendations for further research

In the course of the investigations of this thesis, numerous observations were made of the Port Hills loess, and the manner in which it behaved during the Christchurch Earthquake of 22 February 2011. The Port Hills fissuring may be sub-divided into three categories, Category A, Category B, and Category C, each characterised by distinctive features of the fissures.

- Category A, typified by Bowenvale Valley, Hillsborough Valley, and Huntlywood Ave includes fissures which display evidence of, spring formation, tunnel-gullying, and lateral spreading-like behaviour or quasi-toppling. These fissures are several metres down-slope of the loess-bedrock interface, and are in valleys containing a loess-colluvium fill.
- Category B is typified by the Bridle Path Road fissures and the lower fissures at La Costa Lane, which are also several metres down-slope from bedrock outcrops, but, particularly in the case of Bridle Path Road fissures, are in a much wider valley than those in the first category. The valley contains estuarine silty sediments which liquefied during the earthquake, and springs were formed, at a distance of several hundred metres from the fissures, on the far side of the valley.
- Category C is that of the fissures at La Costa Lane and Maffeys Road, which occurred at higher elevations than the fissures in the preceding categories, being almost coincident with bedrock outcropping.

Three fissuring mechanisms were applied to the formation of the fissures in each of the above categories, each having a differing amount of influence depending on local site conditions. These mechanisms are:

- Bedrock fracturing, whereby high vertical ground acceleration in the area of the fissuring lead to topographically-controlled fissuring, requiring relatively dry loess to behave in a brittle manner in response to propagation of forces from bedrock.

- The trampoline effect, whereby sediment material is subjected to dilational strain when undergoing downward acceleration such that the bulk tensile strength of the near-surface material is reached, which would cause it fail in tension, ultimately forming fissures.
- Lateral spreading, whereby an imbalance of forces acting on the valley flanks, resulting from liquefaction of valley floor sediments, resulted in movement of the soil, as a cohesive body, towards the centre of the valley, leaving the distinctive fissures.

Intra-loess water coursing and tunnel gullying is hypothesised to be an instrumental factor in the fissure formation in the Port Hills. It is considered unlikely that water coursing or tunnel gullying acted as causative, triggering mechanisms for the fissuring, however the presence of water is believed to have exacerbated the soil's propensity to form fissures.

The application of the three fissuring mechanisms of bedrock fracturing, the trampoline effect, and lateral spreading in varying degrees to each of the three fissuring categories has been undertaken using data from investigations conducted throughout this thesis work, and from an understanding of the properties of loess as developed from research into loess soils and failure mechanisms worldwide. Selected recommendations for remedial work on the fissures, in particular that they be infilled using bentonite and SAP-20 gravel mixtures, are outlined in Section 6.4. Section 6.5 provides recommendations for additional research to further develop the fissuring mechanism hypotheses, including the use of trenching, ground penetrating radar, and modelling software.

6.3 Conclusions

It is believed that the loess of the Port Hills at each of the three site categories, failed in tension during the Christchurch Earthquake of 22 February 2011. This was as a result of the loess' tendency to form sub-vertical joint sets, combined with a low moisture content which allowed it to fissure in a brittle manner. Lohnes et al. (1968) made the comment that a cut face in loess will topple inwards along the internal sub-vertical fractures within the loess. This is a useful corollary to the Port Hills case, where lateral support was removed as a result of the shaking intensity of the earthquake producing liquefaction and disturbance in the valley floor sediments.

The mechanism responsible for causing the fissuring is an intricate combination of the trampoline effect, bedrock fracturing, and lateral spreading. These three mechanisms can be applied in varying degrees to each of the fissuring sites in categories A, B, and C, in order to provide explanation for the observations made at each.

The toppling mechanism hypothesis usefully describes the soil movement as a consequence of the aforementioned three causative mechanisms, and provides insight into the manner in which the loess moves. Intra-loess water coursing and tunnel gullying is thought to have encouraged and exacerbated the fissuring, while not being the driving force *per se*. Incipient landsliding is considered to be an unlikely interpretation of the fissuring, however continued infiltration of water into the fissures may have the potential to generate such failures.

In order to provide further substantiation for the fissuring mechanisms it is highly recommended that further research is undertaken. The excavation of a series of trenches at strategic locations crossing the fissure traces. This should show the behaviour of the fissures at depth, and how they are linked to the tunnel gullying in the Hillsborough Valley area. Future investigations are recommended to utilise ground penetrating radar (GPR) as a survey method, as this would provide a greater depth of penetration and enable the depth to the loess-colluvium and bedrock interface to be accurately located. Having concluded that the fissuring is most likely due to the combined effects of the trampoline effect, deep bedrock fissuring, and lateral spreading, it is possible to design three-dimensional models which can utilise input data collected from laboratory analysis and fissure studies to ascertain whether, when subject to the mechanisms listed above, a modelled hillside would respond in the same manner. Such an undertaking could provide valuable insight into the manner in which a hillside responds to earthquake stimuli, and as such may have applications, with suitable adaptations, to similar sites elsewhere.

6.4 Remediation recommendations

The investigations of this thesis have lead the author to believe that it is highly unlikely that the fissure traces are incipient landslides, and as such continued residence in the area is less likely to be hazardous. Should fissures be left unfilled, however, overland flow of rainwater will enter the fissures, ultimately causing further erosion underground, and there is a high likelihood of the development of additional erosion cavities such as that which occurred at 3 Glenview Terrace in the winter of 2011. The subterranean infiltration of water into loess has high potential to cause further ground movement, and as such it is important that the all fissures are infilled using the bentonite and SAP-20 gravel mixtures, as described in Chapter 4.

Some of the remediation methods outlined in Section 2.9, investigated by Laffan and Sutherland (1987) on the lower slopes of the Wither Hills near Blenheim could likely be applied satisfactorily to the tunnel gullies which occur in the Port Hills of Christchurch. The most successful method established by their study was to mechanically reshape severely eroded hill

slopes in order to remove all traces of the tunnel-gullies, and then sow the area with permanent pasture. Clearly this method would be unsatisfactory for residential areas of Christchurch, nevertheless, it could be applied to rural areas. Laffan and Sutherland found that the use of bench terraces to control runoff was unsuccessful as without the application of a form of seal, surface flows of water across loess tends to result in gradual erosion and subsequent rill and gully formation.

6.5 Recommendations for further research

In undertaking the initial research work and investigations in this thesis, investigative methods were established mainly through observing satisfactory analysis methods of other works, as well as managing with privately-owned field areas following the earthquake. As such, access to sites was limited and information on the sites was not always forthcoming. In order to provide further substantiation for the fissuring mechanisms outlined in Section 5.2, it is highly recommended that further research is undertaken. Such research should have a primary goal of providing residents of the affected areas with as much certainty as possible into the stability of their land, and their security should they continue to reside in the area.

6.5.1 Trenching and laboratory analysis

To provide further proof of the toppling mechanism of failure, it would be ideal to excavate a series of trenches at strategic locations crossing the fissure traces. This should show the behaviour of the fissures at depth, and how they are linked to the tunnel gullying in the Hillsborough Valley area. It is recommended that such trenches are up to 2 m deep where possible, and aligned down-slope, perpendicular to the fissuring. Such excavation would enable further loess samples to be collected, and so further laboratory analysis on the strength characteristics of the soils can be undertaken. With limited samples, laboratory testing in this thesis was also limited, however through trenching samples would be available for collection via push tube from various depths at each site.

The shear strength analysis conducted in this research provided results of varying apparent validity when compared to results from tests done on Port Hills loess by previous authors at other sites. Should further investigations be undertaken, it is strongly recommended that loess be either retrieved from site in such a manner that the natural bonds within the loess are maintained, or that Borehole Shear Tests (Section 2.3) are undertaken. Such results would be useful in the further development of the theory of quasi-toppling as a failure mechanism, as they

can offer insight into the ability of the loess to shear in sections, thus ultimately creating the toppling-style failure.

6.5.2 GPR survey

The geophysical resistivity survey conducted in this thesis provided detailed yet ultimately inconclusive evidence of the state of the subterrain at Centaurus Park. Ideally, the survey would have been conducted over a much longer path, but this was not possible due to paved and residential areas. It is advised therefore that future investigations utilise ground penetrating radar (GPR) as a survey method, as this would provide a greater depth of penetration and enable the depth to the loess-colluvium and bedrock interface to be accurately located. Either technique would be unlikely to locate fissures themselves, as their width would be small in comparison to most geophysical resolution, however GPR data combined with the ground resistivity results would provide greater evidence of the subterranean arrangement of the fissuring, with respect to the bedrock interface and the spring behaviour.

6.5.3 FLAC and other modelling software

Having concluded that the fissuring is most likely due to the combined effects of the trampoline effect, deep bedrock fissuring, and lateral spreading, it is now possible to design three-dimensional models which can utilise input data collected from laboratory analysis and fissure studies to ascertain whether, when subject to the three mechanisms listed above in the form of a virtual earthquake, a modelled hillside would respond in the same manner. Such an undertaking could provide valuable insight into the manner in which a hillside responds to earthquake stimuli, and as such may have applications, with suitable adaptations, to similar sites elsewhere.

The modelling software *FLAC* is highly recommended for use in this work. *FLAC* utilised finite-element mesh models to generate three-dimensional geomodels of a particular area, defined by user-specified boundary conditions. In the case of the Port Hills, this could be a section of valley between two ridgelines, such as in a cross-section through the Hillsborough Valley, passing across fissure traces on either side. Input parameters would include the geological constitutive behaviour properties of the loess, and underlying bedrock, using Mohr-Coulomb analysis of laboratory data, as well as topography and the depth to various soils interfaces and the bedrock below. In running the model an initial static gravity loading would be applied, followed by the dynamic conditions of the earthquake loading, as measured by local seismic stations.

A more simple model of the fissuring behaviour can be achieved through a two-dimensional cross-section, using the software *Phase2*. Dr Marlène Villeneuve of the University of Canterbury Geology Department conducted a preliminary analysis of the suitability of *Phase2*, with some promising results. Using generic input parameters for loess and basalt, and an earthquake loading simulation through seismic acceleration, she was able to successfully show that loess mantling bedrock in the manner of the Port Hills, will move down-slope under the effects of an earthquake, leaving areas of negative volume at roughly the height of the fissures, and producing areas of increased volume in the valley floors.

7 References

Alley PJ 1966. Cashmere Hills Loess. New Zealand Engineering 11(10): 424.

Anderson JG 2010. Source and Site Characteristics of Earthquakes That Have Caused Exceptional Ground Accelerations and Velocities. Bulletin of the Seismological Society of America 100(1): 1-36.

Aoi S, Kunugi T, Fujiwara H 2008. Trampoline Effect in Extreme Ground Motion. Science 322: 727-730.

Beavan J, Fielding E, Motagh M, Samsonov S, Donnelly N 2011. Fault Location and Slip Distribution of the 22 February 2011 M_w 6.2 Christchurch, New Zealand, Earthquake from Geodetic Data. Seismological Research Letters 82(6): 789-799.

Beca Infrastructure Ltd 2011. Huntsbury No. 1 Reservoir - Geological Interpretative Report.

Bell DH 1981. Dispersive loessial soils of the Port Hills, Christchurch. Geomechanics in Urban Planning: Proceedings of a Symposium Held in Palmerston North, New Zealand. Pp. 253-261.

Bell DH, Pettinga JP 1983. Presentation of Geological Data. Engineering for Dams and Canals, I.R. Brown (ed) 9(4(G)): I 4.1 - 4.35.

Bell DH, Crampton NA 1986. Panel report: Engineering geological evaluation of tunnelling conditions, Lyttelton-Woolston LPG Project, Christchurch, New Zealand. In: Rimoldi HV ed. Fifth International Congress International Association of Engineering Geology. Pp. 2485-2501.

Bell DH, Trangmar BB 1987. Regolith Materials and Erosion Processes on the Port Hills, Christchurch, New Zealand. 5th International Conference and Field Workshop on Landslides. Chistchurch. Pp. 93-105.

Bell DH, Glassey PJ, Yetton MD 1986. Chemical stabilisation of dispersive loessical soils, Banks Peninsula, Canterbury, New Zealand. In: Rimoldi HV ed. Fifth International Congress International Association of Engineering Geology. Pp. 2193-2208.

Bell FG 1999. Earthquake activity. Geological Hazards, Spon Press.

Bell FG 2007. Engineering Geology 2nd ed. Great Britain, Elsevier.

Birrell KS, Packard RQ 1953. Some physical properties of New Zealand "loess". N.Z. J. Sci. Tech. b35: 30-35.

Blyth FGH 1969. A Geology for Engineers. London, Edward Arnold (Publishers) Ltd.

Bradley BA, Cubrinovski M 2011. Near-source Strong Ground Motions Observed in the 22 February 2011 Christchurch Earthquake. Seismological Research Letters 82(6): 853-865.

Brown LJ, Weeber JH 1992. Geology of the Christchurch Urban Area. Lower Hutt, Institute of Geological and Nuclear Sciences Limited.

Brown LJ, Weeber JH 1994. Hydrogeological implications of geology at the boundary of Banks Peninsula volcanic rock aquifers and Canterbury Plains fluvial gravel aquifers. New Zealand Journal of Geology and Geophysics 37: 181-193.

Browne GH, Field BD, Barrell DJA, Jongens R, Bassett KN, Wood RA 2012. The geological setting of the Darfield and Christchurch earthquakes. New Zealand Journal of Geology and Geophysics 55(3): 193-197.

Campbell JK, Pettinga JP, Jongens R 2012. The tectonic and structural setting of the 4 September 2010 Darfield (Canterbury) earthquake sequence, New Zealand. New Zealand Journal of Geology and Geophysics 55(3): 155-168.

Churchman GJ, Bruce JG 1987. Relationships between loess deposition and mineral weathering in some soils in Southland, New Zealand. In: Eden DN, Furkert RJ ed. International Symposium on Loess. New Zealand, A.A. Balkema. Pp. 11-31.

Claridge GGC, Campbell IB 1987. Loess sources and aeolian deposits in Antarctica. In: Eden DN, Furkert RJ ed. International Symposium on Loess. New Zealand, A.A.Balkema. Pp. 33-45.

Coates G 2002. The Rise and Fall of the Southern Alps. Christchurch, Canterbury University Press.

Crampton NA 1985. Engineering Geological Aspects of the Lyttelton-Woolston LPG pipeline. M.Sc. thesis, University of Canterbury, Christchurch.

Cumberland KB 1944. Soil Erosion in New Zealand - A Geographic Reconnaisance. Soil Conservation and Rivers Control Council, Wellington, N.Z. Pp. 98.

Das BM 2002. Principles of Geotechnical Engineering, Brooks/Cole.

Dellow G, Yetton M, Massey C, Archibald GC, Barrell DJA, Bell D, Bruce JG, Campbell A, Davies TRH, De Pascale G and others 2011a. Landslides caused by the 22 February 2011 Christchurch Earthquake and management of landslide risk in the immediate aftermath. Bulletin of the New Zealand Society for Earthquake Engineering 44(4).

Dellow GD, Massey CI, Davies TRH, Read SAL, Bruce ZRV, Van Dissen R, Barrell D, Jongens R, Heron D, Glassey PJ and others 2011b. Rockfalls and landslides triggered by the February 2011 Christchurch (NZ) earthquake: the GeoNet response. Poster presented at the EGU2011-14230 Special session US4: The 22 February 2011 Christchurch NZ Earthquake. 2011 EGU General Assembly. Vienna, GNS Science.

DeMets C, Gordon RG, Argus DF 2010. Geologically current plate motions. Geophysical Journal International 181: 1-80.

Derbyshire E 2001. Geological hazards in loess terrain, with particular reference to the loess regions of China. Earth-Science Reviews 54: 231-260.

Dijkstra TA, Rogers CDF, Smalley IJ, Derbyshire E, Yong Jin L, Xing Min M 1994. The loess of north-central China: Geotechnical properties and their relation to slope stability. Engineering Geology 36.

Elliot JR, Nissen EK, England PC, Jackson JA, Lamb S, Li Z, Oehlers M, Parsons B 2012. Slip in the 2010-2011 Canterbury earthquakes, New Zealand. Journal of Geophyisical Research 117: 36.

Evans GL 1977. Erosion tests on loess silt, Banks Peninsula, N.Z. 9th ICSMFE Pp. 63-69.

Field BD, Browne GH, Davy BW 1989. Cretaceous and Cenozoic Sedimentary Basins and Geological Evolution of the Canterbury Region, South Island, New Zealand. Lower Hutt, New Zealand Geological Survey.

Fodor P, Kleb B 1994. Engineering Geological Problems in Loess Regions of Hungary. Quaternary International 24: 25-30.

Glassey PJ 1986. Geotechnical Properties of Lime Stabilised Loess, Port Hills, Canterbury. M.Sc. thesis, University of Canterbury, Christchurch.

GNS Science 2011. Scientists find rare mix of factors exacerbated the Christchurch quake. Retrieved 2012 2012, from http://www.gns.cri.nz/Home/News-and-Events/Media-Releases/Multiple-factors

Goldwater S 1990. Slope Failure in Loess. A Detailed Investigation, Allendale, Banks Peninsula, M.Sc. thesis, University of Canterbury, Christchurch.

Griffiths E 1973. Loess of Banks Peninsula. New Zealand Journal of Geology and Geophysics 16(3): 657-675.

Griffiths E 1974. Soils of Part of the Port Hills and Adjacent Plains, Canterbury, New Zealand. Wellington, New Zealand Department of Scientific and Industrial Research.

Hancox GT, Massey C, Perrin N 2011. Landslides and related ground damage caused by the M_w 6.3 Christchurch Earthquake of 22 February 2011. NZ Geomechanics News(81): 53-67.

Harris SA 1983. Infilled Fissures in Loess, Banks Peninsula, New Zealand. Polarforschung 53(2): 49-58.

Hentlass C, O'Grady U ed. 1997. Risks and Realities: A Multi-disciplinary Approach to the Vulnerability of Lifelines by Natural Hazards. Christchurch, Centre for Advanced Engineering, University of Canterbury.

Hoek E, Bray J 1981. Rock Slope Engineering, Taylor and Francis.

Ishihara K 2009. Liquefaction-induced flow slide in the collapsible loess deposit in Tajik. In: Kokusho ed. Earthquake geotechnical case histories for performance-based design. London, Taylor and Francis Group.

Ishihara K, Koseki J 1989. Cyclic Shear Strength of Fines Containing Sands. Proc. Earthquake Geotechnical Engineering, 12 International Conference on Soil Mechanics and Foundation Engineering. Pp. 101-106.

Ives D 1973. Nature and Distribution of Loess in Canterbury, New Zealand. New Zealand Journal of Geology and Geophysics 16(3): 587-610.

Jonsson S, Segall P, Pedersen R, Bjornsson G 2003. Post-earthquake ground movements correlated to pore-pressure transients. Nature 424: 179-183.

Kaiser A, Holden C, Beaven J, Beetham D, Benites R, Celentano A, Collett D, Cousins J, Cubrinovski M, Dellow G and others 2012. The M_W 6.2 Christchurch earthquake of February 2011: preliminary report. New Zealand Journal of Geology and Geophysics 55(1): 67-90.

Keaton JR, DeGraff JV 1996. Chapter 9. Surface Observation and Geologic Mapping. In: Turner KA, Schuster RL ed. Landslides Investigation and Mitigation. Transportation Research Board Special Report 247. Washington, D.C., National Academy Press. Pp. 178-230.

Laffan MD, Sutherland RD 1987. Treatment of tunnel-gully erosion in loess colluvium on the Wither Hills, New Zealand. In: Eden DN, Furkert RJ ed. International Symposium on Loess. New Zealand, A.A.Balkema. Pp. 81-90.

Lohnes RA, Handy RL 1968. Slope Angles in Friable Loess. The Journal of Geology 76(3).

Lutenegger AJ 1987. In Situ Shear Strength of Friable Loess. In: Pecsi M ed. XIIth International Congress of the International Union for Quaternary Research (INQUA). Ottawa, Catena Verlag. Pp. 27-34.

Lutenegger AJ, Hallberg GR 1988. Stability of Loess. Engineering Geology 25: 247-261.

Manga M, Wang C-Y 2007. Earthquake Hyrdology. In: Kanamori H ed. Treatise on Geophysics, Elsevier. Pp. 293-320.

Marshak S 2001. Earth : portrait of a planet. New York, Norton & Company Ltd.

McNally GH 1998. Soil and Rock Construction Materials, E. & F.N. Spon.

Miller DEK 1971. Soil properties affecting tunnel gully ersion. Unpublished M.Agr.thesis, Lincoln University, Christchurch.

Muhunthan B, Pillai S 2008. Teton Dam, USA: uncovering the crucial aspect of its failure. Proceedings of the Institution of Civil Engineers - Civil Engineering 161(CE6): 35-40.

Nobes D, C. 2003. Environmental and Engineering Geophysics: Course Reader for ENGE 480 2010. Christchurch, University of Canterbury.

Pettinga JP, Yetton M, Van Dissen R, Downes G 2001. Earthquake Source Identification and Characterisation for the Canterbury Region, South Island, New Zealand. Bulletin of the New Zealand Society for Earthquake Engineering 34(4): 282-310.

Powrie W 2004. Soil Mechanics Concepts and Applications 2nd Ed. Oxon, Spon Press.

Raeside JD 1964. Loess deposits of the South Island, New Zealand, and soils formed on them. New Zealand Journal of Geology and Geophysics 7: 811-838.

Sanders R 1986. Hydrogeological studies of springs in Akaroa County, Banks Peninsula. M.Sc. thesis, University of Canterbury, Christchurch.

Sciarra N, Calista M, Marchetti D, D'Amato Avanzi G, Pochini A, Puccinelli A 2011. Geo-mechanical characterisation and 3D numerical modeling of complex rock masses: a slope stability analysis in Italy. In: Sainsbury DP, Hart RD, Detournay CJ, Nelson MJ ed. 2nd International *FLAC/DEM* Symposium. Melbourne, Australia, Itasca International Inc. Pp. 189-196.

Sharma PV 1986. Geophysical Methods in Geology 2nd Ed. New York, Elsevier.

Smalley I 1992. The Teton Dam: rhyolite foundation + loess core = disaster. Geology Today 8(1): 19-22.

Smith GN, Smith IGN 1998. Elements of Soil Mechanics. Seventh edition ed, Blackwell Science Ltd.

Smyrou E, Tasiopoulou P, Engin Bal I, Gazetas G 2011. Ground Motions versus Geotechnical and Structural Damage in the February 2011 Christchurch Earthquake. Seismological Research Letters 82(6): 882-892.

Sowers GF, Royster DL 1978. Chapter 4: Field Investigation. In: Schuster RL, Krizek RJ ed. Special Report 176: Landslides: Analysis and Control. Washington, D.C., TRB, National Research Council. Pp. 81-111.

Standards Association of New Zealand 1986. Methods of testing soils for civil engineering purposes. Part 4. Soil compaction tests. Wellington.

Sun P, Peng J-b, Chen L-w, Yin Y-p, Wu S-r 2009. Weak tensile characteristics of loess in China-An important reason for ground fissures. Engineering Geology 108: 153-159.

Tehrani BH 1988. Chemical Stabilisation of Whaka Terrace Loess, Christchurch, M.Sc. thesis, University of Canterbury, Christchurch.

Terzaghi K, Peck RB, Mesri G 1996. Soil Mechanics in Engineering Practice 3rd Edition. United States of America, John Wiley & Sons, Inc.

Trangmar BB 1991. Soil Survey of the Port Hills, Canterbury, New Zealand. N.Z. Soil Bur. Soil Surv. Rep.

Xu L 2010. Comment on "Weak tensile characteristics of loess in China - An important reason for ground fissures" by Ping Sun, Jian-bing Peng, Li-wei Chen, Yue-ping Ying, Shu-ren Wu [Engineering Geology 108 (2009) 153-159]. Engineering Geology 114: 105-106.

Yetton M 1986. Investigation and Remedial Methods for Subsurface Erosion Control in Banks Peninsula Loess. MSc thesis, University of Canterbury, Christchurch. 231 p.

Zhang Z, Lanmin W 1995. Geological Disasters in Loess Areas during the 1920 Haiyaun Earthquake, China. GeoJournal 36.2(3): 269-274.